3rd International Civil Engineering Conference (ICEC 2024)
Department of Civil Engineering
Federal University of Technology, Minna, Nigeria

Potentials of Dekina Cassava Peel Ash In Concrete Production

*Ismail, S.P.,[1]; Kolo, D.N..[1] and Yusuf, A.[1];
[1] Department of Civil Engineering Federal University of Technology, Minna
*Email: paul.pg202321414@st.futminna.edu.ng

ABSTRACT

Basic conventional building materials like cement and aggregates are becoming increasingly expensive due to high cost incurred in their processes, production and transportation. The utilization of locally available materials such as cassava peel ash that can either reduce or replace the conventional ones is being considered. Following review paper summarizes the mechanical and durability characteristics of cassava peel ash compared with ordinary Portland cement. The cassava peel ash was obtained by calcinations of cassava peel to 700^{o}C temperature. The sample was investigated using XRS-FP Analysis, for evaluating the concentration of each component such as SiO_2, Al_2O_3, Fe_2O_3, CaO, MgO, SO_3, K_2O Na_2O and LOI. The phase composition, mechanical and durability properties evolution. The results reveal an oxide composition of 81.14% for the cassava peel ash. These analyses have shown that natural pozzolan based geopolymer has potential to be used as sustainable building materials. It was discovered that the cassava peel ash contains all the main chemical constituents of cement though in lower percentage compared with OPC which shows that it can serve as a suitable replacement if the right percentage is used.

Keywords: Aggregate, Cassava Peel Ash, Cement, and Pozzolana

INTRODUCTION

Building materials account for 40-60% of the total construction cost (Olatokunbo *et al.,2018*) This is attributed to the fact that basic conventional building materials like cement and aggregates are becoming increasingly expensive due to high cost incurred in their processes, production and transportation. The utilization of locally available materials that can either reduce or replace the conventional ones is being investigated. In the same vein, developing nations of the world are challenged with issues of managing domestic and agricultural wastes as a result of the attendant growth in population and increasing urbanization. Reuse of these wastes provide an attractive option that promotes savings and conservation of natural resources from further depletion hence creating a sustainable environment. Solid waste and its resource potential are being appraised for reuse. Agricultural waste such as corn cob ash and cassava peel ash inclusive is recently attracting interest (Olushola and Umoh, 2013). Cassava is known to be a major source of carbohydrates with Africa being the largest centre of production. The cassava tubers are peeled, and the discarded peel forms the first stage of the solid waste. These wastes would even be more problematic in future with increased industrial production of cassava products such as cassava flour and garri.

In view of the need for alternative construction and building materials many researchers have suggested chemical additives and pozzolans from agro wastes. The need for naturally endowed content in the Nigerian construction industry is timely and justifiable. Cassava peel ash is a naturally endowed occurring agricultural waste material abundantly available to the dwellers of the Dekina basin. Construction activities based on these naturally occurring materials are major steps towards industrialization and economic integration of developing countries. This explains the huge interest over the years in utilising such materials as substitute or partial replacement for concrete constituents (Aguwa and Sadiku, 2011).

Concrete account for between 40-60% of the total construction cost (Ayangade *et al.,* 2004), and this is attributed to the fact that basic conventional building materials like cement and aggregates are becoming increasingly expensive due to high cost incurred in their processing, production and transportation. The need to convert this agricultural by-product (cassava peel ash) is the focus of the study. In the same vein, developing nations of the world are challenged with issues of managing domestic and agricultural wastes as a result of the attendant growth in population and increasing urbanization. Reuse of these wastes provide an attractive option that promotes savings and conservation of natural resources from further depletion hence creating a sustainable environment.

Cassava is known to be a major source of carbohydrates with Africa being the largest centre of production. The cassava tubers are peeled, and the discarded peel forms the first stage of the solid waste. Adesanya *et al* (2008) reported that cassava peel constitutes between 20-35% of the weight of tuber, especially in the case of hand peeling. Based on 20% estimate, about 6.8 million tonnes of cassava peel is generated annually and 12 million tonnes is expected to be produced in the year 2020. Indiscriminate disposal of cassava peels due to gross underutilization as well as lack of appropriate technology to recycle them is a major challenge, which results in environmental problem. Thus, there is need to search for alternative methods to recycle them (cassava peels). Salau and Olonade (2011) studied the pozzolanic potential of cassava peel ash (CPA) and their results showed that cassava peel ash possesses pozzolanic reactivity when it is calcined at 700°C for 90 minutes. At these conditions, CPA contained more than 70 percent of combined silica, alumina and ferric oxide

Concrete is the most widely used construction material in the world, second to water as the most utilised substance on earth (Alhaji, 2016). It is obtained by mixing in the right quantities of Cement, water, aggregates and sometimes with admixtures. Aggregates ideally constitute 75% of concrete hence are extremely important in determining the quality of concrete produced, this makes it important that they meet certain standards in order to achieve a strong, durable and economical concrete.

Concrete is widely used as construction material for various types of structures due to its durability. For a long time it was considered to be very durable material requiring little or no maintenance. Many environmental phenomena are known significantly for the durability of reinforced concrete structures. The use of waste materials with pozzolanic properties in concrete production is a worldwide practice.

Salau and Olonade (2011) studied the pozzolanic potential of cassava peel ash (CPA) and their results showed that cassava peel ash possesses pozzolanic reactivity when it is calcined at700°Cfor 90 minutes. At these conditions, CPA contained more than 70 per cent of combined silica, alumina and ferric oxide.

Structural reliability deals with rational treatment of random variable and uncertainties within structural engineering design, inspections, maintenance, and decision making. It may be use to describe uncertainties in basic variable, such as spatial and time variation of external loads, material properties and dimensions under the subdivision of probabilistic distributions.

METHODOLOGY

Ordinary cassava peel ash was used for this experiment which conform to the requirement of BS 8615-1:2019, standard refers to the standard specifying requirement for natural pozzolana and natural calcined pozzolana used with Portland cement. The cassava peel used for this research was obtained from Dekina, in Kogi State. It was ensured that the CPA was clean and free from deleterious materials. The cassava peel was incinerated in an oven at 10°C per minute up to 700°C and was maintained at this temperature for 90 minute to produce the ash. After which the following method was adopted on material.

RESULTS AND DISCUSSION

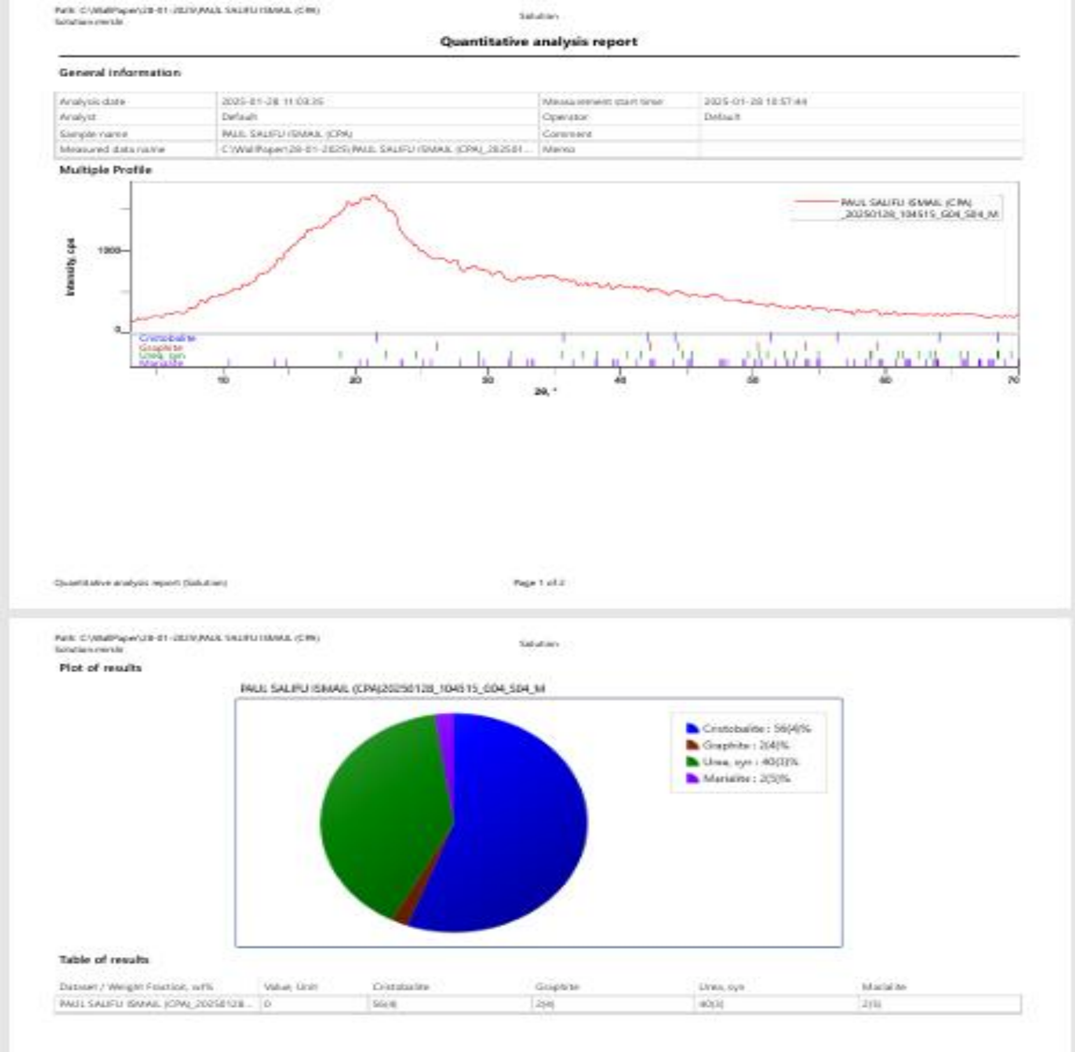

Figure 1: Quantitative Analysis Report of Cassava Peel Ash

1.1 X-RAY DIFFRACTOMETER

This X-Ray diffraction is the method used to study phase and crystal structure of ash by analyzing the diffraction pattern of powder, The information about the composition and structure or morphology of atoms or molecules inside the material is as shown in Figure 1

1.2 X-RAY FLUORESCENCE

Is a relatively and sensitive technique which detect the chemical species at every concentration. which is used to examined the structural changes caused by changes in temperature also, used to examined changes in the composition of the cassava peel ash Which is used to identify critical state in real time. Also, the interaction of different molecules with each other and with the solvent. As shown in Figure 2 and Table 1.

Figure 2 presents the quantitative analysis report of the cassava peel ash. which shows the significant amount cristobalite 56 (4) % and is within the British standard for pozzolanic material, BS 8615-1:2019, hence it is concluded that the silica (SiO_2) forms a suitable chemical composition of natural pozzolan.

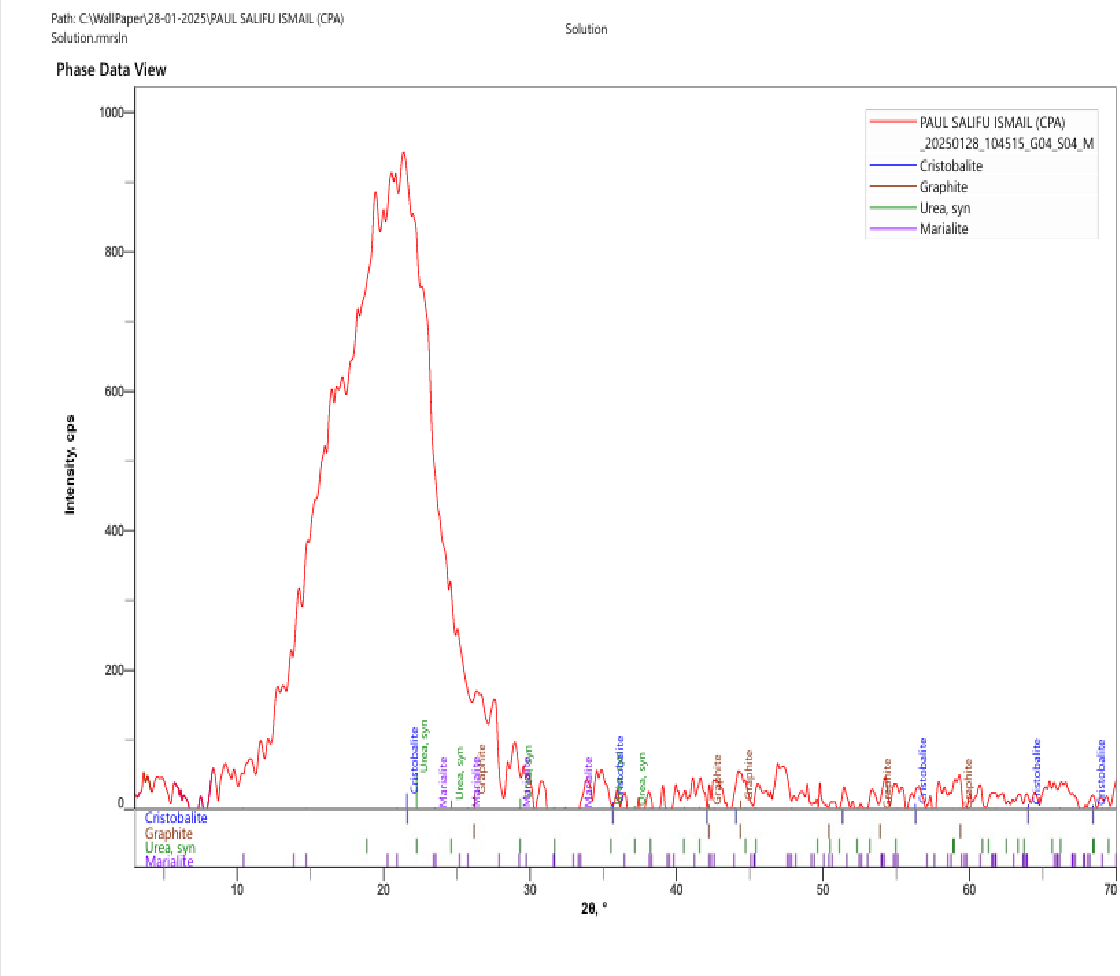

Figure 2: Qualitative Analysis Report of Cassava Peel Ash

Figure 2 presents the qualitative analysis of cassava peel ash with a Figure of merit (3.3). cristobalite. And is within the British standard of natural pozzolan. When compared with graphite, urea, synthesis, marialite, Hence, indicating that cassava peel ash is a suitable pozzolana.

Table 1 presents the oxide composition of the cassava peel ash, the combination of SiO_2, Al_2O_3, Fe_2O_3 is 72.75%. This is in line with ASTMC 618-78 requirement for 70% minimum for pozzolanic materials.

Table 1: Chemical composition of Cement and Cassava Peel Ash

Chemical Composition	Cassava Peel Ash
SiO_2	63.72
Al_2O_3	5.84
Fe_2O_3	3.189
CaO	11.77
MgO	7.94
SO_3	1.79
K_2O	31.75
Na_2O	0.00

CONCLUSION

It is important to note that each natural pozzolan has different effect on cement and concrete properties and can be used in different ratio in a concrete mix. Particularly, the use of natural pozzolans demonstrates lower chloride migration and improve sulfate resistance. The cassava peel ash is deemed suitable for partial replacement of cement in concrete production. Apart from the obvious environmental benefit of supplementary clinker or cement which require a lot of energy and emit higher compressive strength in a later age of cement hydration which continues to increase for a long period of time, they provide long healing properties to the concrete and significantly improve durability which is the main reason for their use

.

REFERENCES

Aguwa, J. I., and Sadiku, S. (2011). Reliability Studies on the Nigerian Ekki Timber as bridge beam in bending under ultimate limit state of loading. *Journal of Civil Engineering and Construction Technology*, 2(11), 253-259.

ASTMC 618-78. Specifications for Coal Fly Ash and Raw or Calcined Natural Pozzolan for Use in Concrete.

Alhaji, B. (2016). Statistical Modelling of Mechanical

properties of Concrete made from Natural Coarse Aggregates from Bida Environ. Unpublished Doctor of Philosophy (PhD) Thesis, Department of Civil Engineering, Federal University of Technology, Minna, Niger State, Nigeria.

BS 8615-1. (2019). Specification for Pozzolanic materials

for use with cement Natural pozzolana and natural calcined pozzolana.

Ofuyatan, O. M., and Olutoge, F. (2014). Assessment of

Strength Properties of Cassava Peel Ash Concrete, *International Journal of Civil Engineering and Technology*, 9(1). 965–974.

Ofuyatan, O., Ede, A., Olofinnade, R., Oyebisi, S.,

Alayande, T., and Ogundipe, J. (2018). Assessment of Strength Properties of Cassava peel Ash-Concrete, *International Journal of Civil Engineering and Technology (IJCIET),* 9(1), 965-974.

Olusola, O., Umoh, A. (2013). Strength characteristics

of periwinkle shell ash blended cement exposed to magnesium Sulphate. *Journal of Civil Engineering science and application,* 15(2).

Salau, M. A., and Olonade, K. A. (2010). Structural

strength characteristics of cement-cassava peel ash, *Civil and Environmental Research*, 2(12).

[62] Farzadkia, M., Akbari, H., Gholami, H. and Darabi, A., "Management of Hospital Waste: A Case Study in Tehran, Iran," *Health Scope,* vol. 7, no. 2, pp. 1-6, 2018.

[63] Rabeie, O. L., Miranzadeh, M. B., Fallah, S. H., Dehqan, S., Moulana, Z., Amouei, A., Mohammadi, A. A., Asgharnia, H. A. and Babaei, M., "Determination of Hospital Waste Composition and Management in Amol City, Iran," *Health Scope,* vol. 1, no. 3, pp. 127-131, 2012.

[64] Olagunju, J. O. and Akinyemi, C., "Hospital Waste Management in Ondo State South West Nigeria," *Environment and Ecology Research,* vol. 3, no. 6, pp. 185-191, 2015.

[65] Yelebe, Z. R., Samuel, J. R. and Yelebe, B. Z., "Biomedical Waste Treatment: A Case Study of Some Selected Hospitals in BayelsaState, South-South, Nigeria," *America Journal of Engineering Research,* vol. 4, no. 6, pp. 160-164, 2015.

[66] Longe, E. O,, "Healthcare Waste Management Status in Lagos State, Nigeria: A Case Study from Selected Healthcare Facilities in Ikorodu and Lagos Metropolis," *Waste Management and Research,* vol. 30, no. 6, pp. 562-571, 2012.

[67] Ahmed, N. O., Gasmelseed, G. A. and Musa, A. E., "Assessment of Medical Solid Waste Management in Khartoum State Hospitals," *Journal of Applied and Industrial Sciences,* vol. 2, no. 4, pp. 201-205, 2014.

[68] Asante, O. B., Yanful, E. and Yaokumah, E. B., "Healthcare Waste Management, its Impact: A Case Study of the Greater Accra Region, Ghana," *International Journal of Scientific and Technology Research,* vol. 3, no. 3, pp. 106-112, 2014.

[69] Amin, R., Gul, R. and Mehrab, A., "Hospital waste management; practices in different hospitals of Distt. Peshawar," *Professional Medical Journal,* vol. 20, no. 6, pp. 988-994, 2013.

[70] Obiora B. Ezeudu, Tochukwu S/ Ezeudu, Uzochukwu C. Ugochukwu." Healthcare Waste Management in Nigeria. Centre for Environmental Management and Control, University of Nigeria, Enugu campus. Enugu 410001.Nigeria. Recycling 2022, 7(6),87

[71] Oteri, J. Bawa, S. Christopher, E.; Nsubuga, P; Dieng, B; Braka, F; Shuaib, F.Pontential for improving routine immuniztion waste managementusing measles vaccination campaign 2017 in Kebbi state, Nigeria. Vaccine 2021, 39, C60 – C65. [Google Scholar]

[72] Suma, Y., Pasukphun, N., Hongtong, A., Keawdunglek, V., Laor, P. and Apidechku, T., "Waste Composition Evaluation for Solid Waste Management Guideline in Highland Rural Tourist Area in Thailand," *Applied Environmental Research,* vol. 41, no. 12, pp. 13-26, 2019.

ACKNOWLEDGEMENTS-

I am eternally grateful to God for all His guidance and protection. I appreciate Him for the wisdom and ability to complete this study.

I must sincerely acknowledge the immense contributions of my late Father Mr Abalaku Anzaya, my Mother Mrs Cecilia Abalaku for their sponsorship which gave birth to achieving this great feat in my educational pursuit. Worthy to mention is Mr Daniel Abalaku and my other siblings who also contributed in other ways.

I cherish the insight that Engr. Prof. T. C. Ogwueleka brought to bear on this work. Iam grateful for the time he spent for continuously reading and correcting my dissertation. I also want to thank Engr. Dr. Samson Balogun for reading through the work and also providing useful suggestions.

My special appreciation goes to Engr. Abdullahi Idris, classmates, friend and well-wishers for their encouragement. I can never forget your care. God bless you.

Investigation of Influence of Geotechnical and Environmental Factors on Road Pavement Failure in North-Central Nigeria: A Review

*[1]Ibrahim, A.; [2]Alhassan, M; [3]Alhaji, M. M.; and [4]Abdulrahman, H. S.
[1] Department of Civil Engineering Federal University of Technology, Minna
[2]Department of Civil Engineering Federal University of Technology, Minna
[3]Department of Civil Engineering Federal University of Technology, Minna
[4]Department of Civil Engineering Federal University of Technology, Minna
*Corresponding author email: agwai2010@gmail.com

ABSTRACT
Pavement failure is a critical issue affecting road infrastructure in Nigeria, particularly in the North-Central region of the country. This review explores the impact of geotechnical and environmental factors on pavement deterioration, emphasizing the challenges posed by poor design, substandard materials, environmental stresses, and inadequate maintenance practices. By integrating insights from existing studies, this paper highlights the need for a comprehensive pavement deterioration model, tailored to the unique conditions of North-Central Nigeria. It also underscores the importance of institutional reforms, advanced analytical techniques, and sustainable maintenance strategies to enhance road performance and longevity in this part of the country.

Keywords: *Climate; Environmental factors; Geotechnical factor; Pavement deterioration; Traffic*

1.0 INTRODUCTION

Road infrastructure is essential for facilitating economic growth and connectivity, yet Nigerian roads face significant challenges due to rapid deterioration. Pavement structures are composed of superimposed layers, designed to work cohesively; however, in Nigeria, defects such as potholes, rutting, corrugation, raveling, flushing, and cracking are prevalent. Contributing factors include poor construction practices, heavy traffic loads, and inadequate maintenance regimes (Okigbo, 2012; Osuolale *et al*., 2012 Mubaraki, 2015; Owoseni, 2019; Abed, 2020). These issues necessitate a systematic approach to road maintenance and the development of predictive models for pavement performance.

Pavement management systems have emerged as a valuable tool for optimizing maintenance and rehabilitation strategies. Accurate prediction of pavement condition and the timing of interventions is crucial for effective resource allocation and informed decision-making. Several studies have explored the development of regression models and machine learning techniques for predicting pavement condition indices and structural capacity (Karballaeezadeh *et al*., 2020; Abed, 2020).

2.0 REVIEWED LITERATURE

Roads remain the most widely used mode of transportation globally due to their convenience in providing door-to-door service and efficiency in short-distance travel. (Alo and Oni, 2018). The ability of road transport to provide access to remote and urban areas alike, makes it indispensable for economic activities, trade, and social interactions. In Nigeria, road transport is the predominant means of mobility, due to the high costs and underdevelopment of alternative transport systems, such as rail and water transport (FMW,1997). However, the increasing number of heavy vehicles and their axle loads contribute significantly to pavement deterioration, thereby escalating maintenance challenges and cost (FMW,1997). Road construction is a capital-intensive investment that requires meticulous planning, design, and execution to ensure long-term functionality. The durability of a pavement depends largely on the quality and integrity of its design, construction standards, and maintenance practices (Alhasan and Mustapha, 2020). Poorly designed pavements are susceptible to early failure, which manifests through various distress indicators, including cracks, potholes, and depressions that compromise ride quality and road safety (Onuoha and Onwuka, 2014). Pavement distress indicators, such as cracks, patches, and rutting, serve as essential markers for evaluating maintenance needs and predicting pavement life cycles (Luo and Prozzi, 2005). The integrity of a pavement depends on its ability to withstand repeated traffic loads, while maintaining essential properties such as skid resistance, surface smoothness and durability ((Khanna and Justo,1997). Inadequate design, overloading, poor construction materials, and environmental factors often lead to defects such as corrugations, rutting, and alligator cracking, which significantly compromise pavement integrity (Hassan, 2006). Pavements are categorized into two main types: flexible and rigid. Flexible pavements distribute loads through aggregate interlock and particle-to-particle contact within the aggregate layers, allowing stress dissipation with depth (Khanna and Justo, 1997). Effective pavement design is crucial to ensuring road longevity and optimal functionality. It involves strategic load distribution, stress management, and material selection, all of which contribute to a durable and sustainable road network (Okigbo, 2012; Gupta, 2004).

2.1 Pavement Deterioration and Structure

Pavement deterioration results from various distresses, including fatigue cracking caused by repeated loading, weathering effects, moisture infiltration, and material disintegration. These factors significantly impact ride quality, road safety, and overall pavement performance (Gary, Smith, & Johnson, 2009) Pavement failures often result from inadequate design specifications, excessive traffic loads beyond design capacity, use of substandard materials, and exposure to extreme environmental conditions. These failures manifest as surface defects, including waves, corrugations, depressions, and rutting, all of which undermine structural integrity and user comfort (Hassan, 2006). Timely intervention through routine maintenance and rehabilitation is necessary to restore pavement serviceability and prevent extensive deterioration.

2.1.1 Pavement Deterioration in Nigeria

Nigerian roads often fail prematurely, with many deteriorating immediately after construction due to environmental stresses, poor drainage, and insufficient oversight. The North-Central region’s climatic conditions, characterized by high rainfall (1077-1787 mm annually) and temperatures ranging from 16 to 35°C, exacerbate these challenges. Combined with heavy traffic, particularly on major routes like Ilorin-Jebba and Mokwa-Bida, these factors significantly contribute to pavement failures (Highway Manual, 2013).

2.2 Geotechnical and Environmental Factors

2.2.1 Geotechnical Factors

Geotechnical properties including soil strength, compaction characteristics, and subgrade stability, play fundamental role in pavement performance. Weak subgrades, characterized by low California Bearing Ratio (CBR) values and high natural moisture content, contribute to pavement instability and accelerated deterioration (Emmanuel *et al*., 2021). Table 1 presents recommended ranges of geotechnical properties for some components of road pavement.

Furthermore, existing pavement deterioration models used in Nigeria are often adapted from standardized global models that do not adequately reflect the region’s unique geotechnical and environmental conditions. These models fail to incorporate key variables such as soil properties, temperature variations, and localized traffic loading patterns, resulting in unreliable predictions of pavement lifespan and maintenance needs (Carvalho *et* al., 2019). The absence of an integrated analytical approach that accounts for these localized conditions has hindered effective road maintenance planning and decision-making.

Pavement condition assessment is crucial for determining appropriate maintenance strategies and ensuring the longevity of road infrastructure (Melyar *et al.*, 2021). In North-Central Nigeria, understanding the specific geotechnical and environmental factors that lead to pavement failure can inform the development of more effective rehabilitation and maintenance programs. Previous studies have emphasized the need to consider both technical and economic factors when evaluating pavement performance, as well as the necessity for standardized performance criteria and deterioration models (Li *et al*., 2013). Various pavement evaluation methods, including the Surface Distress Index (SDI) and Pavement Condition Index (PCI), provide useful insights into road conditions and can guide policy decisions for infrastructure maintenance (Abed, 2020; Melyar *et al*., 2021).

Table 1: Material Properties for Subgrade and Sub base.

Property	Subgrade	Sub base
% passing sieve, No 200 (75µm) (%)	≥35	≥35
Liquid Limit (%)	≤50	≤35
Plastic Index (%)	≤30	≤12
OMC (%)	-7	6-7
MDD (Mg/m^3)	≥1.8	≥1.6
Soaked CBR (%)	≥15	≥30
Unsoaked CBR (%)	≥15	≥80

Source; FMW (2011)

2.2.2 Environmental Factor

Environmental factors such as rainfall intensity, temperature fluctuations, and inadequate drainage systems exacerbate pavement degradation. The North-Central region of Nigeria, which experiences significant variations in climatic conditions, is particularly vulnerable to these influences. Heavy rainfall leads to water infiltration into pavement layers, compromising the structural integrity of the road, while high temperatures contribute to material fatigue and cracking (Olowosulu *et al*., 2020).

Umar *et al*. (2020) stated that environmental conditions, particularly poor drainage and water infiltration, exacerbate pavement deterioration and highlighted that inadequate drainage systems lead to water accumulation, which weakens the subgrade and base layers, resulting in pavement failures. Their study emphasized the importance of proper drainage design and maintenance to mitigate water-related damages. Studies by Akudo *et al*. (2023) have also revealed that seasonal variations, such as heavy rainfall during the wet season, contribute to the weakening of pavement structures. The infiltration of water into pavement layers causes a reduction in shear strength and an increase in pore water pressure, leading to structural failures.

2.3 Pavement Deterioration Models

Predictive models for pavement deterioration are critical for effective maintenance planning. Existing models in Nigeria, are limited in scope, often failing to incorporate critical factors like geotechnical characteristics and environmental influences. This review emphasizes the need for a comprehensive model integrating parameters such as California Bearing Ratio (CBR), natural moisture content, rainfall intensity, and temperature trends. Advanced analytical techniques and mechanistic-empirical approaches offer promising avenues for improving prediction accuracy (Highway Manual, 2013).

2.3.1 Justification for a Comprehensive Model

The unique geotechnical and environmental conditions of North-Central Nigeria demand a tailored pavement deterioration model. Subgrade strength, material properties, and climatic factors significantly influence road performance but are often overlooked in existing models. By addressing these gaps, a comprehensive model can enhance decision-making in road maintenance, reduce costs, and improve infrastructure sustainability.

2.3 Conclusion.

The study identifies weak subgrade soils, poor construction practices, excessive axle loads, and adverse climatic conditions as key causes of pavement failure in North-Central Nigeria. It highlights the inadequacy of existing global pavement deterioration models, which do not account for regional-specific factors like soil properties, climate variations, and traffic patterns. The paper emphasizes the need for a customized model, while reinforcing the importance of geotechnical and environmental factors in pavement performance, it calls for further research on field data, mitigation strategies, and assessment methodologies. A regionally adapted deterioration model is essential for improving road maintenance, reducing costs, and enhancing infrastructure sustainability.

REFERENCES

Abed, M. S. (2020). Development of regression models for predicting pavement condition index from the international roughness index. *Journal of Engineering*, 26(12), 81–94.

Akudo, E. O., Musa, K. O., Akpah, F. A., Ahmed II, J. B., Idowu, S., & Shaibu, M. (2023). Geophysical and Geotechnical Investigations of Failed Sections of Road Pavements in Parts of Northcentral Nigeria. *Communication in Physical Sciences*, 9(3), 256–268.

Alhasan, A., & Mustapha, A. (2020). "Road Construction Standards and Pavement Longevity: A Review." *Journal of Civil Engineering and Infrastructure Development, 12*(4), 78-89.

Alo, O. & Oni, T. (2018). *Transportation Planning and Road Infrastructure Development: A Nigerian Perspective.* Lagos: University Press.

Carvalho, R., Faheem, A., Ferreira, A., & Flintsch, G. (2019). *Pavement deterioration modeling in tropical regions: Challenges and methodologies*. Journal of Transportation Engineering, 145(6), 04019031.

Emmanuel, U. O., Ogbonnaya, I. & Uche, U. B. (2021). An Investigation into the Cause of Road Failure along Sagamu-Papalanto Highway Southwestern Nigeria. *Environmental Disasters*. 8 (3), 1 – 27.

Federal Ministry of Works (FMW). (1997). *Guidelines for Road Design and Maintenance in Nigeria.* Abuja: Government Press

Faisal, R., Ahlan, M., Mutiawati, C., Rozi, M., & Zulherri. (2021). The comparison between the method of Bina Marga and the pavement condition index (PCI) in road damage condition evaluation (case study: Prof. Ali Hasyimi Street, Banda Aceh). *IOP Conference Series: Materials Science and Engineering*, 1087(1), 012028. https://doi.org/10.1088/1757-899X/1087/1/012028

Gary, L., Smith, D., & Johnson, R. (2009). Factors Affecting Pavement Deterioration: A Comprehensive Study. *International Journal of Pavement Engineering, 14*(2), 112-126.

Hassan, M. (2006). "Pavement Defects and Their Implications on Road Safety." *Journal of Transport Engineering, 8*(3), 45-57.

Karballaeezadeh, N., Ghasemzadeh Tehrani, H., Mohammadzadeh Shadmehri, D., & Shamshirband, S. (2020). Estimation of flexible pavement structural capacity using machine learning techniques. *Frontiers of Structural and Civil Engineering*, 14(5), 1083–1096. https://doi.org/10.1007/s11709-020-0654-z

Li, N., Tighe, S., Qian, G., & Liu, Z. (2013). The roles of applied performance indicators in network pavement management—Canadian experience. *International Journal of Pavement Research and Technology*, 6(5), 673–678.

Luo, X. & Prozzi, J. (2005). Pavement Distress Prediction Models for Effective Maintenance Planning. *Journal of Infrastructure Systems, 11*(1), 27-36.

Melyar, M., Isya, M., & Saleh, S. M. (2021). Pavement condition assessment using SDI and PCI method on Geumpang road – West Aceh

Utilization of Bamboo as Reinforcement in Mitigation of In-situ Lateral Earth Pressure in Tropical Residual Soils: Review

*Yahaya, A. M.; [2]Alhaji, M. M.; [3]Alhassan, M. & [4]Adejumo, T. E
[1,2,3,4] Department of Civil Engineering Federal University of Technology, Minna
*Corresponding author email: ymozay@gmail.com

ABSTRACT

The misapplication of concepts developed for transported soils in evaluating in-situ lateral earth pressure in tropical residual soils, coupled with limited data and inaccuracies in traditional measurement techniques, has impeded accurate assessments. These challenges have contributed to failures associated with landslides and slope instability resulting from lateral earth pressure. Bamboo, known for its favorable mechanical properties and sustainability, has gained attention as a cost-effective reinforcement material in geotechnical applications. This review identifies key research gaps in lateral earth pressure evaluation and proposes future directions for optimizing bamboo reinforcement as an innovative technique to mitigate in-situ lateral earth pressure in this understudied soils.

Keywords: *Lateral Erath pressure; Residual soils; Bamboo; Soil reinforcement; In-situ; Residual soils; Transported soils; Pull out capacity*

1 INTRODUCTION

Soil reinforcement is a widely used ground improvement technique that enhances soil stability by incorporating tensile-resistant materials such as metal strips, geosynthetics, and natural fibers (Jaiswal and Chauhan, 2021). Among these materials, bamboo has emerged as a sustainable alternative due to its high strength-to-weight ratio, durability, and environmental benefits.

Research indicates that bamboo reinforcement enhances soil shear strength through frictional interaction, effectively reducing lateral earth pressures (Ahirwar and Mandal, 2018; Samal *et al*., 2023). While synthetic reinforcements are commonly used to counteract lateral earth pressure, their high cost and environmental impact have driven interest in natural alternatives such as bamboo (Fay *et al*., 2012; Pinto, 2003).

Studies on transported soils of temperate regions is extensive, yet a significant knowledge gap persists regarding soils of the tropic. This gap often leads to misapplication of soil mechanics principles, complicating the understanding of their geotechnical behavior (Pitts and Kannan, 1986). In countries like Nigeria, residual soils are prevalent and are formed through intense weathering, resulting in complex heterogeneities that influence their engineering properties (Huat *et al*., 2004; Wesley, 2013).

Geotechnical principles developed for transported soils are seldom been misapplied to these understudied tropical residual soils (Wesley, 2013). Additionally, inaccuracies in traditional measurement methods (Sabouni and Naggar, 2016) and discrepancies between predicted and measured field lateral earth pressure values highlight the need for improved in-situ measurement techniques when dealing with these soils (Alam *et al*., 2021; Hu *et al*., 2022).

To mitigate the risk associated with soil instability resulting from lateral earth pressure, and given bamboo's potential as a reinforcement material (Bang *et al*., 2015), further studies are necessary to evaluate field lateral earth pressure and the utilization of bamboo as reinforcement, across different soils, environments, and excavation conditions to mitigate in-situ lateral earth pressure in the tropical region of the world.

The integration of bamboo as reinforcement in geotechnical applications aligns with sustainable development goals by offering a cost-effective, environmentally friendly solution to mitigate lateral earth pressure in tropical residual soils (Mustapha and Alhassan, 2017; Rochim *et al*., 2020). This study explores bamboo's potential as a reinforcement material, and consequently addressing research gaps in lateral earth pressure measurement, contributing to advancing an innovative reinforcement technique using locally available fibre.

2 LITERATURE REVIEW

2.1 GEOTECHNICAL CHARACTERISTICS AND ENGINEERING BEHAVIOR OF TROPICAL RESIDUAL SOILS

Tropical residual soils form in-situ through prolonged chemical weathering of parent rock under high temperatures and heavy rainfall (Wesley, 2010). Their formation occurs through physical, chemical, and biological mechanisms. In tropical climates, intense weathering produces deep soil profiles with significant mineralogical changes (Gupta, 2011). Biological processes, including root activity and acid production, further contribute to soil formation (Banfield *et al.*, 1999).

Geotechnically, tropical residual soils exhibit variable permeability, compressibility, and shear strength, largely controlled by mineral composition, moisture content, and compaction (Gidigasu, 1976). The upper lateritic hardpan layers offer high shear strength, whereas deeper layers are more compressible. Water content significantly affects soil stability—saturation reduces shear strength and increases landslide risks, while drying induces shrinkage and cracking (Zhang *et al.*, 2017).

Their physical properties, including grain size distribution, bulk density (1.4–1.8 g/cm³), and specific gravity (2.6–2.8), vary with weathering, while moisture content ranges from 16 to 49% (Nixon *et al.*, 1957; Blight, 1997; Huat, 2004).

Studies on decomposed granite soils in Kaduna and residual soils from Nigeria's basement complex regions highlight significant variations in geotechnical behavior with depth, these soils exhibit moderate shear strength, low plasticity, and moderate permeability (Sueoke *et al.*, 1984), whereas residual soils in Ore and Abuja demonstrate different strength characteristics affecting their construction suitability (Idehai *et al.*, 2014). Similarly, southwestern Nigerian residual soils, shaped by alternating wet and dry seasons, display high moisture content, variable plasticity, and specific gravity values between 2.64 and 2.77.

However, further research is needed to assess their long-term performance under varying environmental conditions. The profile and the categories of material type are shown in Figure 1 and the details are presented in Table 1

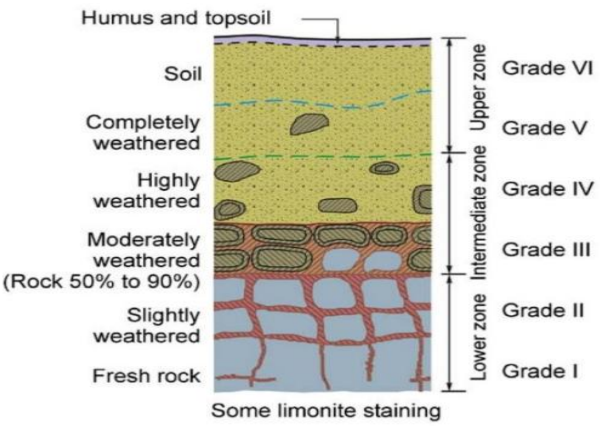

Figure 1: Schematic diagram of typical residual soil profile (Little, 1969).

Anon (1977) proposed a generalized description for a scale to categorize the weathering grades of rock masses, as outlined in Table 1.

Table 1: Weathering Grades of Rock Mass (Anon, 1977)

Term	Description	Grade
Fresh	No visible sign of rock material weathering.	IA
Faintly Weathered	Discoloration on major discontinuity surfaces.	IB
Slightly Weathered	Discoloration indicates weathering of rock material and discontinuity surfaces. All the rock material may be discolored by weathering.	II
Moderately Weathered	Less than half of the rock material is decomposed or disintegrated to a soil. Fresh or discolored rock is present either as a continuous framework or as core stones.	III
Highly Weathered	More than half of the rock material is decomposed or disintegrated to a soil. Fresh or discolored rock is presented either as a discontinuous framework or as core stones.	IV
Completely Weathered	All rock material is decomposed and or disintegrated to soil. The original mass structure is still largely intact.	V
Residual Soil	All rock material is converted to soil. The mass structure and material fabric are destroyed. There is a large change in volume, but the soil has not been significantly transported.	VI

2.2 THEORIES, COEFFICIENTS, AND FUNDAMENTALS OF LATERAL EARTH PRESSURE:

Lateral earth pressure is a fundamental aspect of geotechnical engineering, representing the horizontal force exerted by soil on retaining structures like walls, basements, and foundations. (Das, 2010). Since late 17th century, numerous theories on earth pressure have been proposed by various researchers. Among these; Rankine's theory (which assumes no wall friction) and Coulomb's theory (which incorporates wall friction) are the most widely utilized for calculating active and passive earth pressures. These are collectively referred to as the classical lateral earth pressure theories. Both theories require that the soil mass, or at least a portion of it, be in a state of plastic equilibrium, meaning it is on the verge of failure. In this context, failure is defined as a stress condition that satisfies the Mohr-Coulomb failure criterion.

Lateral earth pressure is classified into three types—*active, passive, and at-rest* (Figure 2), where each is associated with varying soil movement and structural constraints. These classifications underpin the analysis and design of retaining systems, ensuring their resilience against soil forces.

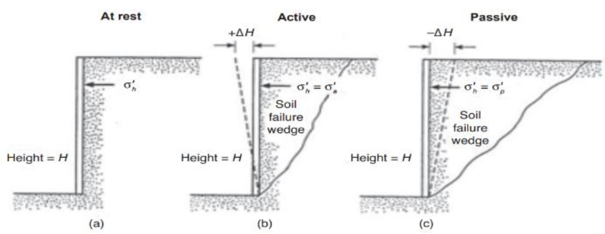

Figure 2: Nature of lateral earth pressure on retaining wall (Das, 2010)

The coefficient of lateral earth pressure (K) represents the ratio of horizontal to vertical stress in soils and is essential in geotechnical engineering. Its value depends on factors such as soil type, density, moisture content, and stress history. The three main states of lateral earth pressure are at-rest (Ko), active (Ka), and passive (Kp), depending on direction of movement of the wall (Figure 3), and with each influenced by different loading conditions.

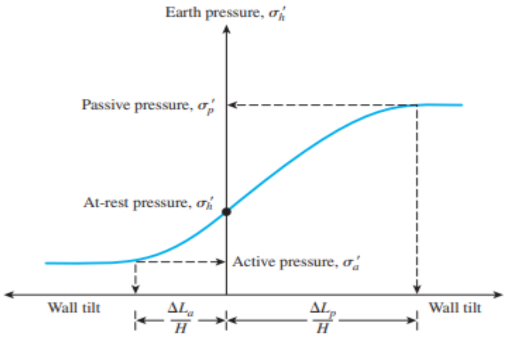

Figure 3: Variation of the magnitude of lateral earth pressure with wall tilt

The following section outlines the equations for different types of lateral earth pressures based on this theory.

The at rest pressure at a depth z is then:

$$po = \mathrm{Ko}\gamma z \tag{1}$$

The total at rest earth pressure (thrust) acting on a wall of height H is:

$$Po = \frac{1}{2}\mathrm{Ko}\gamma H^2 \tag{2}$$

The active earth pressure at a depth z is then:

$$Pa = \mathrm{Ka}\gamma z - 2c\sqrt{ka} \tag{3}$$

$$\mathrm{Ka} = \frac{1-\sin\phi}{1+\sin\phi} \text{ or } \tan^2(45 - \phi/2) \tag{4}$$

is the active earth pressure coefficient.

For Passive Pressure:

$$\sigma p = kp\sigma v + 2c\sqrt{kp} \tag{5}$$

The active earth pressure at a depth z is then:

$$Pp = \mathrm{Kp}\gamma z + 2c\, kp \tag{6}$$

$$\mathrm{Kp} = \frac{1+\sin\phi}{1-\sin\phi} \text{ or } \tan^2(45 + \phi/2) \tag{7}$$

is the active earth pressure coefficient.

The total active earth pressure (thrust) acting on a wall of height H is:

$$Pp = \frac{1}{2}\mathrm{Kp}\gamma H^2 + 2c\, kp\mathrm{H} \tag{8}$$

2.3 In-Situ and Laboratory Techniques for Measuring Lateral Earth Pressure: Implications for Tropical Residual Soil

The primary measurement techniques for the evaluation of lateral earth pressure are categorized into in-situ and laboratory testing methods**,** each providing distinct advantages, depending on soil properties and site conditions (Terzaghi *et al*., 1996).

2.3.1 IN-SITU TESTING METHODS

In-situ methods allow for direct or inferred measurement of lateral earth pressure under real field conditions. One common technique is the use of earth pressure cells**,** which are flat, disc-shaped sensors embedded in soil or structures to measure and transmit pressure data. Strain gauge-based sensors detect deformations in soil or structural elements, providing an estimate of lateral pressure. Optical fiber sensors, such as those utilizing fiber Bragg gratings, offer high-resolution spatial measurements for monitoring geotechnical structures.

2.3.2 LABORATORY TESTING METHODS

Laboratory tests provide controlled conditions to simulate soil behavior and determine lateral earth pressure. The direct shear test evaluates soil shear strength by applying horizontal force to a sample under normal load, helping to estimate lateral resistance. The triaxial compression test assesses soil response under different stress conditions, yielding critical parameters such as cohesion and friction angle.

By selecting appropriate testing methods based on soil conditions and project requirements, engineers can obtain accurate lateral pressure data for designing safe and efficient geotechnical structures. The combination of in-situ and laboratory techniques enhances the understanding of lateral earth pressure distribution and its implications for geotechnical engineering.

While significant progress has been made in studying lateral earth pressure in various soil types, research on tropical residual soils remains limited. Alam *et al.* (2021) examined soil pressure on a temporary trench shoring system in sensitive clay soils, emphasizing discrepancies between measured pressures and theoretical predictions, particularly under surcharge conditions. Their findings suggested that existing analytical models, such as those by Terzaghi and Peck, may underestimate actual pressures, necessitating revisions for improved accuracy. Similarly, Hu *et al*. (2022) investigated lateral earth pressure in finite soils using optical fiber measurements, revealing that Rankine's active earth pressure model overestimates pressure and inaccurately predicts soil failure.

Their study provided an improved theoretical framework for finite soil conditions, enhancing geotechnical design precision.

Massarsch (1975) introduced an innovative pressure cell technique for measuring lateral earth pressure in cohesive soils, demonstrating that measured values were significantly higher than elasticity theory predictions. The study emphasized the influence of pore pressure changes on lateral stress distribution, reinforcing the importance of accurate measurement techniques in soil pressure analysis.

Alkhafaji *et al.* (2022) developed a modified oedometer test for clayey soils, enhancing accuracy in assessing lateral pressure under varying loads. Their findings support the need for improved laboratory techniques to capture the complexities of soil behavior. In the context of tropical residual soils, studies have highlighted the impact of anisotropic soil structures, seasonal moisture variations, and cementation on lateral earth pressure (Wesley, 2010; Blight, 2013; Ali *et al*., 2019).

Generally, while studies have provided critical insights into lateral earth pressure behavior, significant gaps remain, particularly concerning tropical residual soils. There is the need for long-term monitoring and integration of field data with numerical models to enhance predictive accuracy. Addressing these gaps will improve geotechnical design reliability, particularly in regions like Nigeria, where research on in-situ lateral earth pressure variation remains scarce.

2.4 BAMBOO FOR SOIL REINFORCEMENT

Bamboo has emerged as a promising sustainable reinforcement material due to its advantageous physical, mechanical, and durability properties. Rolt (2008) reported that bamboo exhibits tensile strengths ranging from 75–350 MPa, with a typical modulus of elasticity of approximately 18,000 MPa.

Further studies by Nindyawati and Baiq (2016) examined bamboo's role in lightweight concrete, revealing tensile strengths between 133.5–144.2 MPa and pull-out strengths of 0.33–0.48 MPa. Mustapha (2008) demonstrated that embedding circular bamboo specimens in soil increased the applied stress from 226 kN/m² (unreinforced) to 621 kN/m² when three layers of bamboo were used. Similarly, Marto and Uthman (2011) analyzed embankments on soft clay, showing that a Bamboo-Geotextile Composite (BGC) outperformed High Strength Geotextile (HSG) and unreinforced embankments. Their study indicated that the BGC significantly reduced settlement (588 mm compared to 744 mm for the unreinforced case) and minimized lateral movement at depth.

Further research by Aazokhi (2014) on peat soils found that reinforcing with bamboo increased the bearing capacity by 140% with one layer, 224% with two layers, and 279% with three layers. Mustapha and Alhassan (2017) tested Nigerian bamboo in kaolinite clay and observed that using two layers of bamboo reinforcement increased the ultimate bearing capacity from 435 kN/m² to 600 kN/m². These findings highlight bamboo's potential as an eco-friendly and cost-effective reinforcement material for geotechnical applications. Long-term field studies on bamboo's behavior under varying environmental conditions are limited, underscoring the need for further research to optimize its application in geotechnical engineering.

2.5 STUDIES ON THE PULLOUT CAPACITY OF FIBERS

Bamboo reinforcement has emerged as a sustainable approach to improving soil stability and mitigating lateral earth pressure due to its high tensile strength and rough surface texture (Zhang *et al*., 2021). Research has demonstrated that bamboo grids enhance bearing capacity and shear strength by increasing soil cohesion and frictional resistance (Hegde and Sitharam, 2018). Therefore, optimizing design parameters is essential to maximize the benefits of bamboo reinforcement in soil stabilization.

Tardío *et al.* (2018) examined the effectiveness of bamboo-based crib walls in soil bioengineering for erosion control and slope stabilization in Nepal. The research assessed various bamboo species for their mechanical properties, root reinforcement potential, and adaptability to different environmental conditions. Case studies and experimental applications were reviewed to evaluate bamboo's role in slope stabilization. Findings demonstrated that bamboo-based bioengineering techniques significantly enhance slope stability and erosion control.

Bamboo exhibits favorable mechanical properties, with compressive strength ranging from 35–70 N/mm², tensile strength averaging 160 N/mm², shear strength of 6–12 N/mm², and bending strength between 50–150 N/mm². However, its natural durability is limited, lasting only 1–2 years in open-ground conditions due to high starch content, which makes it vulnerable to decay and insect attack. The research recommends further research to optimize bamboo-based design methodologies, enhance structural performance, and assess its long-term effectiveness under diverse climatic and geotechnical conditions. The findings of Tardío *et al.* (2018) reinforce the potential of bamboo as a cost-effective and sustainable material for mitigating in-situ lateral earth pressure.

The study by Cheng *et al*. (2020) examines the bearing characteristics of a Moso bamboo micropile-composite soil nailing (BMCSN) system in soft soil areas in China. The research aims to assess the feasibility of using bamboo micropiles as a sustainable alternative to conventional soil reinforcement techniques, focusing on their load-bearing capacity and deformation behavior. By integrating bamboo micropiles with traditional soil nails. The methodology involves field experiments, laboratory tests, and numerical simulations to analyze the mechanical performance of the BMCSN system. Findings reveals axial force distribution follows an oval pattern, with maximum values **of** 88.5 kN, 105.2 kN, and 127.7 kN from top to bottom, increasing with excavation depth. Pile bending resembles **a** cantilever beam**,** with significant deformation near the foundation pit's bottom, and settlement accelerates when loading reaches a critical level. Earth pressure decreases above the pit bottom during excavation but increases proportionally to loading, with a sudden spike near failure**.**

Numerical simulations align with laboratory results, demonstrating the system's effectiveness in improving bearing capacity. Research reveals BMCSN system significantly improves soil reinforcement by increasing load-bearing capacity and reducing deformation compared to conventional soil nailing alone. The study highlights bamboo's potential as a cost-effective and environmentally friendly reinforcement material but also acknowledges durability concerns. Further research is recommended to refine design parameters, enhance bamboo's resistance to biodegradation, and evaluate long-term performance under varying environmental and loading conditions.

Bang *et al*. (2015) explored the feasibility of using bamboo as an alternative to conventional steel soil nails for excavation and earth-retaining structures in China. It aims to evaluate the mechanical behavior, stability, and overall effectiveness of bamboo soil nailing systems. The research highlights the potential advantages of bamboo, particularly its sustainability, cost-effectiveness, and suitability for soil stabilization applications.

By investigating its performance in retaining structures, the study contributes to the growing interest in eco-friendly reinforcement materials for geotechnical engineering. The findings suggest that bamboo soil nailing systems are a viable and sustainable reinforcement option, offering comparable mechanical performance to steel in certain conditions. The study emphasizes bamboo's economic and environmental benefits, making it a promising alternative for soil stabilization. However, further research is recommended to refine design parameters, optimize bamboo-soil interaction, and evaluate long-term performance under varying soil and environmental conditions to enhance its practical application in geotechnical engineering.

3 CONCLUSION

The utilization of bamboo as a reinforcement material presents a sustainable and cost-effective solution for mitigating in-situ lateral earth pressure in tropical residual soils. Its high tensile strength, frictional resistance, and ability to enhance soil cohesion, shear strength, and bearing capacity make it a viable alternative to synthetic reinforcements, effectively reducing lateral deformations in geotechnical applications. However, existing theoretical models often fail to accurately predict lateral earth pressures, highlighting the need soils modifications that incorporate the unique interaction mechanisms of bamboo-reinforced soils as well as a cost effective method to evaluate in-situ lateral earth pressure in tropical residual.

The integration of both in-situ and laboratory testing methods is crucial for a comprehensive understanding of lateral earth pressure variations over a long period of time. While real-time measurement techniques, such as earth pressure cells and optical fiber sensors, provide valuable insights, cost-effective alternatives must be explored to enhance accessibility in practical engineering applications. Laboratory tests, including triaxial compression and oedometer tests, remain essential for controlled evaluations, complementing field data to refine predictive models.

Future research should focus on optimizing bamboo reinforcement performance under varying soil conditions, moisture levels, and long-term loading scenarios. Additionally, the development of cost-effective evaluation techniques and practical design guidelines based on field and laboratory data will enhance the implementation of bamboo reinforcement in geotechnical engineering. Establishing standardized methodologies for assessing lateral earth pressure in bamboo-reinforced soils will further contribute to the advancement of sustainable reinforcement strategies in tropical regions.

REFERENCES

Ahirwar, S. K., & Mandal, J. N. (2018). Behaviour of bamboo grid-reinforced soil bed. *International Journal of Geotechnical Engineering, 15(7)*, 867–876.

Alam, M., Chaallal, O., & Galy, B. (2020). Protection practices for trench and excavation in Quebec sensitive clay soils: Review of codes, guidelines, and research needs. *Safety Science, 131*, 104918.

Ali, T., Haider, W., Ali, N., & Muhammad, A. (2022). A machine learning architecture replacing heavy instrumented laboratory tests: In application to the pullout capacity of geosynthetic reinforced soils. *Sensors (Basel, Switzerland), 22.*

Alkhafaji, K., Fattah, M., & Al-Recaby, M. (2022). Measurement of the lateral earth pressure coefficient of clayey soils by modified oedometer test. *Engineering and Technology Journal.*

Anon. (1977). The description of rock masses for engineering purposes: Working party report. *Quarterly Journal of Engineering Geology, 10*, 355-388.

Bang, Y., Suh, J., Yang, Y., Yoo, N., & Kim, H. (2015). A study on the application of bamboo soil nailing system through experimental construction. *[Journal Name], 16*, 23–34.

Banfield, J., Barker, W., Welch, S., & Taunton, A. (1999). Biological impact on mineral dissolution: Application of the lichen model to understanding mineral weathering in the rhizosphere. *Proceedings of the National Academy of Sciences of the United States of America, 96(7)*, 3404–3411.

Beyerlein, I., Zhu, Y., & Mahesh, S. (2001). On the influence of fiber shape in bone-shaped short-fiber composites. *Composites Science and Technology, 61*, 1341-1357.

Blight, G. E. (1997). Mechanics of residual soils. *Journal of Geotechnical and Geoenvironmental Engineering, 123(10)*, 946-953.

Cheng, Z., & Deng, Y. (2020). Bearing characteristics of Moso bamboo micropile-composite soil nailing system in soft soil areas. *Advances in Materials*

Science and Engineering, 2020, Article ID 3204285.

Das, B. M. (2010). *Geotechnical engineering handbook.* J. Ross Publishing.

Fay, L., Akin, M., & Shi, X. (2012). Cost-effective and sustainable road slope stabilization and erosion control. *Transportation Research Board eBook.*

Gidigasu, M. D. (1976). *Laterite soil engineering: Pedogenesis and engineering principles.* Elsevier Scientific Publishing Company.

Gupta, A. (1993). The changing geomorphology of the humid tropics. *Geomorphology, 7*, 165-186.

Hegde, A., & Sitharam, T. G. (2018). A state-of-the-art review on soil reinforcement technology using natural plant fiber materials: Past findings, present trends, and future directions. *Materials, 11(4)*, 553.

Hu, H., Yang, F., Tang, H., Zeng, Y., Zhou, J., & Gong, X. (2022). Field study on earth pressure of finite soil considering soil displacement. *Applied Sciences, 12(19)*, 6471.

Huat, B. B. K., See-Sew, G., & Ali, F. H. (2004). *Tropical residual soils engineering.* A.A. Balkema Publishers.

Imoukhuede, M. I., Egai, A. O., & Okiotor, M. E. (2014). Evaluation of the geotechnical properties of residual soils in two different basement complex areas of Nigeria. *British Journal of Applied Science and Technology, 4(36)*, 5000–5013.

Little, A. L. (1969). The engineering classification of residual tropical soils. *Proceedings of the 7th International Conference on Soil Mechanics and Foundation Engineering, 1*, 1-10.

Lu, X., Zhang, Y., & Xu, J. (2006). Influence of fiber morphology in pull-out process of chain-shaped fiber reinforced polymer composites. *Scripta Materialia, 54*, 1617-1621.

Marto, A., & Uthman, B. A. (2011). The potential use of bamboo as green material for soft clay reinforcement system. *Proceedings of the 2011 International Conference on Environment, Science and Engineering, IPCBEE*

Mustapha, A. M. (2008). Physical properties of residual profile found in Minna. *Journal of Technology, 11(3)*, 91-98.

Mustapha, M. A., & Alhassan, M. (2017). Potentials of Nigerian bamboos for use as soil reinforcement. *Nigerian Journal of Technology, 36(2)*, 490-498.

Nindyawati, B. S. U. (2016). Bond strength of bamboo reinforcement in lightweight concrete. *Journal of Civil Engineering and Architecture, 10*, 417-420.

Nixon, I. K., McIntosh, I. K., & Weinert, H. H. (1957). Engineering properties of residual soils. *South African Institute of Civil Engineers.*

Pinto, M. I. M. (2003). Application of geosynthetics for soil reinforcement. *Proceedings of the Institution of Civil Engineers - Ground Improvement, 7(3)*, 103-111.

Pitts, J., & Kannan, R. (1986). Residual soil development on sedimentary rocks of the Jurong Formation in Singapore. *GEOSEA V Proceedings, Geological Society Malaysia, Bulletin 19*, 453-468.

Rochim, A., Latifah, K., & Supriyadi, B. (2020). Characterization of compression and tensile properties of bamboo Jawa (*Gigantochloa atter*) and bamboo Apus (*Gigantochloa apus*) for application as soil reinforcement. *IOP Conference Series: Earth and Environmental Science, 498*, 012040.

Sabouni, A., & El Naggar, M. H. (2016). Analytical solution for lateral earth pressures on cylindrical structures considering ring stiffness. *Canadian Geotechnical Journal, 53(12)*, 1911-1924.

Samal, R., & Sahoo, S. (2023). Static stability analysis of bamboo grid-reinforced slopes. *Proceedings, 56(1)*, 112.

Srivastava, A., Jaiswal, S., & Chauhan, V. B. (2021). Numerical study of geosynthetic-reinforced soil wall subjected to static footing loading. *Progress in Engineering and Technology Innovation, 5(1)*, 1-10.

Sueoka, T., Koyama, S., & Sato, Y. (1984). Geotechnical engineering study on decomposed granite soils in Kaduna District, Nigeria. *Doboku Gakkai Ronbunshu, 1984*, 67-76.

Tardío, G., Mickovski, S. B., Rauch, H. P., Fernandes, J. P., & Acharya, M. S. (2018). The use of bamboo for erosion control and slope stabilization: Soil bioengineering works. In H. P. S. Abdul Khalil (Ed.), *Bamboo - Current and Future Prospects* (pp. 1–20).

Wesley, L. D. (2010). *Residual soils in engineering practice.* John Wiley & Sons.

Wesley, L. D. (2013). Residual soils and the teaching of soil mechanics. *Proceedings of the 18th International Conference on Soil Mechanics and Geotechnical Engineering, Paris*, 3479–3482.

Zhang, X., Kong, L., Yin, S., & Chen, C. (2017). Engineering geology of basaltic residual soil in Leiqiong, southern China. *Engineering Geology, 220*, 196-207.

3rdInternational Civil Engineering Conference (ICEC2024)
Department of Civil Engineering
Federal University of Technology, Minna, Nigeria

Assessment of Index and Compaction Characteristics of Residual Lateritic Soils in Kontagora and Environ for use as Flexible Road Pavement Materials

*Abubakar, I.[1];Alhassan, M.[2];&Adejumo, T. E.[3]
[1] Department of Civil Engineering Federal University of Technology, Minna
[2]Department of Civil Engineering Federal University of Technology, Minna
[3]Department of Civil Engineering Federal University of Technology, Minna
*Corresponding author email:abuuamina86@gmail.com

ABSTRACT

This study assesses the index and compaction characteristics of residual lateritic soils in Kontagora and its surrounding areas for flexible pavement road applications. A total of 20 soil samples were collected, and various tests, including Natural Moisture Content (NMC), specific gravity (Gs), Atterberg limits, and compaction (Maximum Dry Density - MDD and Optimum Moisture Content - OMC), were conducted. The results show significant variation in moisture content (7.87 to 15.4%) and compaction characteristics, with MDD values ranging from 1.83 to 2.13 g/cm³ and OMC between 9.0 and 17.0%. The Atterberg limits indicated Liquid Limits (LL) ranging from 32 to 62%, and Plasticity Index (PI) values between 15.41 and 35.90%, demonstrating a range of plasticity typical for soils from this region. Correlation analysis revealed strong negative correlations between MDD and OMC, and positive correlations between OMC and plasticity indices. The American Association for State Highway and Transportation Officials (AASHTO) classification indicated that most of the soils fall under A-6 and A-7-6 sub-groups, which may not be suitable for use as flexible road pavement materials without modification. The study highlights the need for careful moisture control and possible stabilization methods to enhance the soils' performance in road construction. The findings provide essential insights into the geotechnical properties of residual lateritic soils in the region, informing better decisions in the planning and design of flexible pavements for road infrastructure.

Keywords: *Compaction characteristics; Flexible Pavement; Index Properties;Residual Lateritic Soil.*

1 INTRODUCTION

Assessment of residual lateritic soils is fundamental to road pavement applications, particularly in regions like Kontagora and its environs, where these soils are prevalent. Lateritic soils, commonly found in tropical and subtropical regions, develop through intense weathering of parent rock, resulting in deposits rich in iron and aluminum oxides. Their engineering suitability for flexible pavement construction depends largely on geotechnical properties, which can vary significantly due to differences in formation processes, environmental conditions, and mineralogical composition (Wang and Li, 2015).

For flexible pavement construction, the performance and longevity of the pavement structure are influenced by the quality of materials used in the subgrade and sub-base layers. Properly assessed and utilized, lateritic soils can provide the necessary strength and stability to support traffic loads and mitigate pavement distress (Laldintluanga, 2024). However, their variable index and compaction characteristics necessitate thorough geotechnical evaluation to determine their suitability for road construction. Key parameters such as particle size distribution, Atterberg limits and compaction behavior must be analyzed to ensure compliance with engineering standards. Where deficiencies exist, stabilization techniques may be required to enhance their performance under varying traffic and environmental conditions (Mansur, 2021).

Kontagora, located in Niger State, Nigeria, has substantial lateritic soil deposits that have been widely used in road construction. However, their properties exhibit spatial variability, making a comprehensive assessment essential for effective application in pavement design and construction (Umaru, 2014). Understanding these variations is crucial for optimizing their application and ensuring structural stability. As noted by Winch (2009).The success of civil engineering projects depends on a thorough understanding of material properties and their behavior under field conditions.

This study aims to assess the index and compaction characteristics of residual lateritic soils in Kontagora and its environs, in order to determine their suitability for flexible pavement construction. By evaluating their geotechnical properties, this research provides insights into their engineering behavior and guide best practices for their use in road pavement applications. The findings will contribute to improved material selection and design approaches, ensuring sustainable and durable road infrastructure in the region.

2 MATERIALS AND METHODS

2.1 SOIL SAMPLES COLLECTION

Twenty (20) soil samples used in this study were collected from ten (10) different locations in Kontagora, at a depth ranging from 1.2 to 1.5m below the ground surface The samples were transported to the Civil Engineering laboratory, Federal University of Technology Minna for tests and analysis.

2.2 TESTING METHODOLOGY

To assess the index and compaction characteristics of the residual lateritic soils deposit for pavement application, comprehensive laboratory investigations of the collected soils was conducted. Tests carried out include: Natural Moisture Content, Sieve analysis, Atterberg limits, and Compaction Test. All laboratory tests were in conformity with the guideline as outlined in BS 1377 (1990). Determination of the compaction characteristics was done under the British Standard Heavy (BSH) compactive effort.

3 RESULTS AND DISCUSSION

3.1 NATURAL MOISTURE CONTENT (NMC)

The NMC of residual lateritic soils plays a significant role in their suitability for road pavement applications, as it affects compaction behavior, shear strength, and load-bearing capacity (Ajayi *et al.*, 2024). The NMC values of the soil ranges from 7.87% (K16) to 15.4% (K11), indicating notable variability (Table 2). This variation can be attributed to differences in soil composition, drainage conditions, and environmental factors (Oluyinka and Olubunmi, 2018). Higher moisture content in samples, like K11 (15.4%) and K12 (14.63%) suggests increased clay content or poor drainage, which may reduce soil strength and increase susceptibility to shrink-swell behavior. In contrast, lower moisture content in samples such as K16 (7.87%) and K15 (8.87%) indicates better drainage or coarser soil fractions, which may require moisture conditioning during compaction.

Most samples fall within the 9.0–11.5% range, which is typical for lateritic soils in tropical regions (Oluyinka and Olubunmi, 2018). This range suggests moderate moisture retention, which can support effective compaction and strength development. However, variations in NMC necessitate site-specific compaction efforts to achieve optimal dry density and reduce potential pavement failures. Improperly managed moisture content can lead to excessive settlement, poor load distribution, and premature pavement deterioration, emphasizing the need for precise moisture control in construction practices (Ogaga *et al.*, 2024).

To enhance the performance of these lateritic soils in flexible pavement applications, stabilization techniques such as lime or cement treatment may be required, especially for soils with excessive moisture retention (Jain, 2024). Proper geotechnical assessment and tailored compaction strategies are crucial to optimizing their use as subgrade or sub-base materials. The findings highlight the importance of understanding moisture content variability to ensure durable and stable pavement structures in the region.

3.2 SPECIFIC GRAVITY (GS)

The specific gravity (Gs) values of the soils, as shown on Table 2, range from 2.43 (K10, K14, K15, K17) to 2.67 (K4, K9, K19), indicating moderate variability. Specific gravity is a key index property that reflects the mineralogical composition of soils, with higher values typically associated with iron-rich lateritic soils and lower values indicating the presence of lighter minerals such as quartz or organic matter (Alhaji *et al.*, 2021). Majority of the samples fall within the 2.50–2.63 range, which is typical for lateritic soils and suggests a balance between clay and iron-oxide content (Alhaji *et al.*, 2021). The relatively higher values observed in samples K4, K9, and K19 (2.67) suggest a higher concentration of heavy minerals, which could enhance soil strength, while lower values around 2.43 (K10, K14, K15, K17) may indicate the presence of more weathered or silty materials with lower compaction potential.

The variation in specific gravity has direct implications for soil compaction and stability in road pavement applications. Higher Gs values typically correlate with increased density and load-bearing capacity, making the soil more suitable for subgrade and sub-base layers (Ibrahim *et al.*, 2018). Conversely, soils with lower specific gravity may require stabilization or blending with stronger materials to improve performance under traffic loads (Audu and Okoyido, 2019). Given the observed range, it is essential to consider site-specific assessments and possible treatment methods to optimize the use of these residual lateritic soils in flexible pavement construction.

3.3 PARTICLE SIZE DISTRIBUTION ANALYSIS

Particle size distribution of the residual lateritic soil samples was evaluated against the Nigerian General Specification for Roads and Bridge Works (2016), which stipulates that materials used in road pavement construction should generally have ≤35% fines (Passing No. 200 sieve) for sub-base and subgrade applications to ensure adequate drainage and strength. From the resultson Table 1, several samples, including K1, K2, K6, K7, K8, K13, K14, K19, and K20, have fines content exceeding this threshold, indicating potential susceptibility to poor drainage and reduced shear strength. However, samples such as K3 (22.87%), K9 (35.93%), K10 (32.03%), K11 (11.5%), and K16 (29.27%) fall within the acceptable range, making them more suitable for use in road pavement layers (FMWH, 2016). The variability in fines content suggests that, while some of the soils can be directly utilized, others may require stabilization or blending with coarser materials to meet the standard requirements. Therefore, site-specific assessments and possible modifications are necessary to enhance their performance in road construction.

3.4 CONSISTENCY LIMITS RESULTS

TheAtterberg limits, which include LL, PL, PI, are essential for evaluating the workability and shrink-swell potential of lateritic soils in road pavement applications. According to the Nigerian General Specification for Roads and Bridge Works (1997), lateritic soils used for subgrade and sub-base layers should ideally have LL ≤ 50% and PI between 10 and 30% to ensure adequate strength and minimal deformation under loading. From Table 1, most samples meet the LL requirementexcept for K13 (62.00%), K11 (55.00%), and K14 (55.00%), which suggest a higher clay fraction, leading to increased moisture retention and potential swelling. Similarly, the PI values range from 15.41% (K4) to 35.90% (K13), with K13 exceeding the recommended limit, indicating excessive plasticity, which may result in undesirable deformation under traffic loads (Adewumi *et al.*, 2023).

Most samples exhibit moderate plasticity, making them generally suitable for pavement applications, though variations exist. Samples like K4 (15.41%), K5 (16.96%), and K17 (15.91%) have relatively low plasticity indices, suggesting lower clay content and better stability. Conversely, K13 (35.90%) and K2 (28.07%) have higher PI values, indicating higher cohesion and potential shrinkage issues, which may necessitate stabilization before use. The observed variation in plasticity highlights the need for careful selection and possible improvement measures, such as lime or cement stabilization, to enhance performance in road construction (Audu and Okoyido, 2019). Proper assessment of these soil properties is crucial to ensuring long-term pavement stability and minimizing failures due to excessive moisture sensitivity.

3.5 SOIL SAMPLES CLASSIFICATION

The AASHTO soil classification system categorizes soils based on their suitability for highway subgrade applications, with A-1 to A-3 representing granular materials of high quality and A-4 to A-7 indicating fine-grained soils with increasing plasticity and moisture susceptibility. Majority of the tested samples fall under A-6 and A-7-6 (Table 1), indicating silty or clayey soils with poor drainage and moderate to high compressibility, which may require stabilization for effective use in road construction. Samples K3, K11, and K16 (A-2-7) and K10 (A-2-6) are better suited for pavement applications due to their improved drainage and reduced plasticity, making them preferable for subgrade layers. However, the predominance of A-7-6 soils (e.g., K2, K5, K6, K7, K12, K13, K14, K15, K20) suggests high clay content, requiring stabilization to enhance strength and reduce shrink-swell behavior. Given these classifications, site-specific treatment, including lime or cement stabilization, is essential to improve performance and meet Nigerian pavement construction standards.

3.6 COMPACTION CHARACTERISTICS

MDD and OMC obtained under British Standard Heavy (BSH) compaction energy provide insights into the compaction characteristics and load-bearing capacity of the residual lateritic soils (Table 2). The MDD values range from 1.83 to 2.13 g/cm³, with the highest recorded in K12 (2.13 g/cm³) and K9 (2.10 g/cm³), indicating a well-compacted soil structure with high strength potential. Conversely, K11 (1.83 g/cm³) and K13 (1.83 g/cm³) exhibited the lowest densities, suggesting higher void ratios and potentially lower strength under loading. The variations in MDD are primarily influenced by soil composition, particularly the presence of fines, with higher clay content generally leading to reduced dry density due to increased water retention and lower particle interlock.

The OMC values range from 9.00 to 17.00%, with K13 (17.00%) and K11 (16.70%) requiring the highest moisture for compaction, suggesting high plasticity and fine content. In contrast, K10 (9.00%) and K16 (9.00%) require the least moisture, indicating a coarser soil matrix that achieves maximum density at lower moisture levels. Lateritic soils with higher OMC tend to be more moisture-sensitive, requiring careful moisture control during construction to prevent excessive shrinkage or expansion (Ajayi *et al.*, 2024). The observed range of OMC suggests that some samples, particularly those with OMC above 14%, may require stabilization to optimize their compaction performance and long-term stability in pavement applications.

According to the Nigerian General Specification for Roads and Bridges (1997), lateritic soils intended for use as subgrade materials should have an MDD of at least 1.80 g/cm³, while materials for sub-base and base courses should typically exceed 2.00 g/cm³ (FMWH, 2016). Majority of the soil samples met the subgrade requirement, as all values exceed 1.80 g/cm³. However, only samples such as K5, K8, K9, K10, K12, and K16 surpass 2.00 g/cm³, making them more suitable for sub-base applications. Additionally, the specification recommends an OMC range of 8–18%, meaning all tested soils fall within the acceptable limit. However, the higher OMC values exceeding 14% indicate the presence of fine-grained materials, which may require modification to reduce moisture susceptibility. Overall, while most soils meet the basic subgrade requirements, stabilization may be necessary for improved performance in road pavement layers, particularly for those with lower MDD and higher OMC values.

3.7 COMPACTION CHARACTERISTICS AND INDEX PROPERTIES RELATIONSHIP

The correlation matrix reveals several key relationships between the compaction characteristics and index properties of the residual lateritic soils (Table 3). A strong negative correlation exists between MDD and OMC (-0.7910), which indicates that as the moisture content increases, the compaction density of the soil decreases. This is a common observation in lateritic soils, where higher moisture levels lead to a reduction in particle interlock and overall compaction (Afolayan *et al.*, 2022). Additionally, MDD is negatively correlated with LL (-0.4947) and PI (-0.4797), suggesting that soils with higher plasticity are less compacted. This behavior is due to the ability of finer-grained, high-plasticity soils to retain more water, making them more difficult to compact effectively. On the other hand, the correlation between MDD and NMC is weak (-0.0659), indicating that the natural moisture content does not have a significant influence on the soil's ability to achieve maximum compaction density in this study.

In terms of other index properties, OMC shows a strong positive correlation with both Liquid Limit (0.5984) and Plasticity Index (0.5147), further supporting the idea that soils with higher plasticity require more moisture to achieve optimal compaction. There is also a negative correlation between Sand Content and Liquid Limit (-0.4484) and Plasticity Index (-0.4143), suggesting that soils with higher sand content tend to have lower plasticity and, therefore, require less moisture for compaction. The weak correlation between fine grain content and OMC (0.1187) and MDD (-0.1079) shows that fine-grained content has a more modest effect on compaction behavior. Finally, the strong correlation between PL and PI(0.8209) highlights that these two properties are closely related in defining the plasticity characteristics of the soil. Overall, these correlations emphasize the significant role of fine content and plasticity in determining the compaction characteristics of lateritic soils, with implications for their use in road pavement construction.

TABLE 1: CLASSIFICATION PROPERTIES OF THE SOIL SAMPLES

DESCRIPTION	PASSING NO.10 (%)	PASSING NO.40 (%)	PASSING NO. 200 (%)	LL (%)	PL (%)	PI (%)	AASHTO	COLOUR
K1	87.73	70.57	40.57	33.00	11.51	21.49	A-6	REDDISH
K2	88.43	58.23	41.00	45.00	16.93	28.07	A-7-6	REDDISH
K3	80.63	38.27	22.87	47.00	27.25	19.75	A-2-7	REDDISH
K4	78.93	61.40	38.93	32.00	16.59	15.41	A-6	REDDISH
K5	68.77	50.83	36.97	41.00	24.04	16.96	A-7-6	REDDISH
K6	93.53	75.53	52.97	41.00	19.38	21.62	A-7-6	REDDISH
K7	95.77	76.97	52.63	47.00	21.27	25.73	A-7-6	REDDISH
K8	81.2	51.8	41.73	37.00	14.75	22.25	A-6	REDDISH
K9	74.23	54.07	35.93	36.50	13.07	23.43	A-6	REDDISH
K10	69.97	49.07	32.03	33.00	14.4	18.60	A-2-6	REDDISH
K11	57.73	38.13	11.5	55.00	27.19	27.81	A-2-7	GRAY
K12	61.03	46.9	36.93	47.00	25.96	21.04	A-7-6	GRAY
K13	69.73	57.67	48.4	62.00	26.1	35.90	A-7-6	GRAY
K14	62.1	53.87	43.23	55.00	27.5	27.50	A-7-6	GRAY
K15	61.4	51	39.07	46.00	24.17	21.83	A-7-6	GRAY
K16	63.4	39.7	29.27	46.00	23.74	22.26	A-2-7	GRAY
K17	96.13	67.7	36.23	38.00	22.09	15.91	A-6	GRAY
K18	92.03	65.73	36.1	36.00	16.94	19.06	A-6	GRAY
K19	88.87	73.67	48.6	36.00	13.83	22.17	A-6	GRAY
K20	95.67	74.23	41.4	40.50	20.56	19.94	A-7-6	GRAY

TABLE 2: NATURAL MOISTURE CONTENT, SPECIFIC GRAVITY AND COMPACTION CHARARISTICS OF SOIL SAMPLES

DESCRIPTION	NMC (%)	GS	MDD (G/CC)	OMC (%)
K1	10.40	2.60	2.03	11.00
K2	14.3	2.48	1.92	12.50
K3	9.71	2.57	1.95	12.00
K4	10.7	2.67	1.88	14.50
K5	13.7	2.53	2.02	10.70
K6	9.78	2.5	1.95	15.00
K7	11.18	2.61	1.91	12.50
K8	10.43	2.57	2.00	9.70
K9	10.93	2.67	2.10	10.30
K10	9.71	2.43	2.09	9.00
K11	15.4	2.58	1.83	16.70
K12	14.63	2.57	2.13	13.00
K13	9.79	2.6	1.83	17.00
K14	10.24	2.43	1.89	14.50
K15	8.87	2.43	1.97	13.00
K16	7.87	2.61	2.06	9.00
K17	9.71	2.43	1.99	11.00
K18	10.43	2.63	1.99	12.00
K19	10.25	2.67	1.93	13.00
K20	9.96	2.63	1.91	14.00

TABLE 3: CORRELATION MATRIX FOR MDD, OMC AND INDEX PROPERTIES

	MDD (G/CC)	OMC (%)	NMC (%)	GS	SAND (%)	FINE GRAIN (%)	LL (%)	PL (%)	PI (%)
MDD (G/CC)	1								
OMC (%)	-0.7910	1							
NMC (%)	-0.0659	0.2611	1						
G_S	-0.0712	0.0908	0.0283	1					
SAND (%)	-0.0600	-0.1956	-0.0156	0.1989	1				
FINE GRAIN (%)	-0.1079	0.1187	-0.2838	0.0247	-0.2627	1			
LL (%)	-0.4947	0.5984	0.2019	-0.1830	-0.4484	-0.1020	1		
PL (%)	-0.3208	0.4479	0.1622	-0.2984	-0.3094	-0.3045	0.8209	1	
PI (%)	-0.4797	0.5147	0.1616	0.0193	-0.4143	0.1618	0.7807	0.2841	1

4 CONCLUSION

The assessment of the index and compaction characteristics of the residual lateritic soils in Kontagora and its environs reveals important insights into their suitability for use in flexible pavement road construction. The soils exhibited a range of natural moisture contents, with values between 7.87 and 15.4%, suggesting variability in moisture conditions across the region. This variability, alongside the moderate to strong negative correlation between MD) and OMC, underscores the need for careful moisture control during compaction to achieve optimal pavement performance. The soils' plasticity, indicated by LL and PI, varied considerably, with higher plasticity soils showing reduced compaction densities and suggesting potential challenges in meeting compaction requirements for pavement stability.

Further, the results from the Specific Gravity (Gs), Atterberg limits, and AASHTO classification suggest that the soils primarily fall under A-6 and A-7-6 categories, indicating that they are generally unsuitable for pavement subgrade without modification or stabilization. The correlation analysis further confirmed that moisture content, fine-grained content, and plasticity significantly influence the compaction behavior, with higher plasticity soils requiring stabilization to improve their compaction characteristics. Additionally, the MDD and OMC values of some soil samples did not fully meet the Nigerian General Specification for road and bridges, indicating the necessity for soil stabilization techniques or blending with other materials to enhance their engineering properties for road construction. Therefore, a comprehensive understanding of these geotechnical properties is crucial for designing durable and stable flexible pavements in the region, highlighting the importance of proper soil evaluation and the potential benefits of stabilization methods in enhancing the performance of these soils in road construction.

REFERENCES

Adewumi, R., Sulaiman, W. K., & Shola, A. (2023) Geotechnical Investigation of Pavement Deterioration Along Ikare-Arigidi Road in Ondo State. Civil Engineering Beyond Limits 5(1):1-7. DOI: 10.36937/cebel.2024.1903

Ajayi, O., Konwea, C. I., & Adesanya, O. O. (2024). Engineering Evaluation of Laterite Derived from Sedimentary Rock for Use as Subgrade and Sub-Base Materials. *Indonesian Journal of Earth Sciences*, *4*(2), A833-A833.

Alhaji, M. M., Alhassan, M., Adejumo, T. W., Yahaya, A. M., Saidu, M., & Abdulkadir, H. (2021). Effect of mineralogy on physico-chemical and some geotechnical properties of soils developed over granite, schist, and migmatite gneiss: a case study of Minna, Central Nigeria. *Arabian Journal of Geosciences*, *14*(22), 2343.

Audu, H. A. P., & Okovido, J. O. (2019). Experimental study on effect of lime and cement stabilizers on geotechnical properties of lateritic soil. *International Journal of Engineering Research and Advanced Technology (IJERAT)*, *5*(4), 9-15.

BS 1377 (1990). Methods of tests for Soils for Civil Engineering purposes, London, British Standards Institutions.

FMWH, Federal Ministry of Work and housing General Specification for Roads and Bridge Works (2016)

Ibrahim, A., Alhassan, M., & Alhaji, M. M. (2018). Evaluation of Physical and Geotechnical Characteristics of Residual Profile with Depth of Three Common Basement Complexes in Niger State. Proceeding of the 1st International Civil Engineering Conference, Department of Civil Engineering, Federal University of Technology, Minna, Nigeria.

Jain, P. K. (2024). Enhancing the properties of swelling soils with lime, fly ash, and expanded polystyrene-A review. *Heliyon*, *10*(12).

Laldintluanga, H. (2024). Evaluation of Premature Failure of Flexible Pavement to Hilly Area of Mizoram (Doctoral dissertation, Mizoram University).

Mansur, A.M. (2021). Urbanization Effects on Wetland Ecosystem in Parts of Niger State, Nigeria (Doctoral dissertation). Federal University of Technology, Minna. www.futminna.edu.ng

Ogaga, E., Martins, O., Jimoh, A. O., Okumagbe, A. G., & Emmanuel, A. O. (2024). Assessment of Geotechnical Attributes of Laterites as Sub-base and Sub-Grade Materials in Parts of Northern Anambra Basin Nigeria: Implications for Road Pavement Construction. *Communication in Physical Sciences*, *11*(3).

Oluyinka, L. G., & Olubunmi, O. C. (2018). Geotechnical properties of lateritic soil as subgrade and base material for road construction in Abeokuta, Southwest Nigeria. *International Journal of Advanced Geosciences*, *6*(1), 78-82.

Umaru, A.B. (2014). Influence of Engineering Properties of the Soil, Geological and Hydrometerology Factors On Failures and Distress of Earth dams in North-Eastern Nigeria (Doctoral dissertation). University of Ibadan. www.ui.edu.ng

Wang, H., & Li, M. (2015). Evaluation of effects of variations in aggregate base layer properties on flexible pavement performance. Transportation Research Record, 2524(1), 119-129.

Winch, G. M. (2009). Managing construction projects. John Wiley & Sons.

3rd International Civil Engineering Conference (ICEC 2024)
Department of Civil Engineering
Federal University of Technology, Minna, Nigeria

ASSESSMENT OF WATER TARIFFING FOR MUNICIPAL WATER SUPPLY. A CASE STUDY OF FCT WATER BOARD, ABUJA.

[1]Azih, K.N, [2]Ogwueleka, T.C and [3]Samson, B, [4]Abdullahi, I
1 Department of Civil Engineering, Faculty of Engineering, University of Abuja, – Nigeria.
2Department of Civil Engineering, Faculty of Engineering, University of Abuja, – Nigeria.
3Department of Civil Engineering, Faculty of Engineering, University of Abuja, – Nigeria
4Department of Civil Engineering, Faculty of Engineering, FUT MINNA, – Nigeria
Author to whom correspondence should be address: E-mail azihkenneth@gmail.com;

Abstract: Water tariffing is a crucial aspect of sustainable municipal, Bwari and Gwagwalada water supply, ensuring cost recovery, accessibility, and efficiency in water distribution. This study investigates the effectiveness of the current water tariffing system in the Federal Capital Territory (FCT) Water Board, focusing on revenue generation, affordability, and accessibility. A structured questionnaire was administered to households across selected areas in Abuja, and data were analysed using the Statistical Package for Social Sciences (SPSS) with descriptive statistics and analysis variance (ANOVA). Findings indicate that while the tariff system is considered fair and transparent, concerns persist regarding revenue sufficiency and the affordability of potable water for lower-income households. The study also highlights the need for policy adjustments, increased stakeholder engagement, and alternative water sources to improve service delivery. Recommendations include tariff restructuring, targeted subsidies for vulnerable populations, and enhanced public awareness on water conservation. Implementing these measures will contribute to a more sustainable and equitable water supply system in the FCT.
Key words: Improve service delivery, Tariff restructuring, Targeted subsidies and Water Conservation.

I. INTRODUCTION

Water is one of the most valuable natural resources vital to the existence of any form of life. An adequate supply of safe, clean water is the most important precondition for sustaining human life, for maintaining ecosystems that support all life and for achieving sustainable development [1]. According to [2], about 844 million people globally lack access to clean water supply while 2.5 billion people have no access to adequate sanitation. It was also estimated that 319 million people are without access to improved water supply in sub-Saharan Africa. The consequence of this is that a large proportion of human beings have resorted to the use of potentially harmful sources of water. In this regard, millions of people are locked up in a cycle of poverty and disease. For example, [3] recorded that more than 14,000 people die each day, 11,000 of them being children are under five years of age. [4] inserted that there are more people in the world hospitals today, suffering from water-borne diseases than any other ailment. Some two million children every year – about 6,000 a day – die from such infections. Out of this figure, 1.6 million are from the developing countries [5]. The Water Project [6] concludes that poor water and sanitation conditions cause about 80% of all diseases and more than one-third of all deaths in developing countries. [7] confirmed that with adequate supplies of safe drinking water, the incidence of some illnesses and death could drop by as much as 75%. Emphasizing the importance of water, [8] asserted that safe drinking water is not just a luxury because it's a necessity: it usually creates a distinction between life and death.

Nigeria has 36 State Water Agency (SWAs) and 12 River Basin Development Authorities (RBDAs). Several of these water agencies and authorities still depend on obsolete water equipment. This has been primarily due to reduced management by Government and private sector organization in the water sector compared with other sectors such as oil and gas, energy, housing among others [9]. Despite this, government in recent times has made efforts to ensure provision of water supply in Nigeria, yet only 47 percent of the population had access to an improved water source in 2008. In 2010, 54% had access to safe water in urban households while less than 50% of rural households had access to good portable water in Nigeria as against the National target of 65% [10]. Public water supply is regarded as a measure of access to safe water. However, access to public water supply among Nigerians has decreased extensively from 14% in 1990 to 6% in 2008 [11]. People still depend very much on other sources such as hand-dug wells, ponds, streams, river and shallow wells for their water needs. During the dry season, some of these sources dry up, and households have to invest a substantial amount of their resources to get water of doubtful quality.

In the past most cities and utilities in the world have provided water to their customers almost free of charge because water is considered a necessity, and because water was a relatively cheap and abundant resource. But now with much larger communities requiring service, the only way to ensure that everyone has access to this basic need is to ration it in some way. And perhaps the best way to utilize water to the best and most-valued uses is to put a price on water, and construct appropriate tariff structures to meet different social, political and economic goals in different situations [12].

Drastic changes in water pricing policies are likely to occur in the coming years in particular in the fast-growing urban areas all over the world. Urban populations are growing as never before. While today, 45% of the world population live in urban areas and this population is likely to increase to 61% by 2025 [13].

The Federal Capital Territory Water Board (FCTWB) is the only agency that has the Mandate to supply potable water to the populace of the FCT, it is also responsible for collecting/remitting revenue for water consumed by customer on behalf of the Government.

I Aims

The aim of this research is to evaluate effectiveness and Method of water supply and tariffing for municipal, Gwagwalada, and Bwari water by management in FCT Abuja

II Statement of the Problem

The problem faced by the water sector is that prices and tariffs are almost universally below the full-cost of supply indicating that there are large inefficiencies in the water sector and that water prices need to be raised. The monthly tariff for water from household connections is low and with few connectors and low tariffs, little revenue is generated beyond subsidies provided by the government. Water authorities cannot afford to maintain such systems up to a level that is reliable and so the consumers are forced to supplement the pipe water from traditional sources [14].

In a developing country like Nigeria, tariffs are controversial for many reasons. For policy makers, one objective can be more important than another, which can lead to the adoption of different tariff structures. The impact of such structures on consumers is ambiguous. Despite recent advances, policy makers are not sufficiently informed of the effects on consumer behavior. A lack of competition in the water market implies that policy makers do not have a market test of whether a tariff structure is functioning effectively, with consumers unable to reject a tariff structure that is negatively impacting them [15]. Based on the foregoing, the need to have an effective water tariff structure that will take into consideration consumers' perception is imperative. This study considers effective water tariffing in municipal water supply in FCT Abuja.

IV Justification; -

A water tariff is an important management tool that can be used to assist with the reform of the municipal water and sanitation sector. The pricing of water services is however controversial. There is disagreement over the objectives of water pricing and tariff design. Water pricing decision affect several different objectives or goals of policy makers in conflicting ways. This means that a pricing policy may impact differently on each water tariff objective, thus leading to different conclusions about the attractiveness of the policy. There is also a disagreement on what would happen if different water tariffs were implemented. Inadequate empirical data on how changes in water prices would affect consumers in terms of water use and decision to connect or stay connected is often lacking. There are insufficient numbers of providers of piped water services for consumers to reject inappropriate water tariffs thus giving room for bad ideas to thrive in the water market and policy discussion.

Despite this controversial nature of municipal water pricing and the poor performance of municipal water supply in virtually all Nigeria cities including the Federal Capital Territory Abuja, pricing policy reforms are possible that will benefit almost everyone. The outcome of this study will yield empirical data that will be useful for policy makers and water managers in designing an effective tariff system in the study area.

V. Methodology

This chapter was designed to describe the procedures adopted in this research. The procedures involve the following: research design, population of the study, sample and sampling techniques, instrumentation, validation of the instrument, administration of the instrument and data analysis techniques. This research covered the study that impacts on parameters for effective municipal water tariffing includes interviews, observations, sampling, and data collection of all available information on issues associated with municipal water tariffs in the FCT Water Board.

VI. Study Area

Abuja is located in the central part of Nigeria and it lies at latitude 9.07°N and longitude 7.48°E with an elevation of 840m (2760 ft) above sea level [67]. It has a land area of about 8000km^2, making it almost two and a half times the size of Lagos State. The city is defined by two distinguished rock formations – the Zuma and Aso rock. FCT Abuja has an estimated population of over 3 million people [68]. Its rapid urbanization rate has made it to be the fastest-growing city in Africa [69].
The Abuja area has 2 distinct seasons: the rainy and dry season. Six local area councils were created within the FCT Abuja, namely Abuja municipal, Abaji, Bwari, Kuje, Gwagwalada, and Kwali as depicted in Figure 4. These area councils are further subdivided into districts. It has a total land area of 713 km2 with a tropical climate and predominantly tropical savannah. A total annual rainfall that averages 1100mm per annum has also been recorded for Abuja [70]. Abuja city is located within the Abuja Municipal area and the city is directly administered by the Federal Capital Territory Administration (FCTA). The FCTA has several departments and agencies, supervised by directors, including the Federal Capital Territory Water Board.

The Water supply mains have its sub-station at Bwari Area Council where the treatment plant is located before it is distributed through the pipe network shown in Fig. 3.1 distribution across the Municipal area councils.

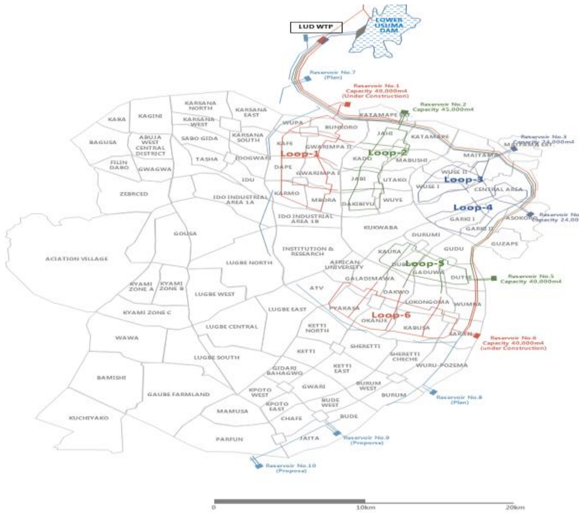

Fig. 3.1 Map Showing Water Distribution network in the study area.

The primary source of water collection comes from the River Usman and being augmented by Gurara River in Kaduna where the Usman Dam is fed to enable optimum production at the peak period. The treatment occurs at the Usman Dam and is distributed to various Tank Locations such as Tank 1 – to Tank 6. The distribution across each tank flow chart is shown in fig 3.2

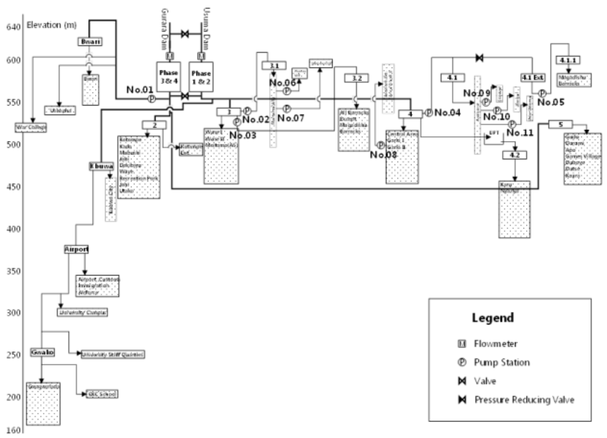

Fig. 3.2 The Tank Flow and Hydraulic Network distribution

VII Data Collection and Sampling Technique

Data were collected with the aid of a structured questionnaire containing open-ended questions. The questionnaire was structured to collect data on:

1. Household Characteristics
2. Economic Characteristics
3. Source Characteristics

Three Hundred (300) questionnaire survey was carried out of which only One Hundred and Fifty (150) respondents who were Household in the selected area for the study responded for proper assessment on the Impact of Parameters for Effective Municipal Water Tariffing, there was an interview of the various heads of Departments of the FCT Water Board administration to obtain accurate information on the management of the Effective Municipal Water Tariffing.

Primary data were collected through questionnaires using random sampling for the health facilities questionnaire. The field survey was inclusive of all areas within research scope.

A Data collection

The following data were required for performing this analysis:

i. FCT Water Board total asset value
ii. Average monthly cost of production
iii. Average monthly Personnel cost
iv. Average monthly Operations and maintenance cost
v. Average Daily Production
vi. Total number of active domestic and commercial customers
vii. Current domestic and commercial tariffs
viii. Questionnaire for consumers' perception of water supply and Tariffing

B. Method of Data Analysis

A simple descriptive test was used to describe the result as obtained from secondary data from the FCT Water board and the fieldwork, with the aid of questionnaires, This analysis is made based on the following assumptions:

i. The government has 30 years to recoup its investment (minimum design life of must engineering infrastructures)

ii. All customers are metered

iii. All customers are billed

iv. The government is not expecting any profit from its investments

v. Wastages are highly minimized (Non-Revenue Water is Zero

This is shown in tabular format and further interpreted using analytical software known as Statistical Package for Social Sciences SPSS) version 22.

ANOVA Model for Water Tariffing System in FCT Water Board

To analyze the differences in respondents' perceptions regarding the water tariffing system managed by the FCT Water Board, a one-way Analysis of Variance (ANOVA) model was applied. This model evaluates whether significant differences exist in perceptions across key variables such as affordability, transparency, sustainability, and service adequacy.

4.3.1 The ANOVA model

$Y_{ij} = \mu + \alpha_i + \varepsilon_{ij}$

where:

- Y_{ij} represents the perception score of respondents concerning a specific aspect of the water tariffing system.
- μ is the overall mean perception score.
- α_i denotes the effect of independent variables such as affordability, revenue generation, and fairness.
- ε_{ij} is the error term, accounting for individual variations in responses.

4.3.2 The hypothesis for the analysis

- **Null Hypothesis (H_0):** There is no significant difference in respondents' perceptions across the various aspects of the water tariffing system in the FCT Water Board.
- **Alternative Hypothesis (H_1):** There is a significant difference in respondents' perceptions across different aspects of the water tariffing system.

The test statistic is calculated using:

$$F = \frac{MS_{between}}{MS_{within}}$$

where:

- $MS_{between}$ represents the mean square variance between groups, capturing differences in perception across key tariffing factors.
- MS_{within} represents the mean square variance within groups, reflecting variability among individual responses.

If the computed F-value is greater than the critical value at a chosen significance level (e.g., 0.05), the null hypothesis is rejected, indicating significant differences in perceptions regarding the FCT Water Board's tariffing system.

Applying this ANOVA model to the study provides insights into how tariffing policies affect different socioeconomic groups. The results will help policymakers understand public concerns regarding affordability, fairness, and sustainability, allowing for informed decision-making to improve water service delivery in Abuja.

Table 4.2.1.4 Analysis of variance (ANOVA)

		Sum of Squares	df	Mean Square	F	Sig
Between People		6.722	9	.747		
Within People	Between Items	73.674	2	36.837	99.636	.000
	Residual	6.655	18	.370		
	Total	80.329	20	4.016		
Total		87.051	29	3.002		

From the table 4.2.1.4 the highly significant **p-value (0.000)** suggests strong differences in how respondents rated the various aspects of water tariffing. The **high F-value (99.636)** indicates that variations between the tested objective questions are much greater than variations within responses, meaning respondents perceived meaningful distinctions among the survey questions. Since the residual variance is relatively low (6.655), the responses are fairly consistent.

Table 4.2.1.5 One-Sample Test

One-Sample Test

	Test Value = 0					
	t	df	Sig. (2-tailed)	Mean Difference	95% Confidence Interval of the Difference Lower	Upper
To evaluate the impact of water tariffing on the affordability and accessibility	14.023	9	.000	3.21500	2.6964	3.7336
To identify potential areas for improvement in current water tariffing system	29.583	9	.000	3.51900	3.2499	3.7881

Result from the table 4.2.1.5 the One-Sample t-test results indicate that respondents strongly believe water tariffing impacts affordability and accessibility (**t = 14.023, p = 0.000, mean = 3.215**) and that the current system needs improvement (**t = 29.583, p = 0.000, mean = 3.519**). Both findings are statistically significant, with confidence intervals excluding zero, confirming that these concerns are widely shared. This suggests that many households struggle with water costs and perceive the tariff system as needing reform. These insights highlight the need for the **FCT Water Board** to review its pricing structure to enhance affordability and service delivery.

C. Results and Discussion

The analysis of the water tariffing system in the FCT Water Board, Abuja, reveals varying perceptions among respondents regarding its effectiveness, affordability, transparency, and impact on households. The demographic breakdown of respondents indicates that the study is male-dominated (57.3%) with a significant proportion of participants aged 50 years and above (47.3%). Most respondents are well-educated, with 31.3% holding MSc degrees and 30.7% being graduates. The income distribution shows that a majority fall within the middle-to-high-income brackets, with 37.3% earning between N150,000 and N250,000 monthly, while only 6.7% earn below N20,000. These factors likely influence perceptions of the water tariffing system.

The effectiveness of the water tariffing system in generating revenue for the FCT Water Board received mixed responses, with a mean score of 2.49 indicating general skepticism. Similarly, the perception of revenue increase over the past year was low, with a mean score of 2.53. However, fairness and reasonableness of the tariff system were rated relatively higher, with a mean of 3.71, suggesting that a significant proportion of respondents believe the charges are justified. In terms of service provision, 33.3% agreed and 29.3% strongly agreed that the FCT Water Board provides adequate services for the current tariff, resulting in a moderate mean score of 3.63.

Transparency and accountability in the tariffing system were perceived positively, with a mean score of 3.73, indicating relative approval. Likewise, communication effectiveness received a mean score of 3.71, suggesting that respondents are generally aware of tariff policies. Flexibility in addressing socioeconomic conditions was rated slightly higher at 3.77, indicating that respondents perceive some level of adaptability in the system. However, concerns were raised about the sufficiency of revenue from tariffing to cover operational costs, as reflected in a low mean score of 2.25, showing a lack of confidence in financial sustainability.

The study also examined the affordability and accessibility of potable water. While the affordability of tariffs was perceived positively (mean = 3.73), many respondents (mean = 2.25) indicated that the current system affects their ability to access potable water. Additionally, the impact of tariffing on household well-being was rated low (mean = 2.13), suggesting that the high cost of water has financial and health implications. Support for low-income households in accessing water was moderately rated (mean = 3.71), and sensitivity to different socioeconomic groups received a similar rating (mean = 3.71), indicating mixed perceptions. Notably, respondents strongly supported alternative water sources for residents who cannot afford the tariff (mean = 3.73) and subsidies for vulnerable populations (mean = 3.01).

Further, the study explored areas for improvement in the water tariffing system. The results showed a strong preference for reviewing and adjusting the system (mean = 3.75) to enhance equity and sustainability. Although transparency and accountability received a moderate score (mean = 3.57), concerns remain regarding the system's responsiveness to different socioeconomic conditions (mean = 3.19). Support for stakeholder engagement in tariff reform was mixed, with a relatively low mean score of 2.58, suggesting a need for increased awareness and participation in policy discussions. However, respondents strongly supported incentives for water conservation (mean = 3.61) and alternative water sources (mean = 3.84), highlighting the demand for sustainable solutions.

Reliability analysis using Cronbach's Alpha (0.705) indicates an acceptable level of internal consistency in the responses, suggesting that the questionnaire was well-structured. The ANOVA test (F = 99.636, p = 0.000) confirms significant differences in how respondents rated various aspects of water tariffing, indicating strong and meaningful distinctions among perceptions. Additionally, the One-Sample t-test results reinforce that respondents widely believe the tariffing system affects affordability and accessibility (t = 14.023, p = 0.000, mean = 3.215) and needs improvement (t = 29.583, p = 0.000, mean = 3.519).

D. Findings

Overall, the study findings highlight critical concerns regarding affordability, accessibility, revenue sufficiency, and equity in the FCT Water Board's tariffing system. While there is moderate satisfaction with fairness, communication, and transparency, the need for a review and adjustment of tariffs, increased stakeholder engagement, and support for vulnerable populations remains evident. These insights provide a strong basis for policy recommendations to ensure a more sustainable and inclusive water tariffing framework in Abuja.

Conclusion

The study underscores the challenges in the water tariffing system in the FCT, particularly in revenue generation, affordability, and accessibility. While respondents acknowledged the fairness and transparency of the current system, concerns about financial sustainability and equitable distribution of water services remain. The findings suggest that adjusting the tariffing structure, engaging stakeholders, and providing support for low-income households are crucial steps toward establishing a more effective and equitable system.

Recommendation

The following recommendation are hereby made:

1. The FCT Water Board should introduce a fairer tariff system that takes household income into account, making water more affordable for low-income earners while ensuring that higher-income households pay rates that match their consumption.
2. To improve revenue collection and financial stability, the board should adopt smart meters, automated billing, and digital payment options, making the process more efficient and reducing financial leakages.
3. It is important to involve the public in decision-making by organizing customer forum, public discussions, and providing easy digital access to tariff policies, ensuring transparency and building trust.
4. Sustainable water management should be encouraged by offering incentives for water-saving technology, and expanding borehole networks to guarantee a reliable water supply for the future.

References

[1] William, J Matthew, Edie Masrsh. Mathewews. Effects of Drought on fish, Across Axes of Space, time and ecological Complexity. June 2003.freshwater Biology. 48(7):1232 – 1253.DOI:10.1046/j.1365-2427.2003.01087x

[2] World Health Organisation (WHO) and United Nations Children's Fund (UNICEF) , "Joint Monitoring Programme," 2023. Progress on WASH in Healthcare facilities 2000-2021 : Special Focus on WASH and Infection Preventionand Control.

[3] WHO and UNICEF Joint Monitoring Programme for water Supply, sanitationand Hygiene. Guidance Note to facilitate Country Consultationon JMP Estimates For Drinking Water Sanitation and Hygiene in Schools, 2021

[4] Brown, M.M., "Clean water – water and waste water management . vol. 10 – 2022. https//DOI.org/10.3389/fenvs.2022.880246

[5] United Nations Children's Fund (UNICEF), "1.6m children die annually due to unclean," The Punch, 2003.

[6] The Water Project, July 2019. [Online]. Available: :http://www.thewaterproject.org/why-water. [Accessed 16 July 2019].

[7] United Nations (UN), "Facts about Water. Fact Sheet, Johannesburg Summit. Johannesburg, South Africa," 16 July 2019. [Online]. Available: www.un.org/jsummit/html/media_. [Accessed 16 July 2019].

[8] Nielson, P., "Global water Shortage and Portable water ssfety; Today's concerv and tomorrow's crisis. http://DOI.org/10.1016/j.envint.2021.106936

[9] Adoga, O., "Nigerian Water Policy and Law: A Need for Global Compliance," 16 July 2019. [Online]. Available: :http://www.martindale.com/natural-resources-law/article-240640.html. [Accessed 16 July 2019].

[10] United Nations Development Programme (UNDP), "UN-Water Global analysis and assessment of Sanitation and Drinking – Water (GLAAS) 2022 report

[11] World Health Organisation (WHO) and United Nations Children's Fund Joint Monitoring Programme (UNICEF JMP),

"Progress on Sanitation and Drinking Wate," Geneva, 2010.

[12] Rogers, P., Silva, R. and Bhatia, R., "Water is an economic good: How to use prices to promote equity, efficiency, and sustainability," Water Policy, vol. 4, pp. 1-17, 2002.

[13] GWP, ""Towards water security - A framework for action" Stockkolm Global Water Partnership," 2000.

[14] C.J Seago., "International Benchmarking of Leakage from Water Reticulation Systems," 2005.

[15] Whittington, D., Boland, J. and Foster, V., "Water Tariffs and Subsidies in South Asia: Understanding the Basics," in Water and Sanitation Program Paper 2. World Bank, Washington DC, 2002.

[16] Fasakin, J.O., "Willingness to pay for the services of commercial motorcycle in akure, Nigeria," Cities, vol. 17, pp. 447-452, 2000.

[17] Pean, L., "AGETIP: Private sector management takes roots in Africa," The Urban Age, vol. 1, no. 3, pp. 9-10, 1993.

[18] Arimah, B.C., " Market segmentation and the impact of landfills on residential property values: empirical evidence from an African city," Netherland Journal of Housing, Building and Environment, vol. 10, no. 2, pp. 157-171, 1995.

[19] Seregeldin ,Ismail. World Bank, "Towards Sustainable Management of Water Resources," World Bank Publications, Washington, 2021. https://documents.worldbank.org/curated/en/382391468173052349

[20] Kalbermatten, J.M., " Should we pay for water? And if so, How?," in Urban Edge, Winter, 1999, pp. 14-15.

[21] Cairncross, S., "Water Supply and the Urban Poor," in The Poor Die Young, London, Earthscan, 1990, pp. 109-126.

[22] World Bank, "Defining and Environmental Development Strategy for the Niger Delta," vol. 1, World Bank, 1995, pp. 1-144.

[23] Immandoust, S.B. and Gadan, S.N., "Are people willing to pay for river water quality, contingent valuation," International Journal of Environment, Science and Technology, vol. 4, no. 3, pp. 401-408., 2007.

[24] Branka, T. and Kelly, G., "Contingent valuation willingness to pay with respect to geographically nested sample: a case study of Alaskan Steller sea lion, W–133," in Western Regional Project Technical Meeting Proceedings, 2001.

[25] Littlefair, K., " Willingness to pay for water at the household level: individual financial responsibility for water consumption," University of London, London, 1998.

[26] Altaf, M.A. and Hughes, J.A., "Measuring the demand for improved urban sanitation services: Results of a contingent valuation study in Ouagadougou, Burkina Faso," Urban Studies, vol. 31, no. 4, pp. 509-551, 1994.

[27] Rogerson, C., "Willingness to pay for water: the international debates," Water SA, vol. 22, no. 4, pp. 73-80, 1996.

[28] Adenike, A.A. and Titus, B.O., "Determinants of Willingness to Pay for Improved Water Supply in Osogbo Metropolis Osun State, Nigeria," Research Journal of Social Sciences, vol. 4, pp. 1-6, 2009.

[29] Dauda, S.A., Yacob, M.R. and Radam, A., "Household’s willingness to pay for heterogeneous attributes of drinking water quality and services improvement: an application of choice experiment," Appl Water Sci , vol. 5, pp. 253-259, 2015.

[30] Coster, A.S. and Otufale, G.A., "Households' Water-Use Demand and Willingness to Pay for Improved water services in Ijebu Ode Local Government area, Ogun State, Nigeria," Journal of Environment and Earth Science, vol. 4, no. 17, pp. 1-10., 2014.

[31] Aribigbola, A. and Omosulu, S.B., "Water Supply Situation in Owo: Implication for Sustainable City development in Nigeria," in The City in Nigeria: Perspective, Issues Challenges and Strategies, Ile-Ife, 2002.

[32] Olugbamila, O.B. and Ogunyemi, O.F., "Assessment of Water supply situation in Owo, Ondo State, Nigeria: Implications for the attainment of the Millennium Development Goal," International Journal of Scientific and Research, vol. 5, no. 9, pp. 1-6., 2015.

3rd International Civil Engineering Conference (ICEC 2024)
Department of Civil Engineering
Federal University of Technology, Minna, Nigeria

AN OVERVIEW: INVESTIGATING THE EFFECT OF COCONUT FIBRE ASH ON THE FLEXURAL STRENGTH OF RE-VIBRATED CONCRETE BEAM

*Oglekwu, F.O [1]; Auta, S. M [2]; & James, O. J [3].
[1,2,3] Department of Civil Engineering, Federal University of Technology Minna, Niger State
*Corresponding author: Email: francisoglekwu@gmail.com

ABSTRACT
Previous studies have reported findings about the possibilities of using coconut fibre ash (CFA) to partially replace cement in the production of concrete. Based on the outcome of previous findings, there is a need for further research to determine the degree of the suitability of using the CFA in re-vibrated concrete beam. This becomes inevitable because some studies reported positive contribution to the compressive strength of concrete with less emphasis on the flexural strength of re-vibrated concrete beam. This study highlights the chemical and physical properties of CFA as reported by previous studies and compared these properties to those of cement. The properties of fresh and hardened concrete that were produced using CFA as partial replacement for cement, as reported in previous works are presented and discussed in this study. Based on the outcome of this study, it has been found that, CFA is a good pozzolona due to its high percentage of silicon oxide, it is readily available and there is a need for large volume consumption of the agricultural waste material. Re-vibrating concrete reduces voids, increases density and strength of the concrete which tends to improves both the compressive and flexural strength of re-vibrated concrete beam.

Keywords: *Concrete properties; Coconut fibre ash; Pozzolana; Re-vibrated concrete; Flexural strength*

1 INTRODUCTION

The most used engineering material for construction in the world today is concrete. Conventional concrete manufacture substantially makes a significant to CO_2 emissions because of the high energy needed to generate Portland cement, the main binder of concrete (Kahan *et al*. 2023; Althoey *et al*. 2023). Recent searches have stated that roughly 0.9 tonnes of CO_2 are released while manufacturing 1 ton of Portland cement, which accounts for approximately 5% of the human-induced CO_2 emissions globally (Althoey *et al*. 2023; Nassar *et al*. 2022). Therefore, in recent years, a vast majority of researchers have searched for sustainable resources for environmentally friendly cement and concrete, to decrease CO_2 emissions. Due to a substantial surge in the demand for sustainable concrete, which is one of the most extensively utilized construction materials globally (Althoey *et al*. 2023).

The over-reliance on the usage of concrete produced from cement (as a binder) for buildings have kept their cost high and this has prevented low-income earners in developing nations of the world from building houses for their local dwellers that make up the greater percentage of their population and most often are agriculturally dependent (Aguwa *et al*.,2016). As a result of the high cost of acquiring the required materials to construct functional and stable houses, a greater proportion of the country's population cannot afford the cost (Aguwa,2009). An easy way out of this, points at suitable means of replacing a proportion of cement with cheap and easily obtainable pozzolanic materials. In (ASTM C618,2012) defined pozzolana as "siliceous or siliceous and aluminous material which in themselves have little or no cementitious properties but in finely divided form and the presence of moisture, react with calcium hydroxide which is liberated during the hydration of Portland cement at ordinary temperatures to form compounds possessing cementitious properties". The global increase in human population has triggered an increase in the demand for scarce and expensive engineering materials for building and engineering infrastructure construction.

Concrete according to (Anzar,2015), is that pourable composite mix of cement, fine aggregates, coarse aggregates and water in the right proportion that hardens into a super-strong material for building. When concrete is re-vibrated, it momentarily liquefies again. The primary chemical process that occurs in the first 120 minutes after the concrete is placed, is the formation of calcium hydroxide, which typically makes up 15 to 25 percent of ordinary Portland cement concrete. The other major product of hydration is calcium silicate hydrate, which usually constitutes about 50% of OPC concrete which gives the concrete its hardness and durability. Initial vibration of concrete may not eliminate defects such as honeycomb and voids causing a reduction in strength and performance. But re-vibration can eliminate such defects (honeycomb and voids) and thereby increasing bond, improving concrete quality, better impermeability, reduction in shrinkage and creep, increasing the compressive strength of the concrete, reduction in surface and other voids as well as cracks in fresh concrete and so on (Krishna et al.,2008). According to (Auta *et al*., 2015) RHA is not recommended to be used as partial replacement for cement in concrete when re-vibration is not envisaged as it results in concrete having very low compressive strength at all ages of curing. An average duration of 90 minutes is recommended for re-vibration of concrete with 20 % RHA as cement replacement for optimal or higher compressive strength. An investigation was conducted on the usage of wood waste ash as a partial replacement for cement in the production of mortar and structural grade concrete, assessment of the fresh concrete properties of self-compacting concrete containing SDA, and it was evident that ash from timber waste was a material capable of replacing cement (Elinwa *et al*.,2008).

Much work has not been reported on the behavior of re-vibrated concrete beam produced from coconut fibre ash (CFA) as a partial replacement for cement. As such, this study aims to examine the effect of CFA on flexural strength of re-vibrated concrete beam made from 0%, 5, 10, 15, and 20% replacements of OPC.

2 PHYSICAL PROPERTIES OF COCONUT FIBRES

Coconut fibre, also known as coir, is derived from the fibrous husk of the coconut plant and is used in the production of coir. Coconut fibres are mostly brown in color with varying lengths and diameters. More-over, other properties such as tensile strength and modulus of elasticity vary depending on the source and usage. A different researcher reported different physical properties of coconut fibre. The details of the physical properties of fibres as per past researchers (Naveen *et al*., 2013: Tensile strength is 175Mpa, water absorption 130 to 180 %, elongation 30 %; Amadi *et al*., 2013: Length 25mm, diameter 0.25mm, aspect ratio 100, tensile strength 405Mpa; Bai *et al*., 2019: Length 18mm, diameter 0.1 to 0.5mm, density 0.67 to 10g/cm^3; Ramakrishna *et al.*, 2005: Length 8 to 10mm, diameter 0.5 to 1.0mm, tensile strength 15 to 327Mpa; Ahmad *et al*., 2021: Length 20 to 30mm, diameter 0.32mm, tensile strength 176MPa, modulus 22.4GPa.

3 FRESH PROPERTIES

Concrete workability is a term that relates to how easily mixed concrete can be placed, compacted, and finished while retaining it homogeneity to the greatest extent possible. Unworkable concrete is one that cannot be easily worked. In unworkable, the cement paste is not sufficiently lubricated and it does not adhere to the aggregates correctly, resulting in significant aggregate segregation. Maintaining the homogeneity of an unworkable concrete mix is very difficult, and compaction of concrete requires a significant amount of work, which has a negative impact on the mechanical and durability performance of concrete.

According to one study, the value of slump flow decreased when the dose of coconut fibres was raised. The increased surface area of coconut fibres requires more water to cover, resulting in less free water for flowability. Moreover, CFA increased internal friction among concrete elements, necessitating more cement paste (Ahmad *et al*., 2020). Adding 0.25 percent coir fibre (by weight of aggregate) reduced slump to 50mm. The slumps of the following variants indicate decreasing values with increasing coir fibre content. This propensity is due to the coir fibres surface shape and physical qualities (Rumbayan *et al*.,2019). According to one study, coir fibres have hydrophilic surfaces and hence repel water (Ahmad *et al*.,2021). In similar manner, several studies have shown that the slump value decreases when coconut fibre is included (Ali *et al*., 2012; Pierad *et al*., 2013; Zhang *et al*., 2019).

According to one study, fresh density rose as the proportion of coconut fibre increased upto 2.0 percent, after which it decreased when compared to reference concrete. Coconut fibre at a dose of 2.0 percent exhibits the highest fresh density when compared to reference concrete (0 percent addition of coconut fibres). However, the fresh density was lowered with the addition of coconut fibres, with a minimum fresh density of 3.0 percent when compared to other coconut fibres reinforced concrete. The increase in fresh density of concrete reinforced with coconut fibre is related to crack prevention since CFA reinforced concrete has fewer plastic shrinkage voids and produces denser concrete (Althoey,2021). However, with the 4 percent addition of CFA, compaction becomes problematic, resulting in porous concrete and lower fresh density. A study claims that adding 1.5 percent CFA by volume to concrete increases density by 15% as compared to the reference concrete (Tadepalli et al., 2013). In contrast, when the fibre content of a specimens increased, the density of the specimens dropped (Ahmad et al., 2020). Due to the fact that fibres are light, their addition to concrete causes cavities in the matrix, which reduces the density of the concrete. As a consequence of the inclusion of low-density coconut fibres, a phenomenon is known as the “filled void effect” occurs, which decreases the density of the concrete when compared to palin concrete (Syed et al., 2020).

Density is an important factor that influences the flowability of concrete. A lack of workability leads to void in occupied space and reduced density (Ramli *et al.*,2023).

4 TREATMENT OF COCONUT FIBRES

To investigate the durability of coconut fibre, several treatments were carried out on the material. For the first minute, each fibre was soaked in an adherent solution (deionized water or natural latex) to ensure that it adhered to the other fibres. During this process, the adherent solution surrounds the coconut fibre, forming bonding layers between the two materials. A coating agent was then applied, which consisted of pozzolanic materials (silica fume or metakaolin). Pozzolans are attracted to the coconut fibre by the adhering solution in which they are dissolved. The production of "chicken fingers" is comparable to the process used in the development of this novel medicine (da Silva *et al.*, 2022).

Using a latex polymer film and a pozzolan layer, the coconut fibre treatment was created to increase the flexural strength and durability of cement-based composites. The performance of the sample treated with silica fume and natural latex was 42.2 percent better than the performance of the sample without any treatment. When fibre samples were subjected to degradation tests, the mass conservation rate increased as a consequence of this treatment (silica fume and natural latex). This treatment resulted in an enhancement in the retention of fibre against the degradation process, according to the microstructural examination of the treated fibres isolated from CF. This treatment (silica fume and natural latex) has the potential to be a viable alternative to the use of CF in the creation of novel cementitious composite materials that have appropriate performance and long-term durability. The compressive and flexural strengths of the structures increased by up to 13 percent and 9 percent, respectively, according to the testing data. However, in terms of durability, the chloride penetration, intrinsic permeability, and carbonation depth increased with CF. The authors propose that the CF could be treated before being used in concrete to ensure that is protected against deterioration (Ramli *et al.,2022).* Coconut fibres were immersed in NaOH solutions with concentration ranging from 2 to 10% for four weeks. The authors discovered that the tensile strength reduced as the concentration of NaOH increased, which they attributed to the fibres becoming more fragile (Wang *et al.*, 2021).

5 MECHANICAL PROPERTIES

5.1 Compressive Strength: is a material's or

structure's capacity to bear loads without cracking or deflection. Compression shrinks a material's size. Concrete compressive strength gives an indication of the concrete properties. This single test determines whether or not concrete was correctly performed. In commercial or industrial construction, concrete's compressive strength ranges from 15N/mm2 to 30N/mm2. Compressive strength is tested on a cube or a cylinder. The American Society of Testing Materials established ASTM C39/C39 for compressive strength testing of cylindrical concrete specimen.

Research also found that fibres increased concrete's compressive strength up to a certain point before decreasing owing to a lack of workability (Ahmad et al., 2020). Even at a larger dosage, the compressive strength of concrete is lower to that of reference concrete. The fibre reinforcement's confinement on the specimen has a favorable impact on compressive strength. Compressive results in lateral expansion, which is limited by the coconut fibres (CF), resulting in increased compressive strength. Because of their strength, the fibres can sustain strain and shear (Ahmad et al., 2020). Compaction becomes problematic at larger dose (more than 2.0%) owing to a lack of workability, resulting in decreased strength. A study reported that in compression to reference concrete, 1.5 percent of the fibres enhanced compressive strength by over 15% (Tadapalli et al.,2013). At 1.0% by volume, fibres significantly improve the mechanical performance of concrete at both the initial and later ages. The greatest 28-day strength increase was found to be 29.15% (Usman et al.,2020). As a result, coconut fibre has an ideal limit. The experiments indicate that the best dosage of coconut fibre for strength is 2.0% by weight of cement (Ahmad *et al*.,2021).

A study indicates that the optimal quantity of coir fibre in concrete is 0.25%, which results in a 19% increase in 28-day compressive strength (Rumbayan *et al*., 2019). However, the optimum dose of fibres varies depending on the type of fibre, the physical aspect such as length and diameter, as well as the concrete mix design and the water-to-binder ratio. A study reported that in CF of 50 mm to 75 mm long, the compressive strength decreases with the increase in fibre content. The decrease in compressive strength could be attributed to the decreased workability of fresh concrete caused by the increased content and length of fibres, as well as the lack of proper compaction during specimen casting, resulting in the formation of air voids. It might be possible due to the dilution of the cement matrix/hardened cement paste caused by the addition of fibres (Ahmad *et al*.,2020).

5.2 Flexural Strength: Flexural strength is the capability of an unreinforced concrete beam or reinforced concrete beam to withstand bending failure. According to ASTM standards, it is by loading 150mm by 150mm concrete beam with a span length that is at least three times the depth (ASTM,2010).

Research found that, when the percentage of coconut fibre is raised by the weight of cement up to 2.0%, the flexure strength improves, but subsequently drops when the percentage of CF is further increased as compared to a reference or standard concrete (Kikuchi et al.,2020).

The inclusion of CF at a rate of 2.0% resulted in the greatest possible flexure strength. After the addition of CF at a rate beyond 2.0%, the flexure strength gradually reduced. The flexural strength of all coconut fibre reinforced concrete is much higher than that of ordinary concrete. Coconut fibre increase flexural capacity by inhibiting the development of fracture. Because of the interfacial between the concrete components and the coconut fibres, the load is quickly transmitted to the coconut fibres. The breaking of cracks is prevented by coconut fibres, which allow the crack to flow around the fibres and transfer the stress. The coconut fibres and concrete matrix resist the load as a whole, resulting in increased flexural strength for the structure (Usman *et al*.,2020). The compaction process becomes more complicated as the quantity of fibre in the mixture increases. Using higher dosage, such as 3.0%, the workability of the concrete worsened, causing porous concrete and drop in flexural strength. According to other findings, the best quantity of CF IS 0.25%, which results in 19 % increase in 28-day flexural capacity (Ali *et al*.,2019). Table 1 shows a summary of the flexural strength of concrete with different doses of CF.

Table 1. Summary of mechanical performance of concrete with coconut fibres.

Author	**Percentage of Replacement**	**Compressive Strength (MPa)**	**Flexural Strength (MPa)**
Abbas *et al.*, (2021)	0 0.1 0.2 0.3 0.4 0.5 0.6	36 38 38 36.5 35 33.5 30	4.8 5.2 5.4 4.98 4.85 4.75 4.50
Srinivas *et al.*, (2021)	0 0.5 1 1.5	8.0 8.66 9.93 4.75	6.33 3.23 3.82 2.80
Kumar *et al.*, (2020)	0 CF: 5% CF ASH: 15%	22.3 19.53 34.87	6.73 5.27 5.33
Khan *et al.*, (2020)	Silica Fume: CF 0:2 5:2 10:2 15:2 20:2	27.2 27.5 28.8 32.4 26.6	6.2 6.6 7.8 8.3 4.7
Raj *et al.*, (2020)	0 0.3 0.4 0.5	9.5 11.5 8.0 7.5	1.4 1.7 1.2 1.1
Wongsa *et al.*, (2020)	0 0.5 0.75 1	31 33 28 25	3.2 5.3 6.2 6.7
Krishna *et al.*, (2018)	0 0.5 1 1.5 2	37.5 35 47.5 51 41.75	-

6 DURABILITY

6.1 Water Absorption

The water absorption test analyses the rate of water absorption of the outer and inner concrete surface. The test includes measuring the increase in mass of concrete samples caused by water absorption as a function of the time when the specimen is exposed to water. Higher water absorption results in less durability since water contains various hazardous compounds that seeps into the concrete, causing concrete breakdown and resulting in reduced durability.

Research revealed that with the addition of CF, the amount of water absorbed increased (Abdullah *et al*., 2011). The effects of fibre volume fraction on heat conductivity and water absorption were not significant (Wongsa *et al*., 2020). A study concluded that the water absorption decreases as the percentage of coconut increase up to 2.0% addition of CF, and decrease occurs gradually, with maximum water absorption observed at 0 % substitution and minimum water absorption observed at 2.0% addition of CF (Ahmad *et al*.,2021). It has also been reported that the inclusion of CF would result in an increase in the tensile strain characteristics of concrete, which would limit the creation and development of early fractures in the concrete (Huang *et al*.,2011). In other words, increasing concrete density reduces water absorption. Due to lack of workability, greater dosage (above 2.0%) resulted in less dense concrete. Because of the increased porosity of the coconut coir fracture mortar compared to the control mortar, according to one research, more water absorption was noticed in CF reinforced concrete than the control mortar. The porous structure of the cement blocks, as well as the presence of an interfacial zone surrounding the particles, are the most important elements influencing water absorption. The findings reveal that as compared to the control mortar; the coconut coir mortar noticed water absorption considerably in the greater amount (Sathiparan *et al*.,2017).

6.2. Permeability

The water absorption by immersion provides an estimate of the total pore volume of the concrete, but it provides no information on the permeability of the concrete, which is more essential in terms of long-term performance.

It is discovered that the permeability of concrete increased with the addition of CF. The continuous pore structure of the specimen has a significant influence on the permeability of the specimen (Hearn et al.,1994). Generally speaking, the wider the width of continuous pores, the more permeable the concrete would be considered to be. It is possible to produce continuous holes under a variety of situations, some of which include the capillary network formed by hydration, the interfacial transition zone between paste and aggregate, the production of micro-cracks, and others (Hearn *et al*.,2021). Not only the interfacial zones between the aggregate and the paste but there will also be a gap between the fibre and the matrix (Savastano and Agopyan, 1999). However, the authors hypothesized that there is another mechanism at work that is also responsible for the disparity. This gap may be linked to the strong water absorption characteristics of the coconut fibre, which is responsible for its existence. During the mixing process, a water film is formed around the fibre's immediate surroundings. The absorption capabilities of the film, as well as the osmosis pressure, will keep the film in place and cause the fibre to inflate. As the hydration process advances, the formation of the permanent shell structure starts to take place. As water is consumed by cement hydration and evaporation, the water film gradually vanishes, finally creating a gap between the fibre/matrix interfacial zone of the composite. When the fibre shrinks back to its former shape after inflating as a result of the drying process, the gap widens even further, creating a larger opening. According to the findings of a study, nitrogen gas travels through the natural fibre during the permeability test because the natural fibre has a porous cellular structure, increasing the likelihood of pore network connection during the test (Persson, 2000).

7 CONCLUSIONS

This paper presents a summary of research progress on coconut fibres. Coconut fibres are an inexpensive, recyclable, low-density, and environmentally acceptable building material. These fibres have excellent tensile qualities, and they may be utilized instead of traditional fibres such as glass and carbon steel fibres as partial replacement of cement in concreting. Based on a detailed review, the following conclusions have been made:

- The flowability of concrete decreased with addition of coconut fibre due to the larger surface of the fibre, which enhanced the internal friction among concrete ingredients, leading to less workability. Furthermore, an increase in fresh density is observed up to 2% addition of coconut fibres.
- Increased durability properties were also observed with addition of coconut fibres. However, less information is available in this regard.
- Mechanical characteristics such as compressive, split tensile, and flexural strength were improved up to a certain dose of coconut fibre, which depends on the physical properties

of fibres such as length, diameter, and aspect ratio. Furthermore, it can also be observed that coconut fibres improved flexure capacity (47%) more efficiently than compressive capacity (12%).

- The optimum dose of coconut fibres is the most important parameter for better performance of concrete, as a higher dosage results in more voids in hardened concrete due to lack of workability, leading to lower mechanical and durability performance of concrete.
- Re-vibration improves both compressive and flexural strength of fibres reinforced concrete beam.

It can be concluded that coconut fibres enhanced flexure capacity more efficiently than compressive capacity. Therefore, further research was recommended to add some pozzolanic materials such as silica fume and fly ash to improved compressive capacity of fibre reinforced concrete for high strength concrete. It is necessary to re-vibrate concrete when its still in it plastic form. It is also necessary to investigate a novel strategy that makes use of the water retention capacity of coconut fibres in order to generate high-performance cement composites using internal curing technology.

Acknowledgments: The authors extend their appreciation to the staff of civil engineering department, Federal University of Technology Minna, Niger State.

8 REFERENCES

Abbas, M., Singh, D., Singh, G. Properties of Hybrid Geopolymer Concrete Properties Using Rice Husk Ash, Fly Ash and GGBS with Coconut fibres. *Mater. Today Proc.* **2021**,45,4964-4970.

Abdullah, A., Jamaludin, S. B.,Noor, M. M., Hussin, K. Composite Cement Reinforced Concrete Fibre: Physical and Mechanical properties and fracture behaviour. *Aust. J. Basic Appl. Sci.* **2011**, 5, 1228-1240.

Aguwa, J.I., Alhaji, B., Jiya, A., Kareem, D.H. Effectiveness of Locust Bean Pod Ash (LBPA) in the Production of Sandcrete Blocks for Buildings (2016) *Nigerian Journal of Technological Development*, 13(1), pp.13-16. DOI 10.4314/njtd.v13i1.

Aguwa, J.I. Study of Compressive Strengths of Laterite-Cement Mixes as Building Material (2009) *Assumption University Journal of Technology* (A.U.J.T.), 13(2), pp.114-120.

Ahmad, J., Zaid, O., Siddique, M. S., Aslam, F., Alabduljabbar, H., Khedher, K. M. Mechanical and Durability Characteristics of Sustainable Coconut Fibres Reinforced Concrete with incorporation of Marble Powder. *Mater.Res. Express* **2021**, 8, 075505.

Ahmad, J., Manan, A., Ali, A., Khan, M. W., Asim, M., Zaid, O. A. A Study on the Mechanical and Durability Aspects od Concrete Modified with Steel Fibres (SFs). *Civ. Eng. Archit.* **2020**, 8, 814-823.

ASTM C618, Standard Specification for Coal Fly Ash and Raw or Calcined Natural Pozzolan for Use in Concrete. ASTM International, West Conshohocken, 2012.

Ali, M., Liu, A., Sou, H., Chouw, N. Mechanical and Dynamic Properties of Coconut Fibre Reinforced Concrete. *Constr. Build. Mater.* **2012**, 30, 814-825

Althoey, F., Ansari, W. S., Sufain, M., Deifalla, A. F (2023) Advancements in low-carbon concrete as a construction material for the sustainable built environment. *Developments in the Built Environment*, 16, 100284.

Althoey, F. Compressive Strength Reduction of Cement Pastes Exposed to Sodium Chloride Solution: Secondary Ettringite Formation. *Constr. Build. Mater*. **2021**, 299, 123965.

Amadi, A.A., Eberemu, A.O., Momoh, O.H. Use of Coir Fibre Reinforced Technique to Improve Strengtth of Cement Kiln Dust Treated Black Cotton Soil Subgrade. *Geosynth. Long Beach* 2013, 223-229.

Anzar, H.M. Improved Concrete Properties Using Quarry Dust as Replacement for Natural Sand (2015) *International Journal of Engineering Research and Development*. 11(3), pp.4652.https://pdfs.semanticscholar.org/6618/1d1fb2e55a797c7cf27556f77e7e4f529fa4.pdf

Auta, S.M., Abanda M.A. Tsado, T.Y. Experimental Study on the flexure strength of a reinforced and re-vibrated RHA concrete beam (2015) *Proceedings of 1st International Conference on green engineering for sustainable development* (ICGESD), B. U. K. Kano, Nigeria in collaboration with Tanta University, Egypt, 8th-10th December, 2015, pp.54-58.

Bai, Y., Liu, J., Song, Z., Chen, Z., Jiang, C., Lan, X., Shi, X., Bu, F., Kanungo, D.P. Unconfined Compressive Properties of Composite Sand Stabilized with Organic Polymers and Natural Fibers. *Polymers* **2019**, 11,1576.

Da Silva, E.J., Marques, M.L., Velasco, F.G., Junior, C.F., Luzardo, F.M., Tashima, M.M. A New Treatment for Coconut Fibres to Improve the Properties of Cement -Based Composites-Combined Effect of Natural Latex/Pozzolanic

Materials. *Sustain. Mater. Technol*. **2017**, 12, 44-51.

Elinwa, A.U., Ejeh, S.P., Mamuda, A.M. Assessing of the fresh concrete properties of self-compacting concrete containing sawdust ash (2008) *Construction and Building Materials*, 22 (6), pp. 1178-1182. DOI: 10.1016/j.conbuildmat.2007.02.004

Hearn, N., Hooton, R. D., Mills, R. H. Pore Structure and Permeability. In *significance of Tests and Properties of Concrete and Concrete-Making Materials*; ASTM International: West Conshohocken, PA, USA, 1994.

Hearn, N., Figg, J. Effect of Microstructural Damage on Barrier Characteristics of Concrete. *In Materials of Science of Concrete VI*; Mindess, S., Skaln, J., Eds.; American Ceramic Society: Columbus, OH, USA, 2001.

Huang, G., Xie, X. Experimental Study on the Effect of Nano-$Si0_2$ to Durability in Hydraulic Concrete. *Yellow River* **2011**, 33, 138-140.

Khan, M., Rehman, A., Ali, M. Efficiency of Silica-Fume Content in Plain and Natural Fibre Reinforced Concrete for Concrete Road. *Constr. Build. Mater*. **2020**, 244, 118382.

Kikuchi, T., Shintani, Y., Hirashima, T., Kohno, M. Mechanical Properties of Steel Fibre Reinforced Concrete at High Temperature. *J. Struct. Constr. Eng*. **2020**, 85, 169-176.

Kumar, G.B.R., Kesavan, V. Study of Structural Properties Evaluation on Coconut Fibre Ash Mixed Concrete. *Mater. Today Proc*. **2020**, 22, 811-816.

Krishna, N. K., Prasanth, M., Gowtham, R., Karthic, S., Mini, K.M. Enhancement of properties of Concrete Using Natural Fibres. *Mater. Today Proc*. **2018**, 5, 23816-23823.

Naveen, P.N.E., Prasad, R.V. Evaluation of Mechanical Properties of Coconut Coir/Bamboo Fibre Reinforced Polymer Matrix Composites. *Sci. Eng*. **2013**, 3, 15-22.

Persson, K. *Micromechanical Modelling of Wood and Fibre Properties*; Lund University, Department of Mechanics and Materials: Lund, Sweden, 2000; ISBN 9178740940.

Pierard, J., Dooms, B., Cauberg, N. Durability Evaluation of Different types of UHPC. In Proceedings of the RILEM-fib-AFGC International Symposium on Ultra-High Performance Fibre-Reinforced ,Concrete Marseille, France, 1-3 October 2013; pp 275-284.

Raj, B., Sathyan, D., Madhavan, M. K., Raj, A. Mechanical and Durability Properties of Hybrid Fibre Reinforced Foam Concrete. *Const. Build. Mater*. 2020, 245, 118373.

Ramakrishna, G., Sundararajan, T. Studies on the Durability of Natural Fibres and the Effect of Corroded Fibres on the Strength of Mortar. *Cem. Concr. Compos*. **2005**, 27, 575-582

Ramli, M., Kwan, W.H., Abas, N.F. Strength and Durability of Coconut-Fibre-Reinforced Concrete in Aggressive Environments. *Constr. Build. Mater*. **2013**, 38, 554-556.

Rumbayan, R., Ticoalu, A. A Study into the Flexural, Compressive and Tensile Strength of Coir-Concrete as a Sustainable Building Material. In Proceedings of the MATEC Web of Conference, Sibiu, Romania, 5-7 June 2019; EDP Science: Les Ulis, France, 2019; Volume 258, p. 1011.

Sathiparan, N., Rupasinghe, M. N., Pavithra, B. H. M. Performance of Coconut Coir Reinforced Hydraulic Cement Mortar for Surface Plastering Application. *Constr. Build. Mater*. **2017**, 142, 23-30.

Savastano, H., Agopyan, V. Transition Zone Studies of Vegetable Fibre-Cement Paste Composites. *Cem. Concr. Compos*. **1999**, 21, 49-57.

Srinivas, K., Akula, K. R., Mahesh, V. Experimental Investigation on Lightweight Concrete by Replacing the Coarse Aggregate with Coconut Shell and Expanded Polystyrene Beads and Using Polypropylene Fiber. *Mater. Today Proc*. **2021**, 46, 838-842.

Syed, H., Nerella, R., Madduru, S.R.C. Role of Coconut Coir Fibre in Concrete. *Mater. Today Proc*. **2020**, 27, 1104-1110

Tadepalli, P. R., Mo, Y.L., Hsu, T.T.C. Mechanical Properties of Steel Fibre Concrete. *Mag. Concr. Res*. **2013**, 65, 462-474.

Usman, M., Farooq, S.H., Umair, M., Hanif, A. Axial Compressive Behavior of Confined Steel Fibre Reinforced High Strength Concrete. *Constr. Build. Mate*r. **2020**, 230, 117043.

Wang, W., Huang, G. Characterization and Utilization of Natural Coconut Fibres Composites. *Mater. Des.* **2009**, 30, 2741-2744.

Wongsa, A., Kunthaqatwong, R., Naenudon, S., Sata, V., Chindaprasirt, P. Natural Fibre Reinforced High Calcium Fly Ash Geopolymer Mortar. *Constr. Build. Mater*. **2020**, 241, 118143.

Zhang, P., Li, Q., Chen,Y., Shi, Y., Ling, Y.F. Durability of Steel Fibre Concrete. *Mag. Concr. Res*. **2013**, 65, 462-474.

Effect of Calcium Carbide Residue on the Compaction Characteristics of Tropical Black Clay Soil

*Tita, B. I.[1]; Alhassan, M.[2]; & Alhaji, M. M.[3]
[1] Department of Civil Engineering Federal University of Technology, Minna
[2] Department of Civil Engineering Federal University of Technology, Minna
[3] Department of Civil Engineering Federal University of Technology, Minna
*Corresponding author email: btitainji@gmail.com

ABSTRACT
This study examines the effect of Calcium Carbide Residue (CCR) on the compaction characteristics of tropical black clay (TBC). The soil (TBC) was stabilized with 0, 2, 4, 6, 8 and 10% of CCR by weight of the dry soil. Laboratory compaction tests were conducted using British Standard Heavy (BSH), West African Standard (WAS), and British Standard Light (BSL) compactive efforts, to evaluate influence of the CCR on the Maximum Dry Density (MDD) and Optimum Moisture Content (OMC) of the soil. The results show that MDD soil increases with increases in percentage of CCR, up to an optimum range of 6 – 8%, particularly under moderate compaction effort (WAS), before decreasing with further increase of CCR. Similarly, the OMC initially decreases at moderate CCR content, indicating improved particle packing, but increases beyond the optimal level due to the hydration demand of cementitious compounds. These findings highlight the potential of CCR as a cost-effective stabilizer for improving the compaction characteristics of tropical black clay, making it a viable alternative for soil improvement in geotechnical applications.

Keywords: *Calcium Carbide Residue, Compaction Characteristics, Tropical Black Clay Soil*

1 INTRODUCTION

Soil compaction is a critical factor influencing the strength and stability of geotechnical structures, as it directly affects load-bearing capacity, settlement behavior, and permeability of the bearing soil. However, certain soils, such as tropical black clay, exhibit poor compaction characteristics due to their high plasticity, low shear strength, and excessive shrink-swell potential (Osinubi *et al.,* 2011). These properties make them unsuitable for direct use in construction, necessitating stabilization to improve their engineering performance. Effective stabilization techniques, particularly chemical stabilization, have been explored to enhance the compaction behavior and overall suitability of such soils for construction applications.

Tropical black clay is an expansive soil commonly found in semi-arid regions where evaporation exceeds precipitation, including the Chad Basin and Upper Benue Trough in Nigeria (Amu *et al*., 2011). The soil is rich in montmorillonite, a clay mineral responsible for its high-water absorption and volume change characteristics (Alhassan and Mustapha, 2015). These properties result in significant challenges in construction, as the soil experiences substantial swelling during wet seasons and shrinkage with cracking during dry seasons. The poor compaction characteristics of tropical black clay contribute to instability in structures and roads, leading to excessive maintenance costs and frequent failures.

To improve the compaction properties of tropical black clay, various soil stabilization methods have been employed, including mechanical and chemical stabilization. Mechanical methods such as densification and compaction can reduce void ratios and increase load-bearing capacity, but these methods are often insufficient for highly plastic soils (Osinubi, 2000). Chemical stabilization, on the other hand, involves the addition of materials such as cement, lime, fly ash, and industrial by-products to alter the soil's properties and improve its compaction characteristics (Arash *et al.*, 2012). However, the high cost and environmental concerns associated with conventional stabilizers have led to the exploration of alternative, cost-effective stabilizers derived from industrial waste.

Calcium Carbide Residue (CCR), a by-product of acetylene gas production, has emerged as a promising stabilizer for problematic soils. CCR contains high percentage of calcium hydroxide, which reacts with clay minerals to improve soil stability by reducing plasticity and enhancing compaction characteristics (Onyelowe and Okafor, 2012). Utilizing CCR not only offers a sustainable approach to soil stabilization but also helps in waste management by repurposing industrial by-products for engineering applications. Several studies have shown that CCR has the potential to enhance the strength, density, and moisture retention properties of expansive soils, making it a viable alternative to conventional stabilizers (Osinubi *et al.*, 2010).

This study investigates the effect of Calcium Carbide Residue on the compaction characteristics of tropical black clay soil. The research evaluated the influence of CCR on compaction parameters, such as MDD and OMC, which are essential in achieving desired soil strength and stability. By analyzing the effectiveness of CCR as a stabilizer, this study contributes to the advancement of sustainable and cost-efficient soil stabilization techniques for geotechnical engineering applications.

2 MATERIALS AND METHODS

2.1 MATERIALS

The materials used for this study are Tropical Black Clay (TBC) and Calcium Carbide Residue (CCR).

2.1.1 TROPICAL BLACK CLAY (TBC)

The tropical black clay was collected by method of disturbed sampling at depth of 1.5m at Gwako village, latitude of 8˚58'22.8" N and longitude of 7˚7'8.4" E along Gwagwalada express way, FCT Abuja, Nigeria. The sample was preserved in polythene bags and transported to the Geotechnical laboratory of Federal University of Technology, Minna.

2.1.2 CALCIUM CARBIDE RESIDUE (CCR)

The calcium carbide residue was obtained from panel beaters at Ketaren Gwarri Mechanic Village in Minna. It was dried, grind and sieved through sieve No. 200 (75µm) before usage.

2.2 METHODOLOGY

Laboratory experiments were conducted to assess the effect of the calcium carbide residue on the compaction characteristics of the tropical black clay. The tests conducted include: Natural moisture content, specific gravity, sieve analysis, Atterberg limit and compaction test. The test procedures were in conformity with BS 1377 (1990). British Standard Heavy (BSH), British Standard Light (BSL) and West African Standard (WAS) energy levels were deployed in the compaction characteristics assessment.

3 RESULTS AND DISCUSSION

3.1 CHEMICAL COMPOSITION OF CALCIUM CARBIDE RESIDUE

Table 1 shows the chemical composition of the Calcium Carbide Residue (CCR) used in the study. The result indicates that calcium oxide (CaO) is the dominant constituent, accounting for 65.04% of the material. This high CaO content makes CCR highly alkaline and suggests its strong cementitious potential. The significant loss on ignition (LOI) of 26.67% further implies the presence of bound water or volatile components, likely due to the formation of calcium hydroxide ($Ca(OH)_2$) upon exposure to moisture. Such characteristics enhance the potential for CCR to be used in soil stabilization. This trend of oxide composition is similar to that reported by (Utser and Taku, 2012; Manasseh and Ejelikwu, 2013).

TABLE 1: SOIL CHEMICAL COMPOSITION OF CALCIUM CARBIDE RESIDUE (CCR)

Oxide	% composition
SiO_2	2.45
Al_2O_3	1.83
Fe_2O_3	0.12
CaO	65.04
K_2O	0.08
Na_2O	0.13
MgO	1.81
SO_3	0.57
MnO	.
P_2O_5	0.71
TiO_2	.
LOI	26.67

LOI = Loss on ignition

3.2 PROPERTIES OF THE TROPICAL BLACK CLAY

The index properties and compaction characteristics of TBC is presented on Table 2. The result indicates that the soil is highly plastic, fine-grained with significant swelling and shrinkage tendencies. The particle size distribution from Table 2 and Figure 1 shows that 75.66% of the soil passes the No. 200 sieve (0.075 mm), confirming its fine-grained nature, which aligns with its classification as a high plasticity clay (CH) under the Unified Soil Classification System (USCS) and an A-7-5 soil, under the AASHTO classification system. These classifications suggest that the soil has poor drainage, low bearing capacity, and high susceptibility to volume changes due to moisture fluctuations. The liquid limit of 66% and plastic limit of 21.53% indicate a soil with a high-water retention capacity, while the Plasticity Index (PI) of 44.47% confirms its expansive nature. This high PI signifies a strong tendency to undergo significant swelling when wet and shrinkage when dry, making it problematic for engineering applications, particularly for roads and foundations. The linear shrinkage of 12.97% further underscores its volume instability, which could result in surface cracks and structural damage when used as a subgrade material. The specific gravity of 2.61 suggests predominance of clay minerals such as montmorillonite, which are known for their high swelling potential.

The compaction characteristics of the TBC vary under different compaction efforts. The MDD decreases as compaction effort reduces, while the OMC increases. Under British Standard Heavy (BSH) compaction, the soil achieves an MDD of 1.83 g/cm^3 at an OMC of 15.3%, indicating that higher compactive effort results in better densification of the soil particles. Under West African Standard (WAS) compaction, the MDD drops to 1.63 g/cm^3, and the OMC increases to 17.6%, suggesting that the soil requires more water to achieve maximum compaction with lower compactive effort. Similarly, with British Standard Light (BSL) compaction, the MDD further reduces to 1.62 g/cm^3, while the OMC increases to 18%, indicating that with minimal compactive effort, the soil retains more moisture and remains less dense. This trend highlights the influence of compaction effort on the soil's structure, as higher energy compaction leads to a denser, stronger soil matrix, which is crucial for improving its engineering performance.

Figure 1: Particle size distribution curve for the tropical black clay

TABLE 2: BASIC PROPERTIES OF THE TROPICAL BLACK CLAY (TBC)

Basic characteristics	TBC		
% larger No.200 sieve (>0.075 mm)	24.34		
% passing No.200 sieve (<0.075 mm) (%)	75.66		
Liquid limit (%)	66		
Plastic limit (%)	21.53		
Plasticity index (%)	44.47		
Linear shrinkage (%)	12.97		
Specific gravity	2.61		
USCS	CH		
AASHTO	A-7-5		
Colour	Greyish black		
	BSH	WAS	BSL
MDD (g/cc)	1.83	1.63	1.62
OMC (%)	15.3	17.6	18

3.3 EFFECT OF CALCIUM CARBIDE RESIDUE (CCR) ON CONSISTENCY LIMIT

Consistency limits of the TBC stabilized with CCR, illustrated on Figure 2, exhibit a progressive reduction in the Liquid Limit (LL) and Plasticity Index (PI) with increasing CCR content, while the Plastic Limit (PL) increases. This trend is indicative of the modification in the clay's plasticity due to the pozzolanic reaction between the calcium-rich CCR and the clay minerals, leading to particle aggregation and improved soil workability.

The LL of the untreated TBC is 66%, signifying high water retention capacity and substantial volume change potential. With the addition of 2% CCR, the LL decreases to 61%, further reducing to 57% at 10% CCR. This reduction aligns with the findings of Gurugubelli *et al.* (2017) and Joel and Edeh (2016), who reported that the introduction of calcium-based stabilizers reduces the clay's affinity for water due to cation exchange and flocculation. Similarly, the PI, which initially measures 44.47%, decreases consistently with CCR addition, reaching 27.33% at 10% CCR. A lower PI indicates reduced swelling and shrinkage tendencies, making the soil more stable under moisture fluctuations. This behavior corroborates the observations of Osinubi *et al.* (2010), who noted that lime and similar stabilizers significantly lower the PI of expansive clays by binding free water within cementitious compounds.

Conversely, the PL increases from 21.53% in the untreated TBC to 29.67% at 10% CCR, implying a reduction in the clay's plasticity and an enhancement in its strength at lower moisture contents. The increase in PL is consistent with previous studies by Isah and Sharmila (2015) and Joel and Edeh (2016), who found that soil stabilization with calcium-based additives enhances soil cohesion and reduces deformability. Overall, the observed changes in the consistency limits confirm the effectiveness of CCR in improving the engineering properties of tropical black clay, making it a viable stabilizer for geotechnical applications.

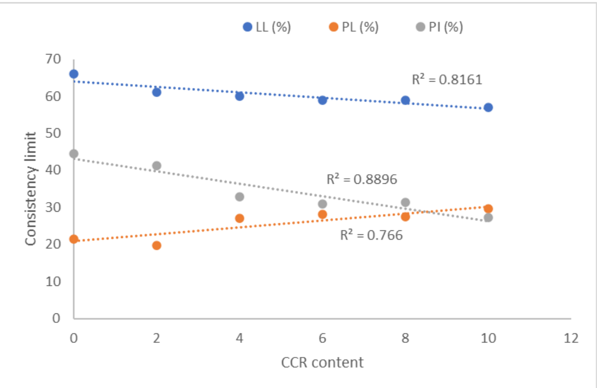

Figure 2: Effect of CCR on the consistency limit

3.4 Effect of Calcium Carbide Residue (CCR) on the Compaction Characteristics

3.4.1 MAXIMUM DRY DENSITY

Maximum Dry Density (MDD) of the tropical black clay stabilized with CCR varies across different compaction efforts, showing a noticeable trend in response to increasing CCR content (Figure 3). Under British Standard Heavy (BSH) compaction, the MDD remains relatively stable between 1.83 and 1.84 g/cm^3 for CCR contents up to 6%, indicating that moderate CCR addition does not significantly affect the soil's compactability under high-energy compaction. However, at 10% CCR, the MDD decreases to 1.79 g/cm^3, suggesting a reduction in particle packing efficiency due to the replacement of soil fines with lighter CCR particles.

Under West African Standard (WAS) compaction, the MDD shows a gradual increase from 1.63 g/cm^3 at 0% CCR to 1.67 g/cm^3 at 8% CCR, before slightly reducing to 1.65 g/cm^3 at 10% CCR. This trend indicates that the inclusion of CCR improves the densification of the soil up to an optimal point, beyond which further CCR addition reduces the soil's compactability. The improved MDD at moderate CCR levels could be attributed to the flocculation and aggregation of clay particles, which enhances particle rearrangement and densification (Akinmade, 2008; Oyediran and Fadamoro, 2015). However, excessive CCR may lead to increase in voids, reducing the overall dry density. A similar trend is observed under British Standard Light (BSL) compaction, where the MDD initially increases slightly from 1.62 to 1.63 g/cm^3 at 4 and 6% CCR, but then decreases progressively to 1.57 g/cm^3 at 10% CCR. The reduction at higher CCR contents suggests that the lower energy compaction does not effectively overcome the increasing particle voids, leading to reduced densification.

Generally, the results indicate that inclusion of CCR up to an optimum level (around 6 – 8%) enhances the compactability of tropical black clay, particularly under medium compaction effort (WAS). However, excessive CCR content beyond 8% reduces MDD across all compaction levels, likely due to the replacement of heavier clay particles with lower-density CCR and an increase in voids.

3.4.2 OPTIMUM MOISTURE CONTENT

The optimum moisture content (OMC) of tropical black clay stabilized with CCR exhibits variations across different compaction efforts (Figure 4), indicating the influence of CCR on the soil's water requirement for maximum compaction. Under British Standard Heavy (BSH) compaction, the OMC remains relatively stable, ranging between 15.3 and 15.5% for most CCR contents, except at 6% CCR, where it drops to 12%. This reduction suggests that at this CCR level, the soil achieves maximum densification with less water, likely due to the improved particle arrangement and binding effect of CCR. However, beyond 6% CCR, the OMC increases again, indicating that higher CCR levels require more moisture for proper hydration and compaction.

Under West African Standard (WAS) compaction, the OMC increases from 17.6% at 0% CCR to 20.2% at 4% CCR, demonstrating that the addition of CCR enhances the soil's water demand at lower compaction effort. This increase could be attributed to the reaction of CCR with the clay minerals, leading to the formation of cementitious compounds that require additional water. At 6% CCR, the OMC drops to 18%, suggesting an optimal point where the soil structure is modified sufficiently to reduce water demand. However, beyond this, the OMC starts to increase again, reaching 19.1% at 10% CCR, further confirming that excessive CCR addition increases the soil's moisture requirement.

Under British Standard Light (BSL) compaction, the OMC follows a similar trend, increasing from 18% at 0% CCR to 21.8% at 10% CCR. This consistent rise suggests that under lower compactive effort, the presence of CCR significantly alters the soil's water retention properties, leading to a higher moisture requirement. The increase in OMC at higher CCR levels can be attributed to the finer particle size of CCR, which creates a greater surface area for water absorption and the need for hydration reactions.

Generally, the results indicate that introduction of CCR affects the water demand of tropical black clay, with an optimal range observed around 6% CCR, where the OMC is lowest across all compaction methods. Beyond this point, increasing CCR content results in a higher moisture requirement, likely due to the increased chemical reactions and the presence of finer particles. This observed trend of OMC variation is also similar to that reported by Isah and Sharmila (2015).

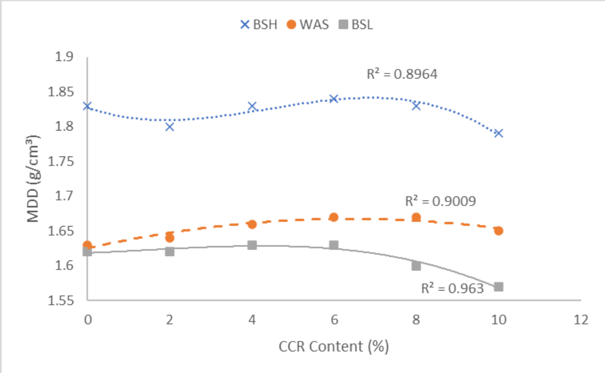

Figure 3: Variation of maximum dry density with CCR content

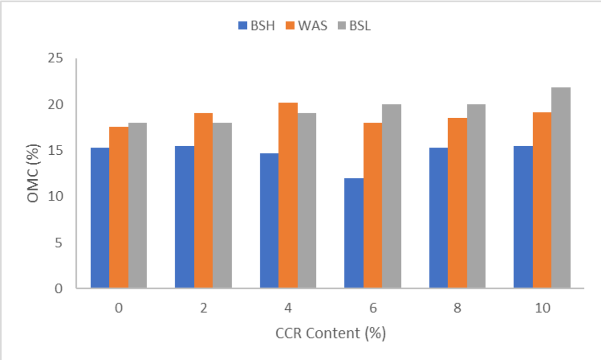

Figure 4: Variation of optimum moisture content with CCR content

4 CONCLUSION

The study has demonstrated that addition of CCR to clay soil, significantly influences its compaction characteristics. The high calcium oxide (CaO) content in CCR enhances its cementitious potential, promoting particle flocculation and aggregation, which affects soil densification. The natural soil exhibits high plasticity, poor drainage, and significant swelling-shrinkage tendencies, making it unsuitable for direct engineering applications. Compaction results show that the MDD increases with CCR addition up to an optimal range of 6–8%, particularly under moderate compaction effort (WAS), before declining at higher CCR contents. This reduction in MDD beyond 8% is attributed to the replacement of heavier clay particles with lighter CCR and an increase in void spaces.

Similarly, the OMC trends indicate that moderate CCR addition initially reduces the soil's water demand due to improved particle arrangement. However, beyond the optimal CCR content, the OMC increases due to the hydration requirements of the cementitious compounds formed. The variation in compaction characteristics across different compactive efforts highlights the role of

CCR in modifying soil structure, with higher compaction energy achieving better densification. These findings suggest that CCR is an effective stabilizer for tropical black clay soil when used within optimal limits, offering a sustainable and cost-effective approach to soil improvement in geotechnical applications.

REFERENCES

Akinmade, O. B. (2008). Stabilization of black cotton soil using locust bean waste ash. *Unpublished MSc thesis, Civil Engineering Department, Ahmadu Bello University*, Zaria.

Alhassan, M. & Mustapha, A. M. (2015). Improvement of deficient soils in Nigeria using bagasse ash - A review. *Proceeding of 17th International Conference on Civil and Building Engineering*, 1040-1049.

Amu, O. O., Owokade, O. S. & Shitan, O. I. (2011). Potentials of coconut shell and husk ash on the geotechnical properties of lateritic soil for road works. *International Journal of Engineering and Technology*, 3(2), 87-94.

Arash, B., Hamidreza, S. & Mehdi, G. (2012). The effect of adding iron powder on Atterberg limits of clay soils. *International Research Journal of Applied and Basic Sciences*, 3(11), 2349-2354.

B. S. 1377 (1990), *Methods of Testing Soils for Civil Engineering Purposes*, British Standards Institute, London.

Gurugubelli, S., Prasad, D. S. V. & Eswararao, B. (2017). A laboratory study on the strength improves of expansive soil treated with calcium carbide residue and fly

Isah, B. W. & Sharmila, S.M.R. (2015). Soil stabilization using calcium carbide residue and coconut shell ash. *Journal of Basic and Applied Engineering Research*, 2(12), 1039-1044.

Joel, M. & Edeh, J. E. (2016). Calcium carbide residue-hydrated lime blend as stabilizing agent. *International Journal of Science and Technology*, 5(12), 606-614.

Manasseh, J. & Ejelikwu, E. J. (2013). Soil modification and stabilization potential of calcium carbide waste. *Advanced Materials Research*, 824, 29-36.

Onyelowe, K. C. & Okafor, F. O. (2012). A comparative review of soil modification methods. *Asian Research Publishing Network, Journal of Earth Sciences*, 1(2), 36-41.

Osinubi, K. J. (2000). Stabilization of tropical black clay with cement and pulverized coal bottom ash admixture. *American Society of Civil Engineers Geotechnical Special Publication*, (99), 289-302.

Osinubi, K. J., Oyelakin, M. A. & Eberemu, A. O. (2011). Improvement of black cotton soil with ordinary portland cement - locust bean waste ash blend. *The Electronic Journal of Geotechnical Engineering*, 16, 785-796.

Osinubi, K. J., Sani, E. & Ijimdiya, T. S. (2010). Lime and slag admixture improvement of tropical black clay road foundation. In: *Transportation research board (TRB) 89th annual meeting CD-ROM*, 10–14 Jan, Washington, DC, USA, 1–18.

Oyediran, I. A. & Fadamoro, O. F. (2015). Strength characteristics of genetically different rice and coconut husk ash compacted shales. *International Journal of Geo-Engineering*, 6(1), 1-14.

Utser, J. T. & Taku, J. K. (2012). Coconut shell ash as partial replacement of OPC in concrete production. *International Journal of Scientific and Technology Research*, 1(8), 86-89.

CIRCULAR ECONOMY FRAMEWORKS FOR MANUFACTURING INDUSTRY-A REVIEW

*Jonah, I.[1,2]; & Abdullahi, A. A.[1]
[1] Department of Mechanical Engineering, Federal University of Technology, Minna
[2]Department of Mechanical Engineering, Kogi State polytechnic lokoja Kogi state
*Corresponding author email: jonahisaac6@gmail.com

ABSTRACT

Manufacturing industries have been played a significant role in terms of production in attempt to improve economy worldwide. However, in a traditional linear economy setting, it becomes unrealistic prove to achieve sustainable production and consumption patterns. The concept of circular economy has been proved to be the only way out in the present environmental issues and unavailability resources, it aims at eventually severing this link, through keeping resources in the loop. Through a systematic literature review, this paper attempts to revisit the concept of circular economy in the manufacturing industries in order to determine whether the body of research has improved beyond framework development and into verified implementation in manufacturing industry.

The review shows that the research field has indeed advanced from purely conceptual framework into empirical studies and research into implementation tools. However, in empirical studies and framework development the sustainability impact of CE practices is completely addressed only through the environmental issues, neglecting the social dimension, economic dimension and even the percentage of virgin material usage for production is neglected. Further, a key finding is that the generality of narrow approaches to sustainability in manufacturing results to a risk that circular economy implementation efforts will become difficult if percentage of virgin materials usage by industries are not evaluated. Holistic approaches are needed to avoid the implementation of solutions that may be framed as circular, but neglect the sustainability component.

Keywords: *Business and supply loop, circular economy, framework, indicators, Manufacturing.*

1.1 INTRODUCTION

To make it clear, circular economy (CE) is a new introduction concept which is achieving growing interest as a way to explain the practices of market agents to protect natural resources and reduce their impacts on natural resources. The main idea of this concept is to review the production and consumption patterns of the current socioeconomic system through the promotion of a series of serious interventions in the contemporary linear production process (i.e., take-make-dispose). These interventions promote a CE model whereby the consumption of raw materials and natural resources can be substantially reduced (Charalampides, Arvanitidis et al. 2014)

The CE is an economic system considered to transform the traditional linear economy and it has been accepted as a potential enabler of sustainable development (Urbinati, Chiaroni et al. 2017) . In a linear economic system, raw materials are sourced, manufactured, used and then discarded; such an end-of-life process leads to environmental degradation due to the continued exploitation of limited resources (Millar, McLaughlin et al. 2019).

CE can now be defined as “an industrial system that is restorative or regenerative by intention and design”(MacArthur 2013, MacArthur 2013) . It the replaces traditional linear economy concept with restoration, taking products and material use from ‘cradle to grave’ to ‘cradle to cradle’ (MacArthur 2013), (McDonough 2002). That is, CE considers discarded products or components as materials and resources for the input of new manufacturing processes. For manufacturing industries facing challenges of resource scarcity and environmental impact, it is important to reduce, reuse and recover resources in production and consumption processes and keep products and materials at their highest utility and value (Kirchherr, Reike et al. 2017), (Lieder and Rashid 2016).

Over the decade now serious attention had been paid worldwide to the new concept and development of framework model for Circular Economy, CE, especially in the manufacturing industries with the aim to provide a better alternative to the dominant economic development model, so called “take, make and dispose will be minimised. (Mendoza, Sharmina et al. 2017), (Reike, Vermeulen et al. 2018) and (Blomsma, Kjaer et al. 2018) pointed out that such circular strategies frameworks can identify or emphasize different (groups of) circular strategies, which can be linked to addressing different types of structural waste. (Blomsma, Kjaer et al. 2018) established the fact that little work has been carried out with regard to ensuring that frameworks are seen as relevant and useful by intending manufacturing industries. For these reasons, there is scope to further develop these frameworks to support visioning in Circular Oriented Innovation (COI). The plastic manufacturing industry in particular is important to global economic development because it provides raw materials for a variety of sectors. However, the industry's linear nature in some countries, as demonstrated by the production-consumption-disposal cycle, has resulted in extensive environmental deterioration and resource depletion. Plastic garbage, in particular, is a major hazard to ecosystems, human health, and the economy. In today's world, plastic waste is one of the environmental contaminants. According to (Karstensen, Engelsen et al. 2020), proved that manufacturing industries waste creates more environmental hazards through greenhouse gas emissions, climate change, and causing global warming. It implies that the traditional linear economy which causes environmental nuisance should be looked into and develop a framework which allows sustainable economy. The Manufacturing Industries in Nigeria is at a critical crossroads, striving with the far-reaching environmental condition of its linear production-consumption-disposal cycle. With serious concerns about plastic pollution, resource depletion, and climate change, the industry immediately needs radical action. To accomplish the circular economy in the plastic manufacturing sector, implementing this new paradigm shift also calls for new frameworks and behavioural changes. Recently research on circular economy has gained significantly attention to researchers, there is a well-established need to consider the circular economy for industrial wastes such as metals, papers, plastics when addressing the challenges of pollution. Most research on plastics focus within the context of achieving a circular economy addresses a specific technology, plastic product, material or intervention that applies to a segment of a supply chain.

1.2 CIRCULAR ECONOMY AND MANUFACTURING INDUSTRY

(Blomsma, Pieroni et al. 2019) presented a framework that introduces a taxonomy of circular strategies, developed for use by manufacturing companies engaging in circular economy (CE) oriented innovation. (De Mattos and De Albuquerque 2018) proposed a framework that analysed how organisation can develop a circular business model, identifying the feasibility factors and respective strategies. (Lanaras-Mamounis, Kipritsis et al. 2022) used a framework for evaluating the progress of firms towards the implementation of circular economy (CE) strategies by utilizing an evaluation matrix which is based on the three-level context of CE, the key “Rs” principles/strategies of CE, and material loops, an empirical analysis was carried out in a sample of plastic industries. (Di Maio and Rem 2015) presented a micro-level indicator, evaluated the recaptured economic value of products through recycling strategies. (Park and Chertow 2014) established the reuse potential indicator (a micro-level CE strategy-oriented indicator) which estimated the reuse capability of waste materials by taking into account alternative waste management technologies. (Felicio, Amaral et al. 2016) proved a single indicator which assesses the achieved level of industrial symbiosis and the resulting presence of by-product and waste synergies in EIPs. (Saidani, Yannou et al. 2019) provided 10 criteria for classification of circular economy CE indicators linked to implementation level (i.e., micro-, meso-, macro-level) and the application level of indicators (i.e., general indicators or indicators for a specific sector). (Bocken, De Pauw et al. 2016) established three types of circular business models, namely, the first type is the closed loop which operates on minimising the use of virgin materials at the manufacturing stage and on the valorisation of materials within their useful lifetime. Another type of business model is the narrow loop which defines CE actions and core strategies that are not closed the loop but to reduce the use of virgin material and their losses. The third business model is the slow loop which intends at increasing the useful lifetime of materials and products in order to reduce the demands for new production and consequently the use of virgin materials. (Elia, Gnoni et al. 2017), (Chun-Rong and Jun 2011), (Saidani, Yannou et al. 2019) developed suitable methods, techniques, and frameworks and evaluated the progress towards CE facilitating governments, firms, and various stakeholders to set, achieve, and monitor realistic CE targets. Such measurement frameworks have been proposed for each level of CE implementation developing various types of indicators. (Felicio, Amaral et al. 2016) established a single indicator and used it to assess the achievement level of industrial symbiosis and the resulting presence of by-product and waste synergies in eco-industrial parks EIPs. (Wang, Lee et al. 2018) developed a framework on a circular composite index used group of indicators and assessed the level of circularity in a sample of 40 Chinese cities. (Pauliuk 2018) presented a framework and recorded inputs, outputs, and material stocks of selected sample firms through LCA thinking. It is based on a single-level indicator which provided interesting insights for many of the CE strategies allowing direct comparisons between them. (Genovese, Acquaye et al. 2017)applied a framework that were involved a combination of emission indicators and compared the environmental impact of linear and circular supply chains, in which the by-products from one sector are considered input for another one.

RESEARCH TRENDS IN DEVELOPMENT OF CE FRAMEWORK

In many research attempts to develop a suitable methods, techniques, and frameworks to measure the achievement towards CE, facilitating governments, firms, and various stakeholders to set, achieve, and monitor realistic CE targets. Such measurement frameworks have been developed for each level of CE implementation though the majority of these studies provide useful classifications for CE indicators. The incorporation of CE strategies into the business models (i.e., material loops) has also addressed in the literature. The shift in the orientation in measuring the frameworks with respect to the CE strategies, widely known as "Rs" models/frameworks has been investigated. With this background, a review of some of the trending works would further widen the research gap in the quest to improve circular economy framework that could be recommended for implementation in manufacturing industries in Nigeria.

FUTURE TREND IN DEVELOPMENT OF CE FRAMEWORK

It has been affirmed that many research works have been done in efforts on developing CE transition methodology and framework from traditional linear economy that is frequently characterised by the presence of structural waste and environmental nuisance as reviewed and overviewed by many researchers. It is of worth research that CE indicators and measurement frameworks should be carefully studied in order to underline the crucial aspects, for holistic framework which will be able to define the integration of CE progress of organisation at all levels. From a waste management standpoint and managerial point of view, as well as percentage of raw material usage, such a framework could be a practical tool for managers and investors to identify the crucial points of CE performance and CE investments, providing information about investment risks and the progress of already funded CE projects. Therefore, some further analysis of plastic manufacturing industries CE indicators is necessary.

2. METHODOLOGY

This paper considered the research method of systematic literature review. An exhaustive search of the literature was performed, before combining narrative and tabular methods for synthesizing literature. The literature on the field of CE is, by now, abundant. It was therefore crucial to limit the scope of the research to only literature relevant to the research questions. A systematic approach was key. The literature review was therefore performed stepwise. This stage included stating the main goal of the study and associated research questions. A search strategy and key criteria for inclusion and exclusion of papers was developed. Thereafter, the data collection step, at which database selection and the identification of appropriate keywords were central elements. This was followed by sorting and exclusion.

Table 1: Developments in Circular Economy Frameworks for Manufacturing Industry

S/N	Conceptual Framework	Factor(s) and Enabler(s)	Production Product	Findings	Research Gap	Reference
1	Assessing the corporate CE practices in relation to all levels of CE implementation (i.e., micro-, meso-, and macro-level),	Examine the effectiveness of the proposed framework and identify key elements which can be further improved.	plastic	Firms show a better performance at the macro-level than the other levels	The frameworks were tested for plastic industry and underscored other manufacturing industries	(Lanaras-Mamounis, Kipritsis et al. 2022)
2	Developing a circular strategies framework for manufacturing companies to support circular economy-oriented innovation	Inappropriate mapping strategies currently applied. Lack of Finding solution for improving circularity across a range of business processes.	Manufacturing companies	It provided guidance in identifying what business areas eco-innovation for CE is possible or necessary.	A tool for inspiring, motivating and aligning people should be further study.	(Blomsma, Pieroni et al. 2019)
3	Performance indicators for a circular economy	Environmental challenges	Post-industrial plastic waste	The results show that the indicator can be a very useful approach to guide waste streams towards their optimal valorization.	Thermosets material or other material types were not addressed	(Huysman, De Schaepmeester et al. 2017)
4	Companies innovate business models and supply chains for a circular economy.	Product/Process/Service innovation.	Manufacturing industries	The findings strengthen the understanding of interlink between the two major types of innovation.	Setting for circular innovation strategy was not addressed.	(Kaipainen, Urbinati et al. 2022)
6	Evaluation of Factors Affecting the Transition to a Circular Economy.	Climate change and reduction carbon emissions.	Both business model and manufacturing processes.	The results of empirical research showed that the factors attention to the environment and attitude towards intention.	Framework model limited to planned behavior but not manufacturing process industries.	(Trần, Phan et al. 2022)
7	Facilitating Circular Economy Strategies Using Digital Construction Tools: Framework Development	Resource constraints, human health and climatic change.	Construction sector.	Framework offers practical insights for construction industry practitioners and helps to investigate several critical barriers.	Framework was not considering other stakeholders in the construction process.	(Jemal, Kabzhassarova et al. 2023)
8	Moving from Linear to Circular Economy: Life-Cycle Assessment on Plastic Waste Management	Environmental issues	Plastic materials	Study revealed that the combined mechanical recycling and pyrolysis with incineration of residuals scenario has the lowest environmental impact.	The model did not provide solution to transitioning to circular economy.	(Almadhi, Abdelhadi et al. 2023)
9	Value-addition to plastic waste towards achieving a circular economy.	Unsustainable waste management practices and environmental issues	Plastics	The new technologies need to employ to close the waste generation loop.	Further research need to be looking into how to expand reuse models, new business models.	(Kumar, Bhujbal et al. 2024)
10	Circular economy for the built environment: a research framework	Sustainability of the built environment	Manufacturing industries	The result shown that the greatest challenges ahead lie not in further technological innovation but rather in the role of people, both as individuals and as a society.	The research undermine the circular economy at macro level.	(Pomponi and Moncaster 2017)
11	Assessment of plastic waste generation and management	Environmental issue and unsustainable waste disposal practices	Plastic	The result shown that the facility to segregate, recycling, and up cycling of plastic waste were not provided	The research only focused plastic materials, however, undermined other materials.	(Oladipupo, Ayanshola et al. 2024)

12	Plastic circular economy framework using hybrid machine	Environmental issues	Plastics	The results shown the maximum recycling rate for the case study.	The research framework focused on plastics waste while other industrial wastes were unexplored.	(Chin, Varbanov et al. 2022)
13	Plastic Pollution, Waste Management Issues, and Circular Economy Opportunities	Plastics management	plastic pollution effects on rural communities and Waste Management Issues	The results revealed that rural communities need to be enlightening the economy opportunities on circular economy through generation of plastics wastes.	The study underexplored other industrial wastes.	(Mihai, Gündoğdu et al. 2021)
14	Understanding circular economy awareness and practices in manufacturing firms	Manufacturing industries	Environmental issues	The research findings shown that with the growing emphasis on CE across the globe by governing bodies, firms are becoming more aware of CE practices.	The study provides manufacturing firms with a thorough understanding of the state of CE practices.	(Liakos, Kumar et al. 2019)
15	Implementation of circular economy approaches in the electrical and electronic equipment (EEE) sector	Electrical Manufacturing industries	Due to large untapped potential in the Electrical Manufacturing industries.	The findings indicate that no single instrument alone from a specific policy domain can address the variety of existing barriers and gaps.	The study covered only Electrical Manufacturing industries understudied other manufacturing industries.	(Rizos and Bryhn 2022)

CONCLUSION

The aim of this research paper was to provide a review of the empirical literature on CE framework in manufacturing industry and to identify the research findings and research gaps taking place between industrial actors and academics to promote further studies. It was found that most published literature from before 2015 was conceptual; this review study finds that literature based on case studies has grown. All case studies reviewed are from after 2015, showing that there is progress towards more empirical research on manufacturing companies relating to CE framework implementation.

ACKNOWLEDGEMENTS

I return all glory, honour, and adoration to God Almighty for the grace and mercy received for carrying out this study.

REFERENCES

Almadhi, A., et al. (2023). "Moving from linear to circular economy in Saudi Arabia: life-cycle assessment on plastic waste management." Sustainability **15**(13): 10450.

Blomsma, F., et al. (2018). "Exploring circular strategy combinations-towards understanding the role of PSS." Procedia CIRP **69**: 752-757.

Blomsma, F., et al. (2019). "Developing a circular strategies framework for manufacturing companies to support circular economy-oriented innovation." Journal_of_Cleaner_Production **241**: 118271.

Bocken, N. M., et al. (2016). "Product design and business model strategies for a circular economy." Journal of industrial and production engineering **33**(5): 308-320.

Charalampides, G., et al. (2014). "Non-energy raw materials in Greece: a tool for sustainable development." Journal of Environmental Protection and Ecology **15**(2): 580-588.

Chin, H. H., et al. (2022). "Plastic circular economy framework using hybrid machine learning and pinch analysis." Resources, Conservation and Recycling **184**: 106387.

Chun-Rong, J. and Z. Jun (2011). "Evaluation of regional circular economy based on matter element analysis." Procedia Environmental Sciences **11**: 637-642.

De Mattos, C. A. and T. L. M. De Albuquerque (2018). "Enabling factors and strategies for the transition toward a circular economy (CE)." Sustainability **10**(12): 4628.

Di Maio, F. and P. C. Rem (2015). "A robust indicator for promoting circular economy through recycling." Journal of Environmental Protection **6**(10): 1095-1104.

Elia, V., et al. (2017). "Measuring circular economy strategies through index methods: A critical analysis." Journal of Cleaner Production **142**: 2741-2751.

Felicio, M., et al. (2016). "Industrial symbiosis indicators to manage eco-industrial parks as dynamic systems." Journal of Cleaner Production **118**: 54-64.

Figge, F., et al. (2018). "Longevity and circularity as indicators of eco-efficient resource use in the circular economy." Ecological economics **150**: 297-306.

Franco, M. A. (2017). "Circular economy at the micro level: A dynamic view of incumbents' struggles and challenges in the textile industry." Journal of Cleaner Production **168**: 833-845.

Genovese, A., et al. (2017). "Sustainable supply chain management and the transition towards a circular economy: Evidence and some applications." Omega **66**: 344-357.

Huysman, S., et al. (2017). "Performance indicators for a circular economy: A case study on post-industrial plastic waste." Resources, Conservation and Recycling **120**: 46-54.

Jemal, K. M., et al. (2023). Facilitating circular economy strategies using digital construction tools: framework development. Sustainability 15 (1), Art no 1.

Kaipainen, J., et al. (2022). "How companies innovate business models and supply chains for a circular economy: A multiple-case study and framework." International Journal of Innovation Management **26**(09): 2240024.

Karstensen, K. H., et al. (2020). "Circular economy initiatives in Norway." Circular economy: Global perspective: 299-316.

Kirchherr, J., et al. (2017). "Conceptualizing the circular economy: An analysis of 114 definitions." Resources, Conservation and Recycling **127**: 221-232.

Kravchenko, M., et al. (2019). "Towards the ex-ante sustainability screening of circular economy initiatives in manufacturing companies: Consolidation of leading sustainability-related performance indicators." Journal of Cleaner Production **241**: 118318.

Kumar, M., et al. (2024). "A review on value-addition to plastic waste towards achieving a circular economy." Science of the total environment: 171106.

Lanaras-Mamounis, G., et al. (2022). "A framework for assessing the contribution of firms to circular economy: a triple-level approach." Circular Economy and Sustainability **2**(3): 883-902.

Li, R. and C. Su (2012). "Evaluation of the circular economy development level of Chinese chemical enterprises." Procedia Environmental Sciences **13**: 1595-1601.

Liakos, N., et al. (2019). "Understanding circular economy awareness and practices in manufacturing firms." Journal of Enterprise Information Management **32**(4): 563-584.

Lieder, M. and A. Rashid (2016). "Towards circular economy implementation: a comprehensive review in context of manufacturing industry." Journal of Cleaner Production 115: 36-51.

MacArthur, E. (2013). "Towards the circular economy." Journal of Industrial Ecology **2**(1): 23-44.

MacArthur, E. (2013). "Towards the circular economy, economic and business rationale for an accelerated transition." Ellen MacArthur Foundation: Cowes, UK **1**.

McDonough, W. (2002). "michael Braungart." Cradle to Cradle: Remaking the way we make things.

Mendoza, J. M. F., et al. (2017). "Integrating backcasting and eco- design for the circular economy: The BECE framework." Journal of Industrial Ecology **21**(3): 526-544.

Mihai, F.-C., et al. (2021). "Plastic pollution, waste management issues, and circular economy opportunities in rural communities." Sustainability **14**(1): 20.

Millar, N., et al. (2019). "The circular economy: swings and roundabouts?" Ecological economics **158**: 11-19.

Moriguchi, Y. (2007). "Material flow indicators to measure progress toward a sound material-cycle society." Journal of Material Cycles and Waste Management **9**: 112-120.

Oladipupo, S. B., et al. (2024). "Assessment of plastic waste generation and management in residential locations, Ilorin, Nigeria: DPSIR analysis and circular economy pathway." Journal of Umm Al-Qura University for Applied Sciences: 1-16.

Park, J. Y. and M. R. Chertow (2014). "Establishing and testing the “reuse potential” indicator for managing wastes as resources." Journal of Environmental Management **137**: 45-53.

Pauliuk, S. (2018). "Critical appraisal of the circular economy standard BS 8001: 2017 and a dashboard of quantitative system indicators for its implementation in organizations." Resources, Conservation and Recycling **129**: 81-92.

Pomponi, F. and A. Moncaster (2017). "Circular economy for the built environment: A research framework." Journal of Cleaner Production **143**: 710-718.

Reike, D., et al. (2018). "The circular economy: new or refurbished as CE 3.0?—exploring controversies in the conceptualization of the circular economy through a focus on history and resource value retention options." Resources, Conservation and Recycling **135**: 246-264.

Rizos, V. and J. Bryhn (2022). "Implementation of circular economy approaches in the electrical and electronic equipment (EEE) sector: Barriers, enablers and policy insights." Journal of Cleaner Production **338**: 130617.

Saidani, M., et al. (2019). "A taxonomy of circular economy indicators." Journal of Cleaner Production **207**: 542-559.

Trần, T. V., et al. (2022). "Evaluation of factors affecting the transition to a circular economy (CE) in Vietnam by structural equation modeling (SEM)." Sustainability **14**(2): 613.

Urbinati, A., et al. (2017). "Towards a new taxonomy of circular economy business models." Journal of Cleaner Production **168**: 487-498.

Wang, N., et al. (2018). "Evaluation of Urban circular economy development: An empirical research of 40 cities in China." Journal of Cleaner Production **180**: 876-887.

3rd International Civil Engineering Conference (ICEC 2024)
Department of Civil Engineering
Federal University of Technology, Minna, Nigeria

STABILIZATION OF CLAY- RAP COMPOSITE WITH CALCIUM CARBIDE RESIDUE AND ZEOLITE FOR ROAD CONSTRUCTION - A REVIEW

*Gomna, B.[1]; Alhaji, M. M.[2]; & Alhassan, M.[3]
[1, 2, 3.] Department of Civil Engineering Federal University of Technology, Minna
*Corresponding author email: babagomna6@gmail.com

ABSTRACT

This paper review the previous studies on the stabilization of clay – RAP composite using calcium carbide residue (CCR) and zeolite as additive. Various studies have categorized clay soils as deficient soils for use as road construction material. The reclaimed asphalt pavement (RAP) have also been studied extensively as material that contained aggregate which can effectively be reutilized to improve deficient soil materials for road construction. However, the mixture of RAP with deficient clay soil was observed to perform satisfactorily without the intrusion of water from external sources. Where water get to the compacted clay-RAP mixture, the compacted specimen loose its strength immediately which makes the mixture to possess low durability. Addition of chemicals like calcium carbide residue (CCR) and Zeolite have been found to improve the engineering properties of individually and as a mixture. The CCR contributes calcium ion while the zeolite contribute both the silica and aluminate which together form a cementitious calcium silicate hydrate (CSH) and calcium silicate aluminate (CSA). The mixture of these two chemicals will serve to increase the durability of the deficient clay soil. Application of response surface methodology will bring out the relationship between all the variables used in the study and which can be used to derive a model equation that later can be applied for response prediction and the determination of optimal conditions.

Keywords: *Clay-Rap Composite; Calcium Carbide Residue; Zeolite; Response Surface Methodology; Stabilization; Unconfined Compressive Strength;*

1.0 INTRODUCTION

The stability and serviceability of most engineering projects or structure depends largely on their foundation and the bearing capacity of soil that supports them (Chesworth, 2008). A road pavement may serve its purpose if the foundation or sub grade meets the minimum required standard in the highway codes. Globally today there is an incessant increase in collapse of buildings and roads due to the foundation failure which result in the loss of lives and properties.

Clay composed of soil particles that are extremely fine (0.002mm in diameter). The particles are composed predominantly of mineral group of kaolinite, illite and montmorillonite (Craig, 1992; Das, 1998). Expansive soils of clay out-crop in large areas have caused persistent difficulties in road construction which is associated with volumetric change when subjected to water content (Houmadi *et al.*, 2009). These soils require stabilization to improve the requisite engineering properties of clay.

Clays are generally composed of micro-crystalline particles of a group of minerals. Since clay science has been the interest of people from different backgrounds, a specific definition of this material is not available (Sirivitmaitrie, C., *et al.*, 2008). Generally, clays are naturally occurring material primarily composed of fine-grained minerals, show plasticity when mixed with appropriate amount of moisture and become hard when dried (Sirivitmaitrie, C., *et al.*, 2011; Das, B., *et al.*, 2015). Das, 2015 indicated the characteristics of clay, which included: (a) Small particle size (usually smaller than 0.002 mm) (b) Net negative charge (c) Show plasticity when mixed with moisture

Clay Mineralogy Clay minerals are crystalline sheet like structure, which consist of hydrous alumino-silicates and metallic ions. There are two fundamental crystal units of clay minerals, i.e. tetrahedral and octahedral. A tetrahedral unit belongs to four oxygen enclosing silicon, where as an octahedral unit composes of six oxygen or hydroxyls at corners surrounding aluminum, magnesium, iron or other ions. The schematic of basic tetrahedral and octahedral unit are presented in Figures 1 and 2, respectively.

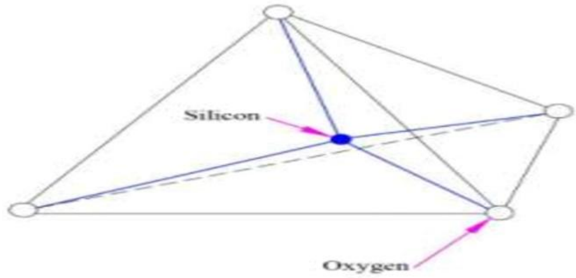

Figure 1.0: Single unit of tetrahedral mineral (Source: Mitchell, J., *et al.*, 2005)

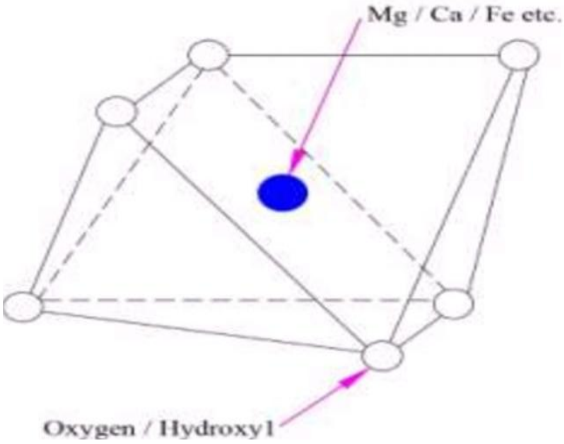

Figure 1.1: Single unit of octahedral mineral (Source: Mitchell, J., *et al.*, 2005)

Based on the arrangement of stacks, bonding, isomorphous substitution, and presence of metallic ions, different clay minerals can be constituted. Some of the common clay minerals are kaolinite, montmorillonite, illite, nontronite, muscovite, (Peng, X., *et al.*, 2006). However, for engineering purpose kaolinite, montmorillonite and illite have particular importance in geotechnical engineering (Hwang, C., *et al.*, 2006).

Kaolinite Kaolinite is known as 1:1 mineral because the inherent crystal structure consists of one tetrahedral and one octahedral sheet. Successive basic layers are bonded together by hydrogen bond between hydroxyls of the octahedral sheet and oxygen of the tetrahedral sheet. Due to this hydrogen bond, a large crystal of kaolinite is developed. The thickness of the basic crystal layer is 0.72 nm. A schematic of the crystal structure of kaolinite is presented in Figure 3.

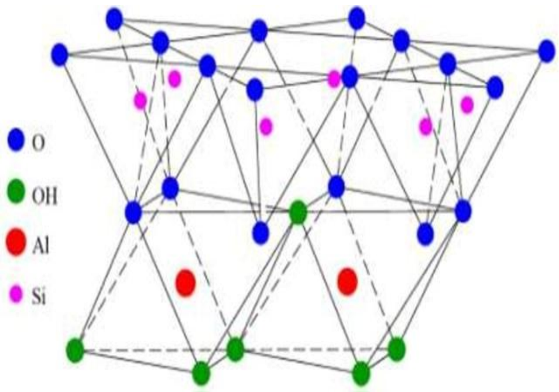

Figure 1.2: Structure of kaolinite crystal (Source: Mitchell, J., *et al.*, 2005)

Montmorillonite The basic unit of montmorillonite consisted of two silica sheets and one alumina sheet. This mineral is known as 2:1 mineral where the distance between the unit cells is approximately 0.96 nm. The top of the silica sheets are bonded by van der Waals force, and there is a net negative charge deficiency in octahedral sheet. Therefore, water and exchangeable ions can center and break the layer. The structural unit of montmorillonite is presented in Figure 4. Because of the layer separation and hydration, montmorillonite mineral is characterized by swelling behavior. In addition, montmorillonite minerals show extensive isomorphous substitution for $Si^{4+}$and Al^{3+} by available cations. According to the literature, Al^{3+} can replace as much as 15% of Si^{4+} in the tetrahedral sheet (Peng, X., *et al.*, 2006). The overall charge deficiency resulting from the ion substitution ranges from 0.5 to 1.2 per unit cell. The typical ranges of cation exchange capacity of montmorillonite are between 80 and 150 meq/100 g. The surface morphology of montmorillonite mineral is characterized by equidimensional flakes, and may appear as thin films. Furthermore, directional strain may cause by large amount of substitution of Fe^{3+} and/or Mg^{2+} for Al^{3+} which may result needle shaped fabric structure in montmorillonite. Due to the inherent configuration and high surface activity, the specific surface area (exclusive of interlayer zone) of montmorillonite can vary from 50 to 120 g /m .

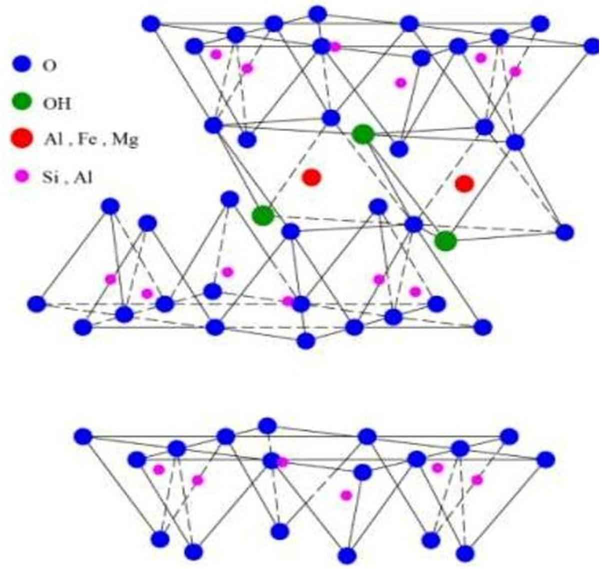

Figure 1.3: Structure of montmorillonite crystal (Source: Mitchell, J., *et al.*, 2005)

Illite Illite mineral is composed of two silica sheets and one alumina sheet, and known as 2:1 mineral. The basic unit configuration is similar to montmorillonite; however, the basic layers are bonded by potassium. The diameters of hexagonal aperture in silica sheet are exactly similar to the ionic radius of potassium (K^+). Therefore, the presence of potassium (K^+) makes the bond between the layers very strong. The schematic of the structure of illite is presented in Figure 5. The overall charge deficiently is mostly in the silica sheets, and ranged between 1.3 to 1.5 units per cell. The additional charge is balanced by non-exchangeable potassium (K^-) ions. The typical cation exchange capacity of montmorillonite ranges from 10 to 40 meq/100 g.

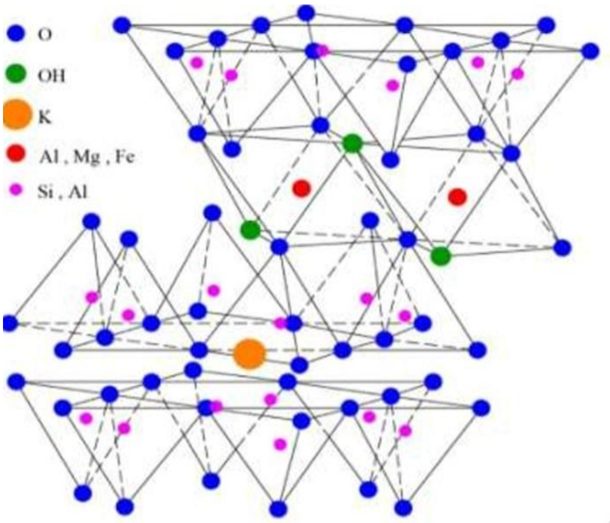

Figure 1.4: Structure of illite crystal [19]

Soil stabilization is the use of stabilizing agents (binder materials) in weak soils to improve its geotechnical properties such as compressibility, strength, permeability and durability to withstand the engineering structural loads (Sherwood, 1993). Improvement in the various geotechnical properties of soil can be achieved by stabilization with suitable materials. Reclaimed Asphalt Pavement (RAP) is the term given to reprocessed and or removed pavement materials which, has been pulverized usually by milling and is used like an aggregate in recycled asphalt pavement (Jeff & Miles, 2006). Therefore, the recycling of pavement materials has become a viable alternative material for consideration in road maintenance and rehabilitation with conservation of resources and environment (Taha *et al.,* 2002).

Calcium carbide residue (CCR) is another form of industrial waste being used by researchers to improve properties of expansive soils (Krammart *et al.,* 2004). It is a by-product obtained from the acetylene gas (C_2H_2) production process. Mixture of CCR with pozzolana which has high silica (SiO_2) or alumina (Al_2O_3) can yield pozzolanic reactions and formation of excess cementitious material. The results have been found to be similar to those obtained from the cement hydration process (Wang *et al.*, 2013).Welding activities in Nigeria has led to the generation of calcium carbide residue deposits.

Zeolites as a pozzolana are aqueous aluminum silicates containing alkali and alkaline earth elements. Their structure is made up of a framework of SiO_4 and AlO_4 tetrahedrons linked to each other's corners by sharing oxygen atoms. Zeolites have been recognized over the decades, but only during the middle of the twentieth century they have attracted the attention of researchers who demonstrated their technological importance in several fields (Cincotti *et al.*, 2006).

Response Surface Methodology (RSM) is a mathematical and statistical technique useful for modeling and analysis of a problem in which a response of interest influenced by several variables with the aim of optimizing the process parameters (Meyers *et al.,* 2002). The design of experiments, the RSM expels systematic errors and reduces the number of experiments required to obtain the optimum values. There are several classes of response surface design that are useful in practice, such as the Central composite design (CCD), Box-Boekhen design, Hybrid design, and Three-design (Khuri and Connell 1996, Mason *et al.,* 2003). The central composite design (CCD) approach was used to design and build model for experimental variables to evaluate and determine their responses of interest. This optimization approach tool can be used in any process or product design and is more helpful for researchers whose area is concerned with the optimization. The major advantages of RSM can be stated as follows (1). No. of experimental run can be reduced (2). Response can be predicted prior to the experimentation phase. (3). It can able to detect the parameter interaction effect on response. CCD and Box-Behnken are two effective designs used in RSM. The central composite design (CCD) is a well-known design for setting a quadratic model. Based on the number of levels and parameters CCD can be classified into CCC, CCI and CCF as described earlier. Box-Behnken method is used for solving the multi objective optimization problem (Meyers *et al*., 2002).

2.0 PROBLEM STATEMENT

Many researchers have used waste recycled reclaimed asphalt pavement (RAP) to stabilize weak soil materials for road construction purposes (Alhaji and Alhassan, 2018; Jeff and Miles, 2006). Weak soils have been stabilized in Nigeria by many researchers using different chemicals and methods to achieve different results. However, optimization of RAP-clay composite using CCR and Zeolite for stabilization has not been given much attention in literature.

The study by (Rehman *et al.,* 2017; Moghal *et al.*, 2016 and Abdullah *et al.,* 2021) indicated that, an enormous amount of energy, time and numbers of experimental trial are required to determining the optimal or best possible solutions using the optimization models, and optimization technique in chemical stabilization to reduce the number of samples required to be tested to achieve optimal chemical mixtures for maximum strength and stability. Over the years, cementitious materials like cement, lime and fly ash has been used for soil stabilization in Nigeria but some researchers like (Alhaji *et al.,* 2014; Ismail *et al.,* 2014; Osinubi and Alhaji, 2008; Prasad *et al.,* 2017; Basha *et al.*, 2005 and Ibrahim *et al.,* 2020) all worked on stabilization of soil using the combination of other materials, methods and the studies recorded higher strength compared to the use of cement alone.

A limited numbers of geotechnical studies have been reported in the literature on the use of RSM technique of optimization, from which we can cite the work of some researchers like (Badri *et a*l 2020; Lu *et al.*, 2015; Myers *et al*., 2016; Shirazi *et al*, 2020, Zhang *et al*., 2020) used and recommended the response surface methodology for the design of experiments (DOE) in civil engineering experimental studies.

3.0 LITERATURE REVIEW

3.1 Response Surface Method Application in Engineering

Response surface methodology (RSM) was introduced by Box and Wilson in the early 1950s; it was a collection of statistical and mathematical techniques useful for the development and optimization of processes (Dwornicka & Pietraszek, 2018). The Concepts and techniques of response surface methodology (RSM) have been applied successfully and extensively in different scientific and research areas (Zangeneh *et al*., 2002). The philosophy behind a response surface method is to sequentially run relatively simple experiments or models in order to optimize a response variable of interest. In other words, we run a small number of experiments sequentially that can provide a large amount of information upon augmentation. Some researchers like (Badri *et al*., 2020; Lu *et al*., 2015; Myers *et al*., 2016; Shirazi *et al*., 2020; Zhang *et al*., 2020) used and recommended the response surface methodology for the design of experiments (DOE) in civil engineering experimental studies.
In general, the response surface can be visualized graphically. The graph is helpful to see the shape of a response surface; hills, valleys, and ridge lines. Hence, the function f (x_1, x_2) can be plotted versus the levels of x_1 and x_2 as shown in Fig. 2.4 (Montgomery, 2005). The RSM optimization involves three primary steps:

i. Statistically calculated trials.
ii. Estimating the coefficients.
iii. Predicting the response and validating the model adequacy with the experimental arrangement (Mahalik *et al.,* 2010).

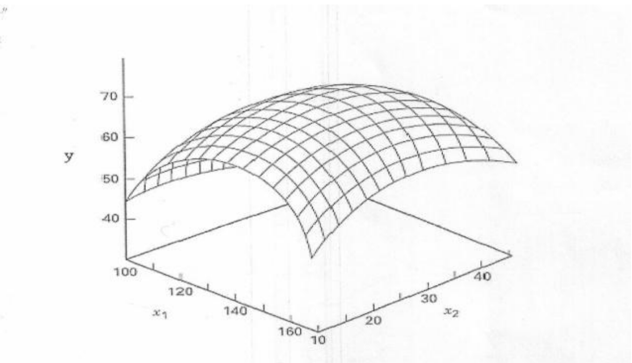

Figure 3.1: Response surface plot (Source: Montogomery, 2005)

In order to understand the surface of a response, graphs are helpful tools. But, when there are more than two independent variables, graphs are difficult or almost impossible to use to illustrate the response surface, since it is beyond 3-dimension. For this reason, response surface models are essential for analyzing the unknown function *f(*x). In such circumstances response surface methodology is recommended to establish an approximate explicit functional relationship between input variables say (x_1, x_2, x_3 ...xn) and output response (y) through regression analysis for the range of expected variation in the input parameters in Equation (3.1).

$Y = f(x_1, x_2, x_3 ...) + e$ ……………………………3.1

Where error "e" represents the noise or error observed in the response y. If we denote the expected response by E(y) = f(x1, x2) = n, then the surface represented by n = f(x_1, x_2) is called a response surface.

The above relationship can be simple linear or factorial model, or more complex quadratic or cubic model. "e" represents other sources of uncertainty not accounted for in "f", such as measurement error on the output response, other sources of variation inherent in the process or the system, effect of other variables and so on. In brief, 2^a factorial design is often used to fit linear and non-linear (second order) response surface models for n number of input variables. These set of input variables are also termed as natural variables as they are given in their respective units. If the response is well modeled by a linear function of the independent variables, then the approximating function is the first order model given by Equation (2.2)

$y = \beta_o + \beta_1 x_1 + \beta_2 x_2 + \ldots + \beta_k x_k + E$ ………………(3.2)

If there is curvature in the system, then a polynomial of higher degree must be used, such as the Second-order model given by Equation (3.3)

$y = \beta_o + \sum \frac{k}{i}{}_{=1} \beta_i x_i \sum \frac{k}{i}{}_{=1} \beta_{ii} x^2{}_i + \sum \sum {}_{I<i\,j} x_j + E$…… (3.3)

The second order or quadratic regression model includes the square terms in addition to the terms above. For a 3-component variable, it may be expressed in Equation $Y = \beta_0 + \beta_{1x1} + \beta_{2x2} + \beta_{3x3} + \beta_{11x1}{}^2 + \beta_{22x2}{}^2 + \beta_{33x3}{}^2 + \beta_{12x1x2} + \beta_{13x1x3} + \beta_{23x2x3} + E$ ……………………………(3.4)

In the above equations x, is the input variables, βo is the regression coefficient this empirical model is called response surface model.

The contour plots can show contour lines of x_1 and x_2 pairs that have the same response value y as shown in in Figure (2.1). There are several classes of response surface design that are useful in practice, such as Central composite design (CCD), Box-Behnken design, Hybrid design, and Three-design (Khuri & Comell 1996, Mason *et al*., 2003).

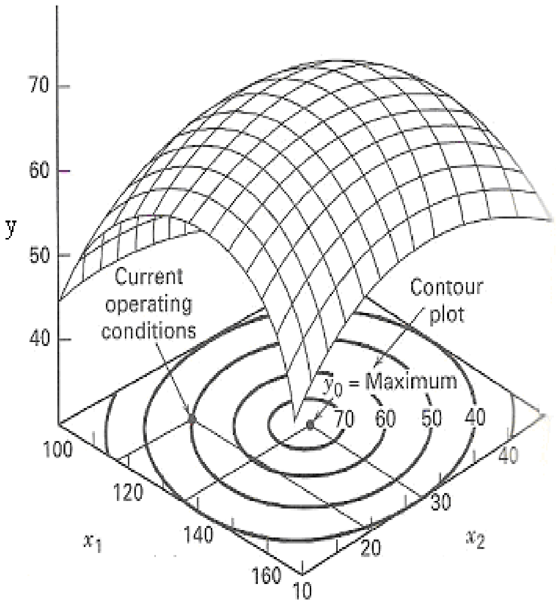

Figure 3.2: Response surface contour plot (Source: Montgomery, 2005).

In a recent study by Zhang et al (2020) that worked on micaceous problematic soil. In the study, RSM modeling was used to model UCS of micaceous soils as a function of the dosage of various additives. The additives included two combinations: (i) slag and fiber, and (ii) slag and polymer. In the end, the performances of micaceous soils were improved by applying a combination of granulated blast furnace slag, fiber and polymer additive. Most of the combinations were found to increase the material strength and ductility. To refine the dosage, response surface method was used to conduct experimental design and develop predictive models for material strength. The developed models formulate the material strength as a nonlinear function of dosages, which was used to optimize additive contents in terms of target requirements.

The model was verified through trials and was used to determine dosages to upscale micaceous soils to field conditions. The combinations of fibers and pozzolanic additives are able to enhance both the strength and ductility.

Lin of al. (2005) performed a study on the effect of Sewage Sludge Ash (SSA) on the strength of silty clay, and found that the Unconfined Compressive Strength (UCS) performance of soil is enhanced two or three times with the decrease of swelling properties. Also, the increment in the amount of Sewage Sludge Ash (SSA) results in increase in the cohesion and decrease in the angle of internal friction. Lin et al (2007a) employed SSA and hydrated lime for improvement of the engineering properties of soft soil. It is found that the addition of SSA+ lime increases the UCS of soft cohesive soil as much as three to seven times and reduces the swelling properties. They concluded that SSA-lime mixture could be introduced to soft cohesive soil in order to improve its geotechnical properties such as compressive strength, California bearing ratio and swelling in the soil stabilization applications modeled using the RSM.

Lin *et al*. (2007b) performed an investigation on the use of Sewage Sludge Ash (SSA) as a soil stabilizer for improvement of the strength characteristics of soft cohesive soil such as compressive strength, bearing capacity and shear strength. They found that the UCS performance of soil treated with Sewage Sludge Ash SSA is 14-2 times better than that of untreated soil. Chen & Lin (2009) used Sewage Sludge Ash (SSA) mixing with cement in order to improve the strength properties of soft soil. While the UCS value increases roughly three-seven times of native soil, the swelling potential decreases up to 60%. They concluded that SSA could be used together with cement for the stabilization purposes.

Lia *et al* (2013) proposed a response surface optimization design method for the foundation pit soil nailing, and Algin (2016) used RSM in the multi objective optimization analysis to present the optimized design solution of a jet grouted raft.

Khoshnevisan *et al*. (2017) used response surface-based robust geotechnical design of supported excavation by means of a spreadsheet-based solution. Lafifi *et al*. (2019) on the other hand, used a combination of Taguchi's design of experiment (DOE), RSM to optimize geotechnical parameters of a synthetic soil for pressure-meter test.

Du *et al*., (2011), used Calcium Carbide Residue (CCR) and lime as binders to treat over-wetted clays being used us as embankment filling material. It was concluded from their tests that CCR treated soils have better performance than that of lime treated soils and can be adopted as an alternative binder to treat over-wetted soils being used for highway embankment. Bandyopadhyay *et al*., (2016) worked on stabilization of soil using ground granulated blast furnace (GGBS) and CCR. It was concluded that with increase of CBR values, the optimum moisture content (OMC) increased and maximum dry density (MDD) decreased which was due to the water absorbing nature of CCR.

4.0 APPLICATION OF DESIGN OF EXPERIMENTS (DOE)

The choice of the design of experiments can have a large influence on the accuracy of the approximation and the cost of constructing the response surface. An important aspect of RSM is the design of experiments (Box and Draper, 1987), usually abbreviated as DOE. These strategies were originally developed for the model fitting of physical experiments but can also be applied to numerical experiments. The objective of DOE is the selection of the points where the response should be evaluated. Most of the criteria for optimal design of experiments are associated with the mathematical model of the process. Generally, these mathematical models are polynomials with an unknown structure, so the corresponding experiments are designed only for every particular problem. In a traditional DOE, screening experiments are performed in the early stages of the process, when it is likely that many of the design variables initially considered have little or no effect on the response. The purpose is to identify the design variables that have large effects for further investigation. A detailed description of the design of experiments theory can be found in Box & Draper (1987), Myers & Montgomery (1995), among many others. A particular combination of runs defines an experimental design. The possible settings of each independent variable in the N dimensional space are called levels.

The Box-Whilson Central Composite Design, commonly called a Central Composite Design (CCD), is the most popular of all second-order designs. This design consists of the following parts:

i. A complete or a fractional of 2k factorial design whose factors' settings are coded as (Low-1, High = 1), this is called the factorial portion.
ii. An additional design, star points, which provides justification for selecting the distance of the star points from the center; the CCD always contains twice as many star points as there are factors in the design ($2k$)
iii. Thus, the total number of design points in a CCD is $n = 2^k + 2k + 1$.

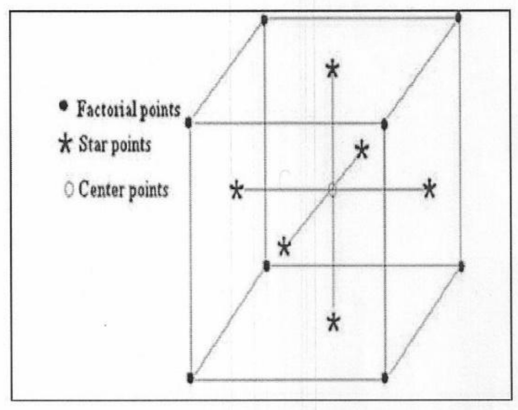

Figure 4.1 Structure of composite Design (Source: Pradeep ***et al*., 2020)**

A CCD is obtained by augmenting the first-order design of a 2k factorial with additional experimental runs, the 2k axial points, and the center-point replications. This design is consistent with the sequential nature of a response surface investigation. The analysis starts with a first-order design and a fitted first-degree model, followed by the addition of design points to fit a higher second-degree model. The first-order design in the preliminary phase gives initial information about the response system and assesses the importance of the factors in a given experiment. The additional experimental runs are performed for the purpose of obtaining more information. This information helps to determine the optimum operating conditions of the independent variables by using the second-degree model. In the CCD, the values of α and 1, are chosen for their desirable properties, where α is the axial point and 1 the number of center point replicates. (Khuri *et al*., 2017; Khuri & Cornell; 1996).

The number of tests required for CCD is given by:
$2^k + 2k + 1$………………………………………….(3.5)
Where,
N = total number of runs or experiments
k = number of independent variables or factors.
nc = number of center points if the distance from the center of the design space to a factorial point is ±1 unit for each factor, the distance from the center of the design space to a star point is $|a| > 1$. The precise value of α depends on certain properties desired for the design and on the number of factors involved.

5.0 CONCLUSION

The use of CCR and Zeolite additives in the literature was found to enhance the pozzolanic reaction, improve the microstructure, and increase the resistance to degradation of the soil foundation. The use of central composite design (CCD) or Box-Behnken method using the analysis of variance (ANOVA) to evaluate the degree of accuracy held by the derived model based on several responses, to determine the best experimental design in order to identify the relationship between variables. The results from the papers showed significant improvements in the mechanical properties of the stabilized clay, indicating it potential as sustainable and cost – effective materials for road construction, reducing the risk of incessant road failures, and minimizing environmental impacts by providing valuable insights into the use of industrial by-products and natural minerals as additives for soil stabilization.

6.0 REFERENCES

Alhaji, M. M., Jibrin, R., Etsuworo, N. M. & Alhassan, M. (2014). Stabilization of A-6Lateritic Soil Using Cold Reclaimed Asphalt Pavement, *International Journal of Engineering and Technology*, 4 (1), 52-57.

Badri R.M., AL Kaissi, Z.A., & Alobaidi (2020). Investigating the rheological properties of asphalt binder incorporating different crumb rubber content based on a Response Surface Methodology. J.king Saudi Univ. *Eng. Sci.*3(2), 230- 579.

Basha, E. A., Hashim, R., Mahmud, H. B. & Muntohar, A. S. (2005), Stabilization of Residual Soil with Rice Husk Ash and Cement, Construction and Building Materials, 19, 448-453.

BS 1377. 1990. Methods of test for soils for Civil Engineering purposes. BritishStandardInstitute,London, UK.

Chesworth, W. (2008). *Encyclopedia of Soil Science.* Dordrecht, Netherland; Springer

Cincotti, A.Mameli, A.M.Locci, R.Orru.G.Cao (2006), *Industrial and Engineering Chemistry Research*45(3), 1074-1084.

Das, B., "Principles of foundation engineering", Cengage learning, 2015.

Houmadi, Y.Mamoune, S.M.A. and Belakhdar k.(2009) swelling and Geotechnical Cartography of Saida Soils. *Jordan journal of Civil Engineering*, 3(1), 32-40.

Hwang, C., "Determination of material functions for unsaturated flow", Ph. D. dissertation, University of Colorado, Boulder, Co, USA, 2002.

Ismail, A. Baghini, M. S. Karim, M. R., Shokri, F., Al-mansoba., R. A., Firoozi, A. A. & Firoozi, A. A. (2014). Laboratory Investigation on the Strength Characteristics of Cement-Treated Base, *Applied Mechanics and Materials*, 507, 353-360

Jeff, R. & Miles, P.E. (2006). Guidelines for Use of RAP. No. 13, 87-94.

Khuri, AI, Cornell, JA. (1996) *Response Surfaces*. 2nd Ed. New York: Dekker.

Krammart, P. & Tangtermsirikul, S. (2004) Properties of Cement made by partially replacing Raw Material with solid waste ashes and Calcium carbide waste. *Construction and building Materials*, 18(8), 62-69.

Lu, J. Xu & R. LiX. (2015). Application of Response Surface Methodology in organic matter soil stabilization. *Electronic Journal Geotech. Eng.* 20, 3633-3646.

Mahalik, K. Sahu, J., Patwardhan, A.V. &Meikap, B. (2010) Statistical modelling and optimization of hydrolysis of urea to generate ammonia for flue gas conditioning. *J. Hazard. Mater. 182*, 603–610. ***Google Scholar***. **CrossRef** [**PubMed**]

Mason, R.L., Gunst, R.F & Hess, J.L. (2003) *Statistical design and analysis of experiments*: With application to engineering and science, John Wiley & Sons.New Jersey,USA.

Mitchell, J., SOGAK, "Fundamentals of soil behavior", New York: John Wiley & Sons, 2005.

Myers RH, Montgomery DC, Vining GG. (2002) *Generalized Linear Models with Applications in Engineering and the Sciences*. New York: John Wiley & Sons.

Myers, R. H., Montgomery, D. C., & Anderson-Cook, C. M. (2009). Response Surface Methodology: Process and product optimizationusing designed experiments, 3rd ed., John Wiley & Sons, New Jersey,USA.

Myers, R.H., Montgomery D.C., & Anderson-Cook, C.M., (2016). Response Surface Methodology: *Process and Product Optimization Using Designed Experiments*. John Wiley & Sons Inc. USA

Osinubi, K. J & Alhaji, M.M. (2008) optimal use of Bagasse Ash on Cement Stabilized Laterite. *NSE* Technical Transactions, 44(1), 1-6.

Peng, X., Horn, R., Peth, S. & Smucker, A., "Quantification of soil shrinkage in 2D by digital image processing of soil surface", Soil and Tillage Research, vol. 91(1): p. 173-180, 2006.

Prasad, D., Borthakur, N. & Das, S. (2017). Effect of Rice Husk Ash and Cement Mixtures on

Sherwood, P. (1993). Soil Stabilization with cement and lime. *State of the Art Review*. London:

Shirazi M., Kademalrasoul A. & Safieddin, A.S.M., (2020). Multi-objective Optimization of Soil Erosion Parameters using Response surface Methodology in the Emamzadeh Watershed. *Acta Geophysics*. 68, 505-517.

Sirivitmaitrie, C., Puppala, A. J., Chikyala, V., Saride, S. & Hoyos, L. R., "Combined lime and cement treatment of expansive soils with low to medium soluble sulfate levels", American Society of Civil Engineers, Proceedings of the Geo Congress, pp. 646-653, 2008.

Sirivitmaitrie, C., Puppala, A. J., Saride, S. & Hoyos, L., "Combined lime-cement stabilization for longer life of lowvolume roads", Transportation Research Record: Journal of the Transportation Research Board, vol. 2204(1): pp. 140-147, 2011.

Taha, R. AL-Harthy, K.A &Muamer A. (2002), Cement Stabilization ofReclaimed Asphalt Pavement Aggregate for Road Bases and Sub-bases *Journal of Materials in Civil Engineering, ASCE,* 3(14), 239-248.
Transport Research Laboratory, HMSO.

Wang Y.L.,Dong S.J., Liu L.L. & Cui, S.P. (2013). *Material Science Forum* 1(743), 171-174.

Zhang, J., Deng, A. & Jaksa, M. (2020). Optimizing Micaceous soil stabilization using response surface methodology. *J. Rock Mech. Geotech. Eng*. http://doi.org/10.1016/j.jrmge.2020.05.05

ANALYZING GEOTECHNICAL FACTORS CONTRIBUTING TO PAVEMENT FAILURE: A CASE STUDY OF THE MINNA-PAIKO ROAD IN NIGER STATE

*Bello, M.[1]; Alhassan, M.[2]; & Alhaji M. M.[3]
[1] Department of Civil Engineering Federal University of Technology, Minna
*Corresponding author email:mhobello@gmail.com

ABSTRACT
Pavement failure poses a significant challenge to transportation infrastructure worldwide, impacting economic development and societal well-being. This paper investigates the geotechnical factors contributing to pavement failure along the Minna-Paiko road in Niger State, Nigeria. The study employed a combination of field investigations, including visual inspection, soil sampling, and laboratory testing, to characterize the subgrade soil properties. The results revealed that the subgrade soil along the Minna-Paiko road is characterized by low bearing capacity, poor drainage, and susceptibility to volume changes. These geotechnical deficiencies, coupled with inadequate pavement design and construction practices, have significantly contributed to the observed pavement distresses, including cracking, rutting, potholes, and edge failures. The paper concludes with recommendations for improved geotechnical investigation, pavement design, construction, and maintenance practices to mitigate future pavement failures along this critical roadway.

Keywords*: Pavement failure, Geotechnical factors, Subgrade soil, Minna-Paiko Road, Niger State, Nigeria, Case Study.*

1 INTRODUCTION

Road infrastructure plays a vital role in connecting communities, facilitating trade, and driving economic growth. However, the effectiveness of roads is often compromised by premature pavement failures. Pavement failure is defined as the deterioration of the pavement structure to a point where it no longer provides a safe, comfortable, and functional riding surface. These failures can manifest as cracking, rutting, potholes, edge failures, and other forms of distress (Aliyu & Eberemu, 2018).

The Minna-Paiko road in Niger State, Nigeria, is a critical transportation artery connecting the state capital, Minna, to other significant towns and agricultural areas. However, this road has been experiencing significant pavement failures within a relatively short period after construction and/or rehabilitation. These failures disrupt traffic flow, increase travel time and costs, and pose safety hazards to road users.

While traffic loading and environmental factors contribute to pavement deterioration, geotechnical factors relating to the subgrade soil properties are often the primary culprits. Understanding these geotechnical factors is crucial for developing effective pavement design and construction strategies to ensure long-term pavement performance (Ahmed, 2014).

This study aims to investigate the specific geotechnical factors contributing to pavement failure along the Minna-Paiko Road corridor. By identifying the underlying causes of the failures, this research will contribute to improved pavement design and maintenance practices, ultimately enhancing the durability and service life of this crucial transportation infrastructure.

1.1 Description of the Study Area

Paiko-Minna Road originates from Diko junction to Kaduna-Abuja dual carriageway way. It passes through towns and villages such as Maje, Izom, Lambata, Kwakuti, Farin Doki, Gwam, Wabe, Paiko, Pogo, and terminates in Minna. The study area is located between latitude 9°16’N, longitude 6°33’E (Minna). The entire length of the road is about 12.1km. The existing highway is of standard 7.3m wide single carriageway with asphaltic concrete surfacing and base course of naturally occurring lateritic soil. It exhibits various conditions ranging from the newly repaired portion to the fair, and to completely failed sections. Figure 1. shows the Minna-Paiko road in Minna, Nigeria.

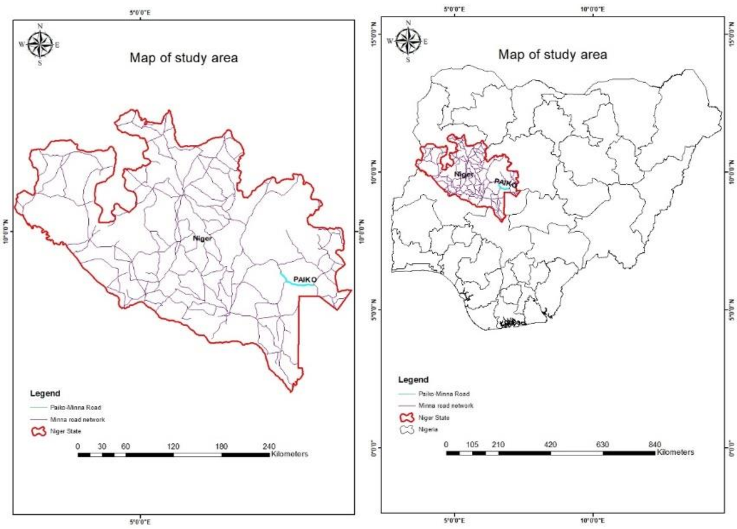

Figure 1: Map of Study Area

2 LITERATURE REVIEW

Previous research highlights the significant influence of geotechnical factors on pavement performance. Several studies emphasize the importance of understanding the subgrade soil properties, including:

i. Bearing Capacity: Low bearing capacity of subgrade soils can lead to excessive pavement deformation under traffic loads, resulting in rutting and cracking (Ahmed, 2014).

ii. Drainage: Poor drainage can saturate the subgrade soil, reducing its strength and leading to accelerated pavement deterioration. This is particularly critical in areas with high rainfall (Jones & Smith, 2010).

iii. Volume Change: Expansive soils, which swell and shrink with changes in moisture content, can exert significant stresses on the pavement structure, causing cracking and unevenness (Nelson & Miller, 1992).

iv. Soil Type and Gradation: The type and gradation of subgrade soil influence its permeability, stability, and resistance to erosion. Well-graded soils generally provide better support for pavements compared to poorly graded soils (Das, 2010).

v. Compaction: Adequate compaction of the subgrade and pavement layers is crucial for achieving the desired strength and stability. Poor compaction can lead to premature pavement failure (Huang, 2004).

Studies specific to Nigeria have also highlighted the challenges posed by expansive clays and inadequate drainage in many regions (Ezeokonkwo & Olofsson, 2015; Aliyu & Eberemu, 2018). These findings emphasize the need for site-specific geotechnical investigations to characterize the subgrade conditions adequately and tailor pavement design accordingly.

3 METHODOLOGY

The methodology employed in this study comprised the following steps:

a) Site reconnaissance and visual inspection: A preliminary site reconnaissance was conducted along the Minna-Paiko road to identify areas exhibiting significant pavement failures. The type and extent of distresses (cracking, rutting, potholes, edge failures) were documented and photographed.

b) Soil Sampling: Disturbed soil samples were collected from the subgrade at representative locations along the road alignment, focusing on areas where pavement failures were observed. Samples were taken at depths representative of the subgrade layer, typically within 1 meter of the pavement surface.

c) Laboratory Testing: The collected soil samples were subjected to a series of laboratory tests to characterize their geotechnical properties. These tests included:

   i. Particle Size Analysis (Sieve Analysis and Hydrometer Test): To determine the soil gradation and classification.

   ii. Atterberg Limits (Liquid Limit, Plastic Limit, and Plasticity Index): To assess the soil plasticity and potential for volume change.

   iii. Moisture Content Determination: To determine the in-situ moisture content of the soil.

iv. Compaction Test (Standard Proctor Test): To determine the optimum moisture content and maximum dry density for compaction.
v. California Bearing Ratio (CBR) Test: To assess the bearing capacity of the subgrade soil under saturated conditions.
vi. Permeability Test: To evaluate the drainage characteristics of the soil.

- Data Analysis and Interpretation: The laboratory test results were analyzed and interpreted to assess the suitability of the subgrade soil for pavement construction. The data was compared with established geotechnical criteria and guidelines for pavement design.
- Correlation and Conclusions: The results of the laboratory tests were correlated with the observed pavement distresses to identify the specific geotechnical factors contributing to the failures. Conclusions were drawn regarding the causes of pavement failure and recommendations were made for improved pavement design and construction practices.

Ultimately, the study involved two aspects; Field investigations and laboratory tests.

Field investigation

The field investigation was in three folds;

i. Condition survey of the road,
ii. Dynamic cone penetration test, and
iii. Sample collection along the road.

Condition Assessment

As part of the condition evaluation process, a five-point rating system was used for the principal categories of distress along the route, along with their intensities and extents. The World Bank/Organization for Economic Cooperation and Development (OECD) five-point rating system, which is shown below, was used to assess the state of the road:

1=Excellent (No pavement distress exists)
2=Good
3=Fair
4=Critical
5=Poor (Complete pavement deterioration)

The average rating for each major category of distress in a segment of road pavement is the condition rating of that section. The average of each section's rating represents the overall state of the pavement.

Dynamic cone penetration

The dynamic cone penetration test is a test carried out to find the resistance value of the cone against the soil that helps us to determine different mechanical properties of soil such as strength, bearing capacity, and so on. The CBR values are calculated from penetration resistance readings, obtained from the DCP test on site. The California Bearing Ratio (CBR) values were then used to judge the stability of the required pavement structures.

A sub-grade sounding test was also carried out along the road as shown in Plates I at specific intervals (at failed and unfailed sections) using a Dynamic Cone Penetrometer (DCP). This was done at somewhat smaller horizontal intervals in order to assess the subgrade strength (in-situ CBR). The Dynamic Cone Penetration (DCP) test was performed using a 60-degree cone head dynamic penetrometer and a lightweight 10 kg rammer. The number of blows for every 10 cm penetration was noted during the penetration test, which was carried out to a maximum depth of 1.20 meters. However, the average measurements for a stratum thickness of 20 cm were used for analysis and presentation. Using the correlation depicted in Equation 1, the strength (CBR) of the pavement structures (subgrade) was determined by averaging the number of strikes.

$$Log\ (CBR) = 2.48 - 1.057Log(PI) \quad (1)$$

Where PI = Penetration Index or Penetration Rate

Plate I: DCPT test in progress

The test measures the materials' insitu resistance to penetration and was carried out in compliance with TRL (2008) of the UK. A metal cone was driven into the ground during the test by continuously hitting it with an 8 kg weight rammer that was dropped from a height of

575 mm. To obtain a continuous measure of the penetration resistance up to 5 1.5 meters below the ground surface, the cone's penetration was measured and recorded following each strike.

Collection of samples

The pavement investigation was done by digging trial pits of 1.0 m x 1.0 m and soil samples were collected at some selected critical and stable locations along shoulders and median of the highway and dynamic cone penetration test was carried out. The depth at which samples were collected ranged from 0.8 m to 1.7m based on the terrain of each location. Samples were preserved in polythene bags to avoid contamination and moisture loss and were transported to the laboratory for further investigation.

Samples were collected from subgrade, subbase and base layers of the road. The collected samples were taken from different locations along the road, at both unfailed (Plate III) and failed (Plate II) sections from trial pits at dug collection points.

Plate II: Collection of Samples

Plate III: Collection of Samples

The natural moisture content of the samples was determined within 48 hours in the laboratory. This was followed by air drying of the samples, by spreading them out on trays at enclosed area at room temperature for four days. Large soil particles (clods) in the samples were broken with a wooden mallet.

Laboratory Test

All the collected soil samples were tested based on procedures outlined in BS. 1377 (1990). The tests included index properties, compaction characteristics and strength properties test.

Natural moisture content determination

The ratio of the mass of water to the mass of solids in a specific mass of soil is known as the natural water content, or natural moisture content. The moisture content was calculated using Equation 2.

$$NMC = \frac{M_2 - M_3}{M_3 - M_1} * 100 \qquad (2)$$

Where;
NMC= natural moisture content
M_1= mass of empty cans
M_2= mass of empty cans plus wet samples
M_3= mass of empty cans plus dry samples.
The procedure was repeated for all the remaining soil samples.

Index properties test

Particle Size Distribution

300g of air-dried soil sample was weighed as total mass in (g) and soaked with water for 24hrs, the soaked sample was washed through BS sieve 0.075mm. The material retained on BS sieve 0.075mm was then transferred into tray and dried in oven at 105^0C to 110^0C. After allowing it to cool, it was weighed as mass of soil after washing. The dried sample was placed on the top of set of sieves and mechanical sieve shaker was operated for 10min and the amount of soil retained on each sieve was weighed and recorded, while the percentage of soil passing each sieve was calculated and the grading curve plotted on a semi-log graph.

Atterberg limits

a) Liquid Limit

The test was carried out in accordance with BS 1377 (1990); part 2. 300g of air dried sample passing through BS sieve 0.425mm was weighed and placed on glass plate and distilled water was added to the sample and mixed for at least 10min. Using two palates knifes, the mixed soil sample was placed into cup with palate knife up to the brim. The excess sample was striked off to give a smooth level.

b) Plastic Limit and Plasticity Index

Plastic limit and plasticity index were carried out in accordance with BS 1377 (1990); part 2. 40g of clay sample passing through BS sieve 0.425mm was placed on a glass plate and then mixed thoroughly with water. The mixed sample was rolled between the palms and flat glass plate to form a thread of 3mm diameter. The process continued until the thread crumbled when the diameter is 3 mm. The sample of the thread was collected for moisture content determination and plasticity index was calculated using Equation 3.

$$P = LL - PL \tag{3}$$

(c) Specific Gravity Test

Specific gravity of clay soil was carried out in accordance with BS 1377 (1990); part 2. The specific gravity will then be calculated using Equation (4).

$$GS = (\frac{W2-W1}{(W4-W1)-(W3-W2)} \tag{4}$$

Where: G_s is the Specific Gravity.

W_1 is the mass of density bottle (g)

W_2 is the mass of bottle +dry soil (g)

W_3 is the mass of bottle + dry soil + water (g)

W_4 is the mass of bottle + water (g)

Strength properties

a. Compaction test

The compaction test was carried out in accordance with the procedure outlined in BS 1377 (1990). The empty mould and moisture content cans were weighed and recorded. The height and diameter of the mould was recorded. 3000g of the air-dried soil sample was measured and poured into the mixing tray. Using a wooden hammer, lumps of the sample were pulverized. Relatively little quantity of water was added to the soil, mixed properly, and divide into 5 portions. The collar of the mould was placed back on the mould and secured. Each portion was placed as a layer into the assembled mould and compacted using 4.5kg rammer. 25 blows were applied to each layer. The collar was removed, excess soil trimmed, and the surface of sample at the top was scraped to level with the top of the mould's rim. If there are voids, the remaining materials was used to fill these voids. And scraped again to level. The mould and sample were weighed without the collar, and recorded. Using the knife, samples were taken from the top and bottom of the mould and placed in two different labelled moisture content cans, and placed in oven for 24 hours to dry, for moisture content. The masses of the cans and wet samples were recorded. The samples were then extracted from the mould, unto the mixing tray. The wooden hammer was used to pulverize the sample and it was remixed with additional quantity of water, and the whole procedure was repeated until the system failed. This is when the mass of sample and mould drops. The bulk and dry densities for each trial were calculated using Equations 4 and 5.

$$\rho_b = \frac{Mass\ of\ wet\ soil}{volume\ of\ mould} \tag{4}$$

$$\rho_d = \frac{\rho_b}{1+w} \tag{5}$$

where

ρ_b = bulk density (Mg/m3)

ρ_d = dry density (Mg/m3)

W = moisture content

Compaction test was also carried out on samples collected from the stone base.

b. California bearing ratio (CBR)

The California Bearing Ratio (CBR) test is a penetration test carried out to evaluate the mechanical strength of sub-grade, sub-base or base course materials. It measures the shearing resistance, controlled density and moisture content. In order to characterise the soil for use as base or sub-base materials, CBR is applied both soaked and unsoaked.

A 6000g of the air-dried soil was weighed and mixed with the percentage of water base on the predetermined OMC of each energy level will be added and mixed thoroughly. The mould base place and collar will be fixed and put on flat surface, concrete floor. For modified energy level the moist sample is divided in five portions, each portion will be compacted into CBR mould by using 4.5kg rammer giving each layer 62 blows. The collar will then be removed, the excess sample is trimmed and the sample is placed in polyethene leather for 7, 28 and 60days before testing. After curing of day of each sample, the samples will be tested using CBR machine by recording force reading of 0.25mm intense penetration for both top and bottom.

CBR was calculated from Equation 3.8 and 3.9

$$\text{CBR at 2.5mm } = \left(\frac{Px41.6}{1000}\ divided\ by\ 13.24\right)x100 \quad (3.8)$$

where

P = proving ring reading at 2.5mm, using

41.6 = proving ring constant

$$\text{CBR at 5.0mm} = \left(\frac{Px41.6}{1000}\ divided\ by\ 19.96\right)x100 \quad (3.9)$$

Average of the two values was taken as CBR of the material.

CBR test was also carried out on samples collected from the stone base.

4 RESULTS AND DISCUSSION

Condition Survey Result

The road is generally rated fair (4) to poor (5), the shoulders are generally in fair to poor condition along the investigated road segment, and drainage is generally insufficient over the whole stretch of the road, according to the Table 1 below. As a result, the road's overall condition might be considered fair to poor.

Table 1: Result of condition assessment of the road

Pavement Section			Distress Condition Rating [5 Point Scale]			Carriageway Condition Rating [Pavement]	Shoulder Rating	Drainage Adequacy	Remarks
From	To	Length (m)	Cracks Rating	Pot Hole Rating	Rut/Depression Rating				
0	500	500	5	5	5	5	5	5	Poor condition
500	800	300	4	3	4	3	4	5	Fair Condition
800	900	100	5	5	5	5	5	5	Poor condition
900	1000	100	4	4	4	3	4	5	Fair Condition
1000	1100	100	5	5	5	5	5	5	Poor condition
1100	1400	300	3	3	3	3	4	5	Fair Condition
1400	1700	300	5	5	5	5	5	5	Poor condition
1700	1800	100	3	3	3	3	4	5	Fair Condition
1800	2000	200	5	5	5	5	5	5	Poor condition
2000	2300	300	3	3	3	3	4	5	Fair Condition
2300	3000	700	5	5	5	5	5	5	Poor condition
3000	3700	700	3	3	3	3	4	5	Fair Condition
3700	3900	200	5	5	5	5	5	5	Poor condition
3900	5000	1100	4	3	4	3	4	5	Fair Condition
5000	5200	200	5	5	5	5	5	5	Poor condition
5200	5300	100	4	3	4	3	5	5	Fair Condition
5300	5600	300	5	5	5	5	5	5	Poor condition
5600	6100	500	3	4	4	3	5	5	Fair Condition

It can be observed from Table 1 that:

1. The road is generally rated to be in fair (4) to poor (5) condition.
2. The shoulders of the studied road are generally in poor condition.
3. There is no drainage along the entire stretch of the road.

Therefore, the condition of the road can be categorized as fair to poor.

Dynamic Cone Penetrometer Test (DCPT) Result

The DCPT result of the samples taken from the study area is summarized and presented in Table 2. The results indicated that the California Bearing ratio (CBR) values from the DCPT result on both failed and unfailed sections of the subgrade material on the road were mostly above the minimum (10%) specified by the Specification for Road and Bridge Work (2016). Four tested sections of the subgrade at chainages 1+00 (6.7%), 1+100 (6.7%), 3+000 (8%), and 5+000 (9%) presented CBR values below 10% respectively. This is indicative of a weak subgrade material with low strength and bearing capacity (Al-Refeai & Al-Suhaibani, 1997).

On the other hand, the sub-base material showed that a few sections of the road had CBR values above the minimum (30%) as recommended by the NGS (2016). All other results of the CBR for the sub-grade showed values less than 30%. In the context of sub-base materials for road construction, a California Bearing Ratio (CBR) value below 30% obtained through a Dynamic Cone Penetrometer (DCP) test indicates that the material has relatively low bearing capacity and strength, making it less suitable for use as a sub-base without treatment or additional reinforcement (Feitosa Monteiro *et al.*, 2016).

Table 2: Summary of DCPT on tested road section

					CBR from DCPT (%)		
	From	To	Length (m)	Condition of Section	Subgrade	Sub base	Base
0+500	0	500	500	Failed	22.5	28	32
0+800	500	800	300	Failed	19.3	30	37
0+900	800	900	100	Failed	17.3	27	31.5
1+00	900	1000	100	Failed	6.7	18	19
1+100	1000	1100	100	Failed	6.7	9	22
1+400	1100	1400	300	Failed	15.3	28	36
1+700	1400	1700	300	Failed	26	30.5	36
1+800	1700	1800	100	Failed	21	34.5	38
2+000	1800	2000	200	Failed	22	36	38
2+300	2000	2300	300	Failed	18	19	22.3
3+000	2300	3000	700	Failed	21	26	40
3+700	3000	3700	700	Failed	8	27	38.5
3+900	3700	3900	200	Failed	19.5	29	37.5
5+000	3900	5000	1100	Failed	9	12.5	30.3
5+200	5000	5200	200	Failed	29	31.5	35
5+300	5200	5300	100	Failed	10	15.25	29.7
5+600	5300	5600	300	Failed	7.25	12	18
6+100	5600	6100	500	Failed	26	36.5	39

Furthermore, the CBR results of the base materials showed no section (both failed and unfailed) reached the minimum standard of 80% recommended for CBR value for road base material by the NGS (2016). However, the failed sections of the road presented lower CBR values in comparison to the unfailed sections.

These trends are generally attributed to the softening of the pavement structure by the infiltrating water resulting from the failure of the protective wearing course and the general absence of roadside drainage facilities along the entire stretch of the road. Additionally, the base layer serves as the primary structural layer in a pavement system, distributing traffic loads to the sub-base and subgrade. A CBR below 80% suggests the material lacks the strength needed to perform this function effectively, which could lead to premature pavement failure. Such material might deform under heavy traffic loads, leading to rutting or settlement (AASHTO, 1993).

Summary of Geotechnical Test on Sub-grade Materials

A summary of the geotechnical tests comprising the specific gravity (Gs), sieve analysis, moisture content, Atterberg limit, compaction, soil classification, and CBR for sub-grade materials is presented in Table 3.

Table 3: Summary of properties of sub-grade materials

Sample	Gs	Percentage Passing Sieve 200	Moisture Content	Atterberg Limits		Compaction Characteristics		Soil Classification	Soaked CBR (%)
				LL (%)	PI (%)	MDD (Mg/m^3)	OMC (%)	AASHTO	
0+500	2.67	35.7	2.2	34	13.2	1.69	13.1	A-7-6	8.30
0+800	2.64	35.9	2.1	34.6	12.6	1.69	13.1	A-7-6	7.10
0+900	2.65	36.7	3	40.6	14.4	1.68	14.8	A-7-6	7.30
1+00	2.55	38.1	2.9	40.6	15.3	1.67	14.8	A-7-6	6.00
1+100	2.62	36.9	2.8	34	13.2	1.7	13.8	A-7-6	7.20
1+400	2.65	36.2	2.7	28.2	3.9	1.72	13.8	A-4	5.20
1+700	2.64	39.1	3.7	27.2	8.3	1.7	13.8	A-4	6.10
1+800	2.60	35.5	3.8	22.5	11.5	1.71	11.8	A-6	10.20
2+000	2.59	34.5	3.4	22.1	15.8	1.71	11.8	A-6	7.25
2+300	2.57	34	3.2	23.1	15.2	1.63	16.3	A-6	8.10
3+000	2.55	37.9	2.8	38.3	23.6	1.63	16.3	A-7-6	5.10
3+700	2.57	36.5	3.2	23.6	14.1	1.74	9.8	A-6	11.40
3+900	2.65	36.6	3.6	23.6	14.1	1.74	9.8	A-6	7.20
5+000	2.64	35.1	2.7	27.7	18.8	1.66	12.1	A-6	6.50
5+200	2.60	34.7	3.5	36.8	11.9	1.65	12.1	A-7-6	7.00
5+300	2.60	36	3.2	30.9	16.4	1.65	12.1	A-7-6	8.10
5+600	2.67	33.7	3.1	27.7	18.8	1.62	12.1	A-6	6.80
6+100	2.56	36.2	3	30.4	18	1.71	13.8	A-7-6	6.70

*Gs= Specific Gravity

Table 3 indicated that the specific gravity of the sub-grade material ranged from 2.55-2.67. Specific gravity between 2.55 and 2.67 implies that the subgrade material likely consists of typical mineral soils with good compaction characteristics and moderate bearing capacity. While generally suitable for road subgrades, further evaluation of gradation, compaction, and moisture sensitivity is crucial to confirm its adequacy for the intended application (Braja, 2010).

The sieve analysis result presented in Table 3 showed that the percentage passing 75μm sieve ranges from 33.7% - 39.1%. This indicates a subgrade material with a moderate to high fine content, primarily composed of silts and clays. This may imply moisture sensitivity that makes the material prone to water retention, swelling, and shrinkage. Furthermore, it translates to reduced load-bearing capacity, especially under saturated conditions which may necessitate stabilization. This sub-grade material might be suitable for low-traffic roads if compacted and well-drained. However, for heavy-traffic roads, additional treatment or stabilization is required (ASTM, 2007).

Furthermore, the liquid limit result presented in Table 3 showed a range between 22.1% and 40.6%. This indicates moderate lower LL (22.1–30%) plasticity soils that include silts and clay which implies better strength and stability to higher LL (30.1–40.6%) which indicates greater moisture sensitivity and deformation risk. Its suitable for low-traffic roads if compacted and drained. For high-traffic roads while soils with LL > 30% may need stabilization (AASHTO, 1993; Braja, 2010).

The plasticity index for the sub-grade material ranged between 3.9% and 23.6%. Low PI (3.9–10%) demonstrates low-plasticity soils like silty sands, with good stability and lower water sensitivity while moderate to high PI (10.1–23.6%) signifies clayey soils with higher cohesion but more prone to swelling, shrinkage, and strength loss when wet. PI < 12% is more suitable for subgrade without additional treatment while PI > 12% may require stabilization for better performance, especially for high-traffic roads (Bowles, 1996; Koti, 2018).

The maximum dry density (MDD) test results for the sub-grade materials ranged from 1.62Mg/m^3 to 1.74Mg/m^3. This represents typical fine-grained soils for subgrade construction. Soils with higher MDD values (1.74 Mg/m^3) are better suited for road foundations, while those with lower values (1.62 Mg/m^3) may require additional treatment to meet load-bearing requirements.

The optimum moisture content (OMC) test results for the sub-grade materials ranged from 9.8% to 14.8%. This may suggest that the subgrade material consists of silts and clays, with moderate moisture requirements for compaction. Proper moisture control during compaction is crucial to ensure the subgrade's load-bearing capacity and durability in road construction (Braja, 2010; Bowles, 1996).

The subgrade samples were classified mostly as A-4 (fine-grained, silty soil), A-6 (fine-grained, clayey soil), and A-7-6 (fine-grained, high plastic clay) on AASHTO soil classification (AASHTO, 1993). The soaked CBR values for the sub-grade material ranged from 5.1% to 10.20%. These values are lower than the minimum 10% CBR specified by Nigeria General Specification for Road and Bridge Works - NGS (2016). This and the observed absence of side drains along the entire stretch of the road explain the larger percentage of causes of pavement collapse and eventual road failure.

Summary of Geotechnical Test on Sub-base Materials

A summary of the geotechnical tests comprising the specific gravity (Gs), sieve analysis, moisture content, Atterberg limit, compaction, soil classification, and CBR for the sub-base materials is presented in Table 4.4.

Table 4: Summary of properties of sub-base materials

Sample	Gs	Percentage Passing Sieve 200	Moisture Content	Atterberg Limits		Compaction Characteristics		Soil Classification	Soaked CBR (%)
				LL (%)	PI (%)	MDD (Mg/m^3)	OMC (%)	AASHTO	
0+500	2.52	46.19	4.5	28.82	7.9	2.18	4.9	A-6	30.9
0+800	2.54	48.43	4.9	31.44	7.5	2.17	5.4	A-7-5	32.6
0+900	2.60	46.59	4.3	27.52	7.2	2.14	4.5	A-6	32.4
1+00	2.58	45.87	5.4	26.42	8.3	2.09	3.8	A-6	35.6
1+100	2.60	46.9	4.8	34.32	7.1	2.21	3.4	A-7-5	39.4
1+400	2.62	46.76	10.2	29.11	7.9	2.25	7.2	A-6	35.3
1+700	2.48	46.32	7.5	27.64	8.3	2.19	6.5	A-6	36.7
1+800	2.50	48.12	4.2	26.31	7.7	2.13	4.4	A-6	38.4
2+000	2.55	45.37	6.5	25.61	7.1	2.16	5.2	A-6	34.2
2+300	2.48	45.63	5.5	29.02	8.6	2.08	3.1	A-6	34.5
3+000	2.51	48.21	6.4	32.41	6.2	2.24	7.1	A-7-5	33.7
3+700	2.53	45.39	5.0	33.09	7.4	2.34	6.5	A-7-5	31.3
3+900	2.58	45.36	5.5	31.13	6.3	2.12	4.5	A-7-5	31.2
5+000	2.50	47.33	6.8	28.23	7.3	2.16	5.5	A-6	30.5
5+200	2.50	47.85	7.2	25.80	9.1	2.22	5.5	A-6	29.8
5+300	2.55	48.32	5.2	26.55	6.9	2.17	4.8	A-6	33.4
5+600	2.45	44.27	8.5	29.43	6.6	2.26	7.2	A-6	32.6
6+100	2.47	46.19	7.3	36.8	11.9	2.35	9.8	A-7-6	31.4

Table 4 indicated that the specific gravity of the sub-base material ranged from 2.45-2.62. This implies that the subgrade material likely consists of typical mineral soils with good compaction characteristics and moderate bearing capacity. While generally suitable for road subgrades, further evaluation of gradation, compaction, and moisture sensitivity is crucial to confirm its adequacy for the intended application (Braja, 2010).

The sieve analysis results for sub-base material presented in Table 4 also showed that the percentage passing 75µm sieve ranges from 44.27% - 48.43%. This indicates sub-base material with high fine content, which is generally unsuitable for sub-base use without stabilization. Proper treatment or material replacement is necessary for reliable performance in road construction (ASTM, 2007).

The liquid limit result for the sub-base ranged between 25.80% and 36.8%. This indicates moderate lower LL (25.80–30%) plasticity soils that include silts and clay which implies better strength and stability to higher LL (30.1–36.8%) which indicates greater moisture sensitivity and deformation risk. Its suitable for low-traffic roads if compacted and drained. For high-traffic roads while soils with LL+ > 30% may need stabilization (AASHTO, 1993; Braja, 2010).

The plasticity index of the sub-base material ranged between 6.2% and 11.9%. This suggests a sub-base material with low to moderate plasticity, suitable for many road construction projects. Proper compaction and drainage are critical to ensuring its performance, and stabilization may be necessary for soils with higher PI values in this range, particularly under heavy traffic or in wet conditions (Bowles, 1996; Koti, 2018).

The maximum dry density (MDD) test results for the sub-base materials shown in Table 4 ranged from 2.08Mg/m^3 to 2.35Mg/m^3. A maximum dry density (MDD) between 2.08 Mg/m^3 (2080 kg/m^3) and 2.35 Mg/m^3 (2350 kg/m^3) for sub-base material in road construction indicates the material's compaction potential and its suitability as a load-bearing layer.

The optimum moisture content (OMC) test results for the sub-base materials ranged from 3.1% to 9.8%. This reflects the water content required to achieve maximum dry density (MDD) during compaction.

Low OMC (3.1–5%) indicates coarse-grained materials such as sands and gravels, which require less water for compaction due to their lower surface area and minimal fine content while moderate OMC (5.1–9.8%) suggests the presence of silts or minor clay content, increasing the water demand due to greater surface area and cohesion. (Braja, 2010; Bowles, 1996).

The sub-base samples were classified mostly as A-6 (fine-grained, clayey soil), A-7-5 (silty soil), and A-7-6 (fine-grained, high plastic clay) on AASHTO soil classification (AASHTO, 1993). The soaked CBR values for the sub-base material ranged from 29.8% to 39.4%. These values are higher than the minimum 10% CBR specified by Nigeria General Specification for Road and Bridge Works - NGS (2016). This indicates the evidence of relative quality control measures taken during the construction/rehabilitation stages of the road.

Results of Base Course Materials Testing

A large portion of the road has crushed granite as base course material. These materials were tested for particle size distribution, compaction characteristics and CBR. The results are presented below.

Properties of the stone base materials

Particle size distribution of crushed stone base materials

Results of particle size distribution of the crushed stone base course materials collected along the road are presented in Figures 2 to 19.

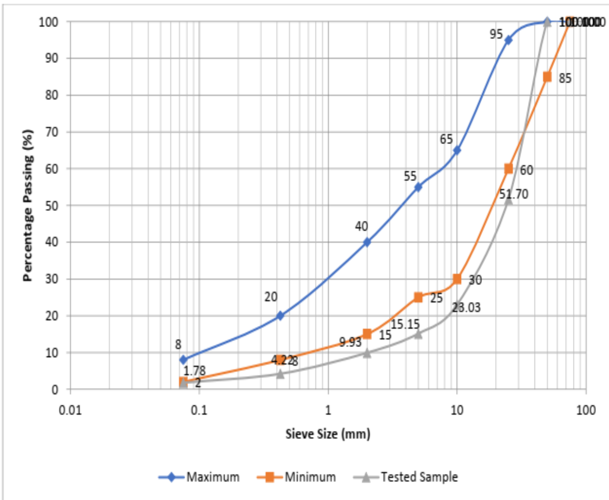

Figure 2: Grading envelope (gradation A) for base course sample taken from CH 0+500

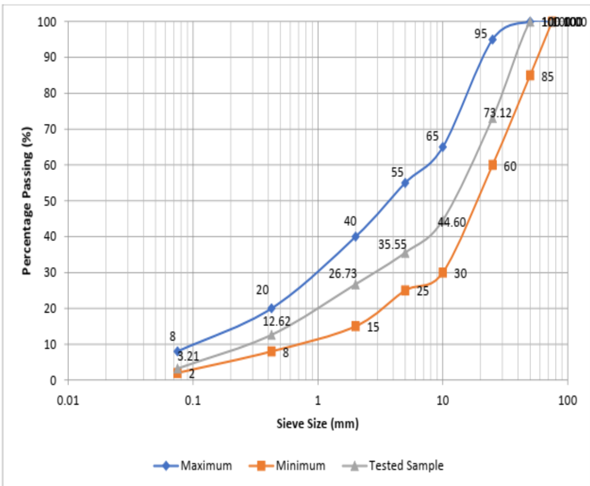

Figure 3: Grading envelope (gradation A) for base course taken from CH 0+800

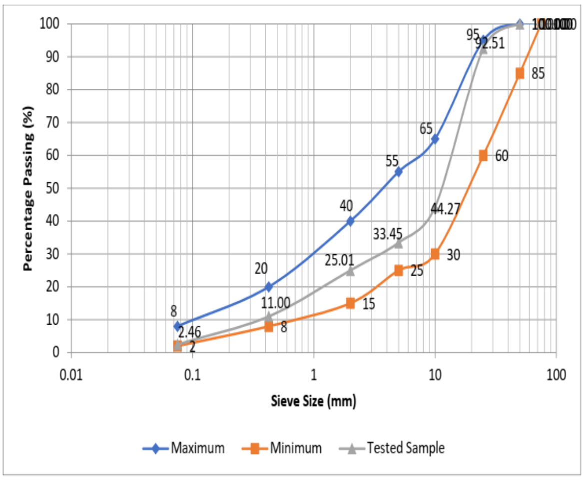

Figure 4: Grading envelope (gradation A) for base course sample taken from CH 0+900

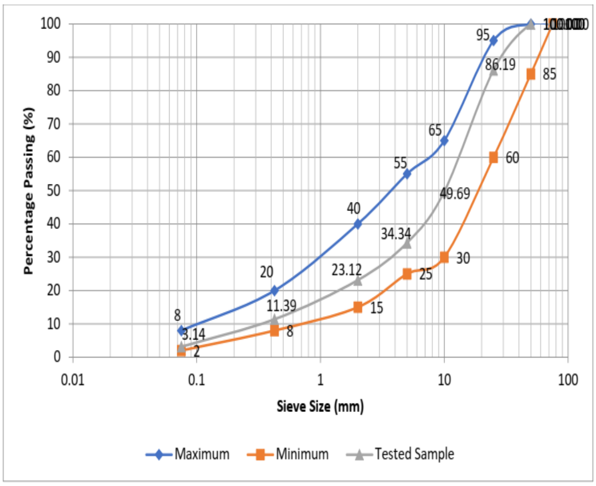

Figure 5: Grading envelope (gradation A) for base course sample taken from CH 1+00

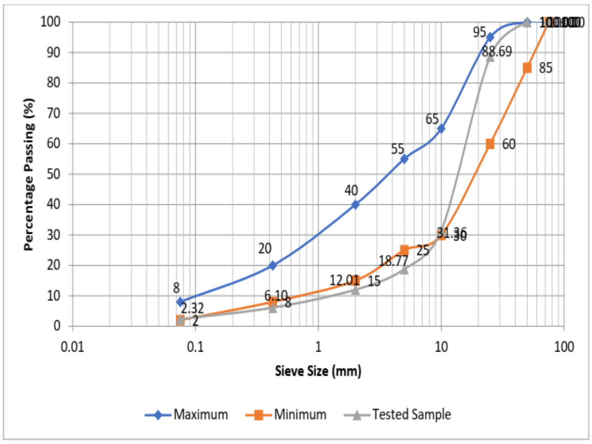

Figure 6: Grading envelope (gradation A) for base course sample taken from CH 1+100

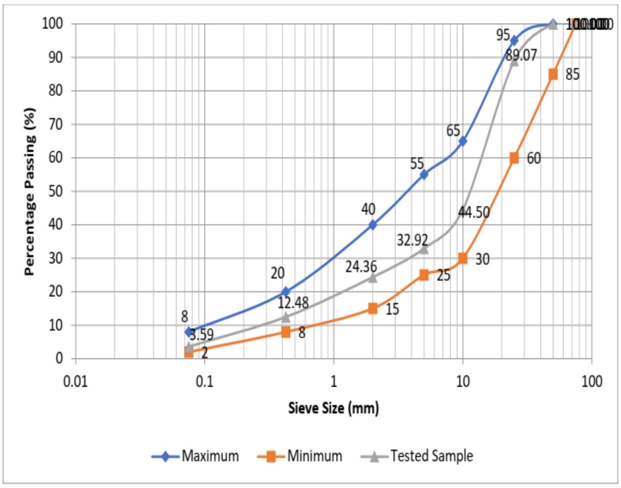

Figure 7: Grading envelope (gradation A) for base course sample taken from CH 1+400

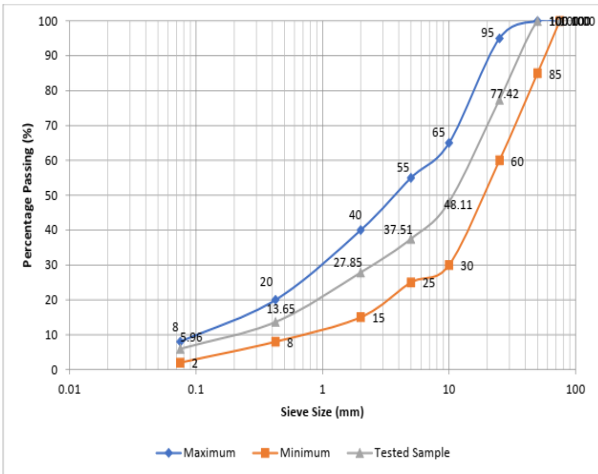

Figure 8: Grading envelope (gradation A) for base course sample taken from CH 1+700

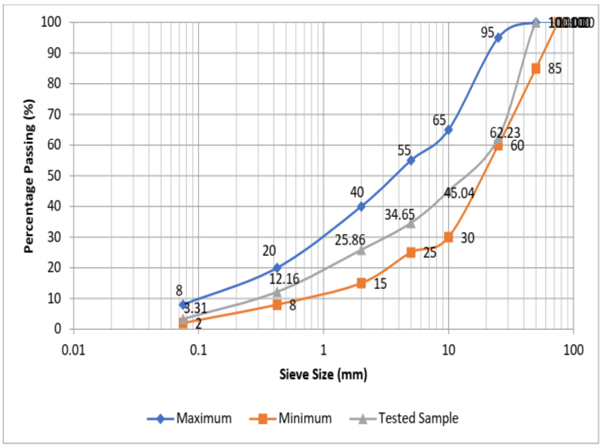

Figure 9: Grading envelope (gradation A) for base course sample taken from CH 1+800

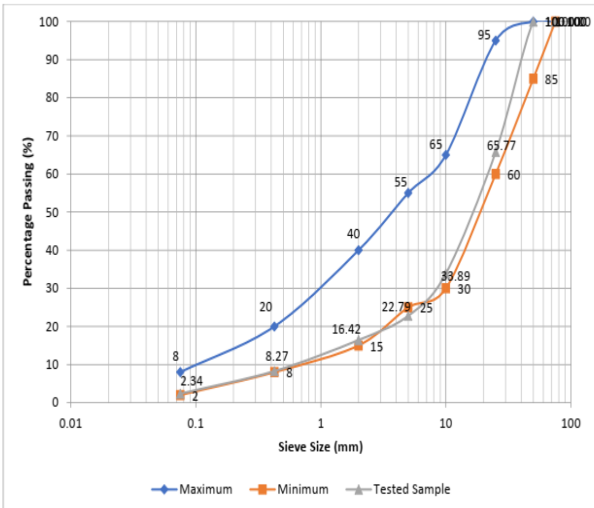

Figure 10: Grading envelope (gradation A) for base course sample taken from CH 2+000

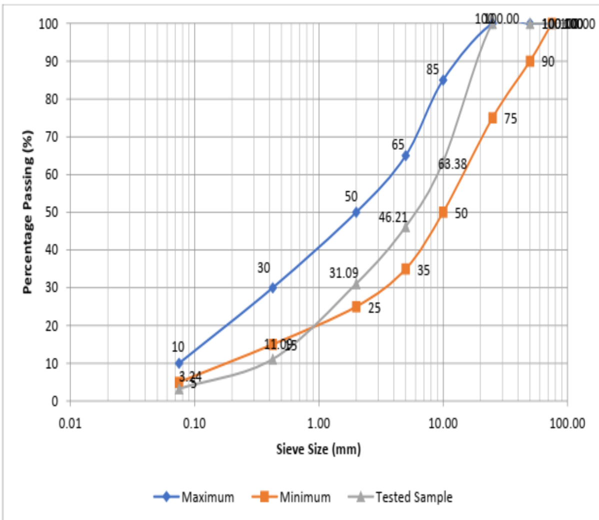

Figure 11: Grading envelope (gradation C) for base course sample taken from CH 2+300

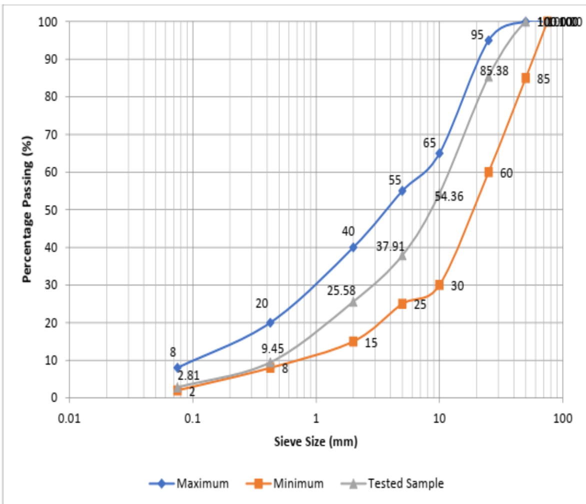

Figure 12: Grading envelope (gradation A) for base course sample taken from CH 3+000

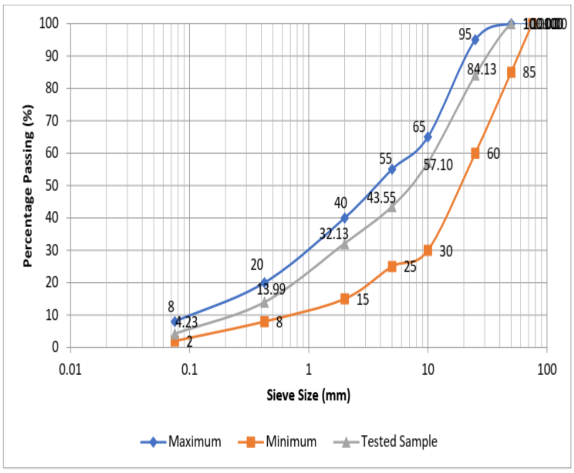

Figure 13: Grading envelope (gradation A) for base course sample taken from CH 3+700

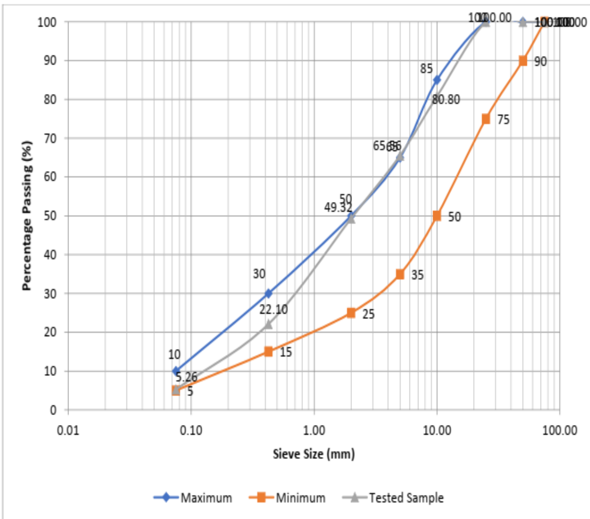

Figure 14: Grading envelope (gradation C) for base course sample taken from CH 3+900

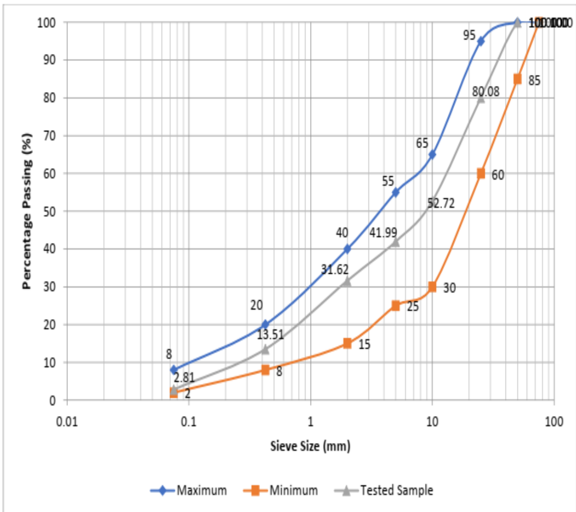

Figure 15: Grading envelope (gradation A) for base course sample taken from CH 5+000

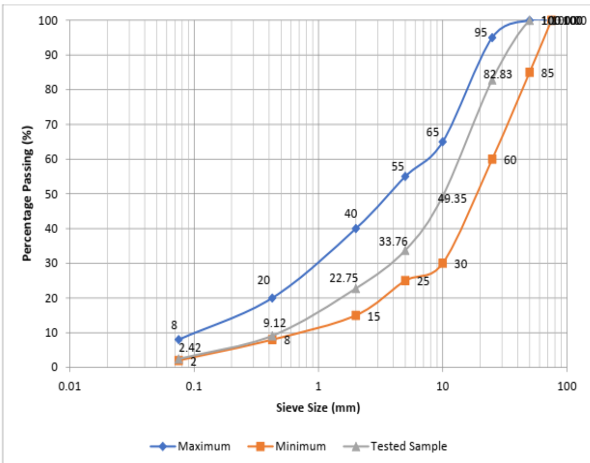

Figure 16: Grading envelope (gradation A) for base course sample taken from CH 5+200

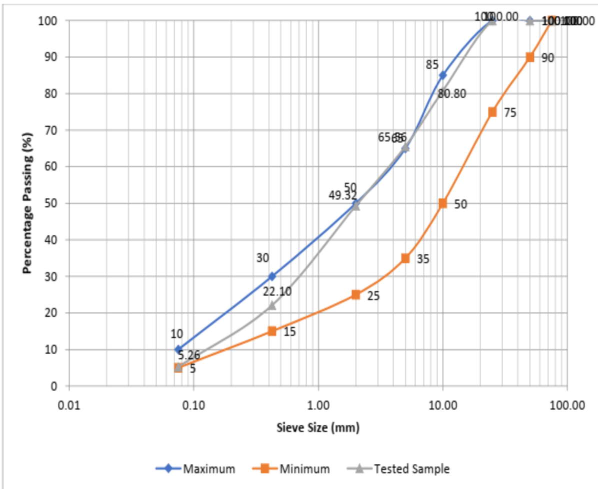

Figure 17: Grading envelope (gradation C) for base course sample taken from CH 5+300

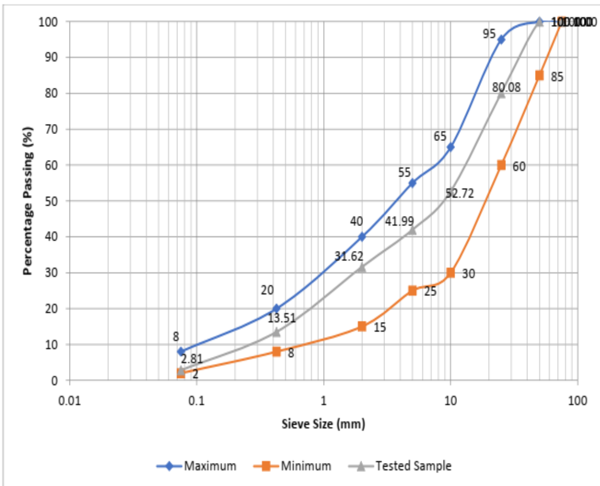

Figure 18: Grading envelope (gradation A) for base course sample taken from CH 5+600

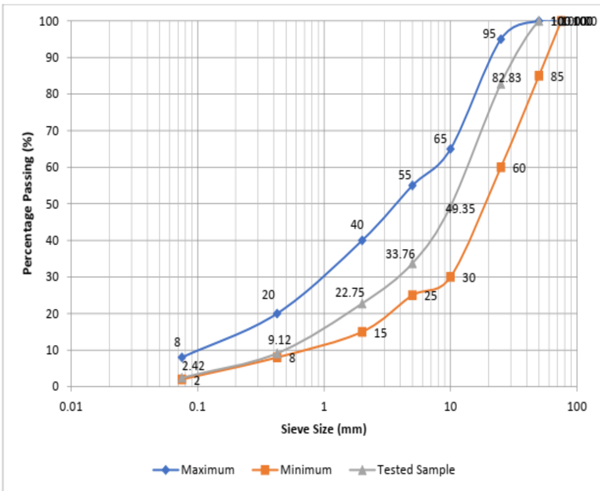

Figure 19: Grading envelope (gradation A) for base course sample taken from CH 6+100

It can be observed that all the base course material (stone base) tested fit into gradation as recommended by the Nigeria General Specification for Road and Bridge Works- NGS (2016). However, samples from CH 0+500 (see Figure1) generally fell below the lower limit of the zone. Samples from CH 2+300 and CH 3+900 (see Figures 11, 14, and 16) fit into gradation C, with samples from CH 2+300 having lower fine content below the minimum specified by the Nigeria General Specification for Road and Bridge Works (2016). The observed trend also indicated evidence of relative quality control measures during the construction/rehabilitation stages of the road base.

Results of Strength Properties of the Base

The results of compaction characteristics (MDD and OMC) of the stone base materials are presented on Table 4.5.

Table 5: Summary of Strength properties of the stone base materials

Sample	Compaction Characteristics	
	MDD (Mg/m^3)	OMC (%)
0+500	2.18	4.5
0+800	2.19	5.5
0+900	2.16	7.6
1+00	2.19	10.4
1+100	2.17	12.7
1+400	2.16	12.4
1+700	2.18	9.6
1+800	2.17	8.3
2+000	2.15	7.1
2+300	2.19	4.8
3+000	2.15	3.2
3+700	2.16	4.2

3+900	2.19	5.5
5+000	2.19	6.8
5+200	2.17	7.4
5+300	2.16	6.5
5+600	2.16	5
6+100	2.18	4.5

The result presented in Table 5 showed that the MDD of the stone base material along for the study area ranges from 2.15 to 2.19 Mg/m^3 while the OMC ranges between 3.2% to 12.7%. This indicates the moisture level at which the material achieves its maximum dry density during compaction. A lower OMC reflects coarse-grained materials such as crushed stone, while a higher OMC suggests finer particles or clay content. These values are within those typical for stone base materials of the stated gradation zones.

Results of CBR of the stone base materials

The results of CBR of the stone base materials are also presented on Table 5. From the table, it is observed that CBR values of the tested stone base materials ranges between 18% to 40%, which are typical values for crushed stone base materials as reported in literature (Braja, 2010; Koti, 2018).

5 CONCLUSION AND RECOMMENDATION

5.1 Conclusion

It can be concluded from the current study that the result from the condition assessment of the road indicated that it can be generally referred to as being in fair to poor condition.

The sieve analysis on the subgrade material indicated that the tested area might be suitable for low-traffic roads if compacted and well-drained. The liquid limit demonstrated that the road has greater moisture sensitivity and deformation risk signifying its suitability for low-traffic roads if compacted and drained. Additionally, the plasticity index results demonstrated low-plasticity soils with good stability and lower water sensitivity to moderate clayey soils with higher cohesion but more prone to swelling, shrinkage, and strength loss when wet.

Furthermore, the subgrade samples were classified mostly as A-4 (fine-grained, silty soil), A-6 (fine-grained, clayey soil), and A-7-6 (fine-grained, high plastic clay) on AASHTO soil classification (AASHTO, 1993).

The soaked CBR values for the sub-grade material ranged from 5.1% to 10.20%. These values are lower than the minimum 10% CBR specified by Nigeria General Specification for Road and Bridge Works - NGS (2016). This and the observed absence of side drains along the entire stretch of the road explain the larger percentage of causes of pavement collapse and eventual road failure.

On the other hand, the sieve analysis result from the sub-base samples indicated material with high fine content, which is generally unsuitable for sub-base use without stabilization.

The sub-base samples were classified mostly as A-6 (fine-grained, clayey soil), A-7-5 (silty soil), and A-7-6 (fine-grained, high plastic clay) on AASHTO soil classification (AASHTO, 1993).

However, the soaked CBR values for the sub-base material ranged from 29.8% to 39.4% which were higher than the minimum 10% CBR in comparison to the sub-grade material samples. Therefore, it can be concluded that there is evidence of relative quality control measures taken during the construction/rehabilitation stages of the road.

5.2 Recommendations

From the study, the following are recommended:

1. Proper investigation should be carried out to ascertain the depth of the subgrade material to be removed before placement of other pavement structures, during reconstruction/rehabilitation of the road.
2. Side drains should be provided to reduce ponding and infiltraion of surface runoff into the pavement structure, during reconstruction/rehabilitation of the road.

6 REFERENCES

AASHTO. (1993). *AMERICAN ASSOCIATION OF STATE HIGHWAY AND TRANSPORTATION (AASHTO) Design of Pavement Structures*.

Ahmed, I. (2014). Geotechnical properties of subgrade soils and their influence on pavement performance. *International Journal of Pavement Research and Technology, 7*(4), 368-376

Ahmed, M. Y. (2012). Evaluation of geotechnical properties and structural strength enhancing road pavement failure along Sylhet-Sunamganj highway, Bangladesh. *Journal of Soil Science and Environmental Management*, *3*(5), 110–117. https://doi.org/10.5897/jssem12.024

Aliyu, M., & Eberemu, A. O. (2018). Evaluation of geotechnical properties of subgrade soils and their effect on pavement performance in some parts of Nigeria. *Journal of Civil Engineering and Construction Technology*, *9*(2), 22-30.

ASTM. (2007). *Standard Test Method for Particle-Size Analysis of Soils 1*.

Braja M. Das. (2010). *Principles of Geotechnical Engineering* (7th ed.). CENGAGE Learning.

British Standard. (2003). Bs 1377-2: 1990. *BS-1377-part-2, March*.

Das, B. M. (2010). *Principles of geotechnical engineering* (7th ed.). Cengage Learning.

Department of Transport and main Roads. (2020). *Manual Pavement Rehabilitation* (Número February). Department of Transport and Main Roads.

Ezeokonkwo, I. G., & Olofsson, B. (2015). Assessment of pavement failure mechanisms in some parts of South-Eastern Nigeria. *Journal of Transportation Engineering*, *141*(12), 04015027.

Huang, Y. H. (2004). *Pavement analysis and design* (2nd ed.). Pearson Prentice Hall.

Jones, D., & Smith, A. (2010). The role of drainage in pavement performance. *Transportation Research Record: Journal of the Transportation Research Board*, *2154*(1), 1-8.

Nelson, J. D., & Miller, D. J. (1992). *Expansive soils: Problems and practice in foundation and pavement engineering*. John Wiley & Sons.

Nelson, J.D. and Miller, D.J. (1992). Expansive soils: problems and practice in foundation and pavement engineering. John Wiley & Sons, inc. New York.

NGS (2016). Nigeria General Specification for Road and Brdge Works.

3rd International Civil Engineering Conference (ICEC 2024)
Department of Civil Engineering
Federal University of Technology, Minna, Nigeria

ESTIMATION OF STREAMFLOW IN SHIRORO DAM USING SOIL AND WATER ASSESSMENT TOOL (SWAT) MODEL

Sunday Emmanuel Ogunmola[1], Ibrahim Abayomi Kuti[2] and Peter Aderemi Adeoye[3]
[1]Agric Services Department, Upper Niger River Basin Development Authority, Minna, Niger State.
[2]Department of Agricultural and Bioresources Engineering, Federal University of Technology Minna, Niger
[3]Department of Agricultural and Bioresources Engineering, Federal University of Technology Minna, Niger State.
Corresponding author email: ogunplanet82@yahoo.com

ABSTRACT
The focus of hydrological studies has been on climate change, while much attention has not been focused on the effect of Best Management Practices on streamflow. Streamflow was likely to be estimated using the Sequential-Uncertainty-Fitting method of the Soil and Water Assessment Tool (SWAT-SUFI2). The streamflow was divided into datasets: calibration (2011-2018) and validation (2019-2021). Nash-Sutcliffe Efficiency (NSE) method was used to evaluate the performance of the models. The results showed that Nash–Sutcliffe efficiency (NSE) and coefficient of determination (R^2), PBIAS, P- factor, and R-factor for monthly streamflow in conservation practice were 0.52, 0.53, -4.5, 0.13, and 0.1 in the calibration. The validated models were 0.58, 0.63, 20.5, 0.28, and 0.47 at the Shiroro sub-basin 5. Similar results were found for streamflow in contouring during calibration, but the PBIAS was -2.8. The corresponding values are 0.64, 0.65, -8.1, 0.31, and 0.48 for validation. In the Shiroro sub-basin, strip cropping was confirmed by NSE and R^2 (0.58 and 0.58) during calibration. Also, the PBIAS, P, and R-factors have values of -2.7, 0.13, and 0.19, respectively. The equivalent values were 0.65, 0.65, 1.3, 0.28 and 0.39 during validation. During calibration, the values of the Nash–Sutcliffe efficiency (NSE) and coefficient of determination (R^2), PBIAS, P-factor, and R-factor were 0.58, 0.58, -3.2, 0.09, and 0.07 for the terrace. The corresponding values for validation include 0.58, 0.65, 23.3, 0.11, and 0.05. The SWAT models are satisfactory. Water policymakers need to discourage farmers from the use of non-conservation practices around Shiroro Dam.

Keywords: *Streamflow, SWAT model, Shiroro Dam and Best Management Practices.*

1. INTRODUCTION

Streamflow is a critical component of the water cycle and refers to the volume of water that flows through a river or stream over a given time (Fan, 2023). Fresh liquid water suitable for humans can be found in rivers and reservoirs as surface water or in aquifers as groundwater. Although the total amount of fresh water accessible has stayed constant over time, water demands are growing by the day due to population increase, economic development, urbanisation, and other factors. Rainfall patterns will likely be affected by climate change, resulting in increasing volatility and issues in stream flow and water supply management. Runoff prediction plays an important scientific and practical role in engineering projects and water resource management (Kushwaha et al., 2013), such as the design and management of reservoirs. The most valuable and commonly used tool for the prediction of runoff is the hydrological model (Hinmanshu et al., 2019). One of the best models is the SWAT model, which represents the hydrologic process and the interaction between them (Jain et al., 2017). This model requires hydroclimatic parameters such as observed streamflow, rainfall, and minimum and maximum temperature and represents the physical properties of the catchment. The model can be calibrated using sequential fitting algorithm 2 (Abaspour et al., 2017).

The SWAT model is used to simulate long-term streamflow, sediment, and phosphorus (Pandey *et al.*, 2016); it was developed by the USDA Agricultural Research Service (ARS) to forecast the effect of activities related to land management on the transport of hydrology, pollutants and sediment in complex, large watersheds (Bera and Mati 2021). Several researchers have applied the SWAT model for discharge/runoff prediction (Pandey *et al.*, 2016) and sediment load (Kuti and Ewemoje, 2021; Krause et al., 2005; Song et al., 2015; Himanshu et al., 2017). The model performance of these studies was satisfactory. Daramola *et al.* (2019) estimated sediment yield in Shiroro Dam using the SWAT model—however, there is no available information about the simulated discharge in the catchment. In addition, Adeogun et al. (2022) predict the effect of BMPs on sediment yield; however, there is no available information on the effect of BMPs (terracing, contouring and strip cropping) on simulated streamflow. The main objective of the study is to estimate stream flow behaviour under different Best Management Practices (BMPs) in the Shiroro watershed and find out the most sensitive parameters which are critically responsible for the hydrologic response with pre-defined conditions.
The outcome of this study would be used by policymakers, land managers, and researchers to inform decision-making processes. The application of BMPs,

such as terracing, contouring, and strip cropping, resulted in varying effects on streamflow. Specifically, terracing increased streamflow by approximately 4%, while contouring and strip cropping increased it by about 7% and 9%, respectively. Conversely, non-conservation practices led to a significant increase in streamflow by 19%. The implementation of contouring and strip cropping BMPs is expected to reduce flooding downstream by approximately 2 times, highlighting the potential benefits of these practices in mitigating flood risks.

2.0 METHODOLOGY

2.1 Description of the study area

The study area, Shiroro Dam, which is about 66 km, is situated at the former Shiroro village in North-Central Nigeria. It can be found between Latitude 9.35°N, Longitude 6.45°E and Latitude 11.28°N Longitude 8.55°E, with an appraised land area of 32,125 km^2. The watershed has a mean elevation of 683 m above sea level (Figure 3.1). The Shiroro dam derives its water sources from the Kaduna watershed (32,125 km^2), which consists of four sub-watersheds. These four sub-watersheds are named after some commonly known rivers - Dinya, Gutalu, Sarkinpawa and Kaduna. The Dinya (365 km^2) consists of a basin; Gutala (2,672 km^2) and Sarkinpawa (3,413 km^2) on the other consists of seven basins, whilst the largest of them, the Kaduna sub-watershed (25,675 km^2) contains 69 basins. The northern part of the watershed is a little drier than the south. The sedimentary geology nature of the study area, alongside the predominately sandy soil with Guinea and Sudan savannah vegetation cover, makes the study area susceptible to soil erosion, which is a major sediment yield driver.

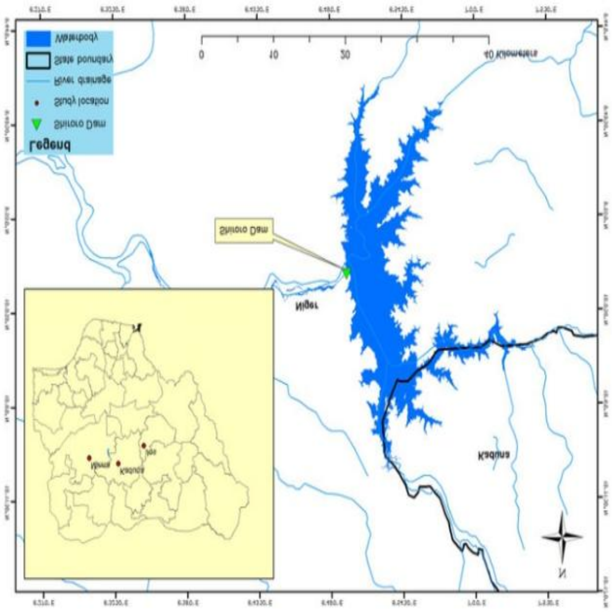

Figure 1: Location map of Shiroro

2.2 Climate of the study area

The Shiroro Lake watershed receives in excess of 100 mm with a peak value of about 280 mm –300 mm in July. Rainfall amount is in excess of 300 mm in the western half of the area. The highest rainfall receipt of over 400 mm is to be expected in September during a normal rainy year but can drop sharply to a maximum of 130 mm – 150 mm during a low rainfall year. The onset of the seasonal rainfall is between 20 – 30th April, and the length of the rainy season is between 161- 200 days.

The maximum temperature (< 35 ^{0}C) is recorded between March and June, while the minimum is usually between December and January (Niger State, 2012). The climate of the area is tropical and belongs to the tropical wet and dry (AW) of Koppen's climatic classification (Eze, 2004). However, the creation of Shiroro Lake has led to a change in climatic conditions in and around the lake area (Ezugwu, 2013).

2.3 Land use

The watershed and hydrological response unit of Shiroro was divided into 18 sub-basins with a total of 35 hydrological response units. Fig. 2 indicates that agricultural land (51.24%) has the highest percentage of land use, and next to it is water (45.14%), followed by forest (3.54%) and office building (0.07%). Ferric luvisols and lithosol cover the Shiroro sub-basins. Ferric luvisol covers 80.3% of the land, while the remaining 19.7% contains lithosol.

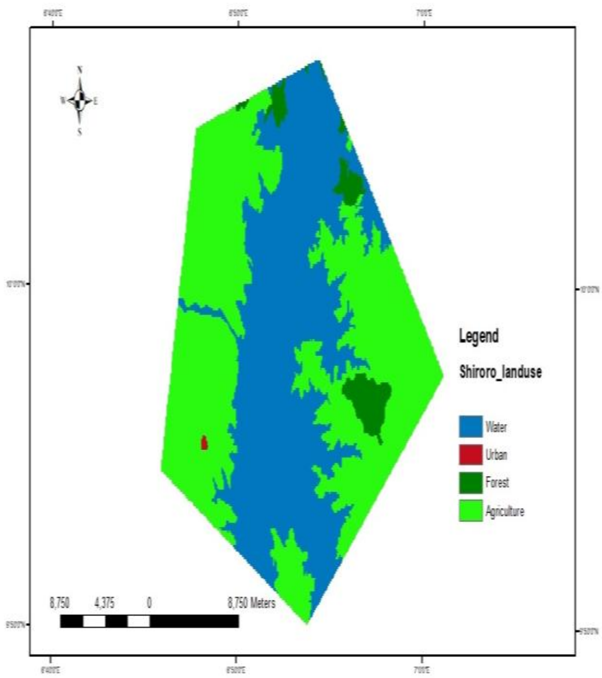

Figure 2 Landuse of the study area

3.1 Estimation of streamflow using the SWAT model

SWAT is a model that predicts streamflow (Abbaspour *et al.*, 2015) and eroded sediment and nutrients (Kuti and Ewemoje, 2021). In line with landuse and land slope, SWAT also splits a basin into sub-basins and separates them into hydrological response units (HRU). The water balance equation estimates streamflow through the hydrological cycle employing SUFI2 (Abbaspour *et al.*, 2015).

3.2 Data collection

The 90-meter DEM was downloaded from the website of the Shuttle Radar Topography Mission (http://srtm.csi.cgiar.org). A land-use map was taken from the United States Geological Survey website with a resolution of 2 km (https://www.usgs.gov). A soil map was downloaded from the website of the Food and Agriculture Organization's database (2009) with a resolution of 1 km (http://www.fao.org).
The data, including rainfall, temperature, wind speed, relative humidity, and solar radiation, were obtained from the Upper NigerRiver Basin Authority (Shiroro Dam, 2023). The climatic data covers 11 years (2011 - 2021).

3.3 Watershed delineated and hydrological response units

The boundaries of Shiroro Dam were delineated using a polygon tool from Google Earth. The model was built using the ArcSWAT 2012 interface (Kuti and Ewemoje, 2021). The flow direction and accumulation of the streams (area of 5904.37 ha) were extracted from the DEM. The outlets in each location were selected and defined before the model sub-basin parameters were calculated. These further divided the entire watershed into 18 subbasins, which were also subdivided into 35 hydrological response units (HRUs) based on soil, land use, and slope in Shiroro Dam. One HRU is assumed to be a standardised unit for calculating water balance. The meteorological data were prepared between 2011 and 2021. The model writes input data and runs the Soil and Water Assessment tool (SWAT). The simulation runs for eleven years (2011-2021). The watershed delineation in Shiroro Dam is shown in Figure 3.

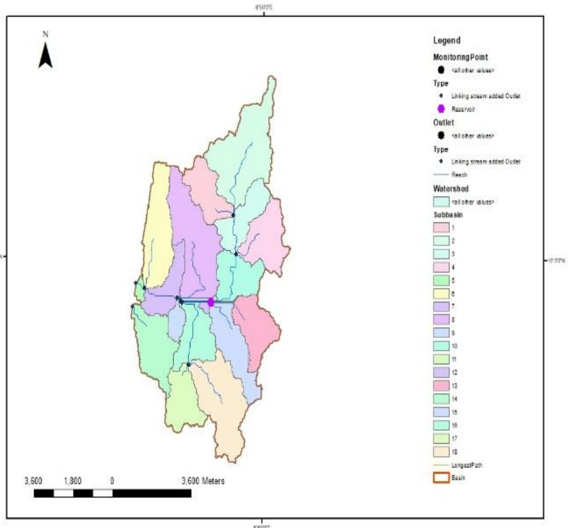

Figure 3. Shiroro watershed delineation

3.4 Calibration And Validation of Streamflow using SUFI2

Tables 1 and 2 show the modification of SWAT input parameters and input variables for SWAT. Streamflow prediction was executed by employing the SWAT procedure (Kuti and Ewemoje, 2021; Abbaspour *et al.*, 2015). The Latin hypercube method was used to calibrate, validate, and estimate uncertainty. The streamflow records were divided into two sets: the first dataset was used for calibration (2011-2018), and the second dataset was used for validation (2019-2021). This calibration and validation were conducted under different Best Management Practices: terracing, contouring, strip cropping and non-conservation practice (ridge along the slope) by changing the values of SCS runoff curve number for moisture condition and USLE equation support practice factor in ARCSWAT. It was also used to identify the input variables that change inflow.

Table 1: Modification of SWAT Input Parameters in ArcSWAT

S/N	BMPs	Original Value	Modified value
1	Terrace	91	71
		1	0.10
2	Contour	91	75
		1	0.5
3	Strip cropping	91	75
		1	0.38

Table 2: SWAT Input Parameters in ArcSWAT

SWAT Parameters	Minimum value	Maximum value	Fitted value
r__CN2.mgt	-0.2	0.2	-0.40
v__ALPHA_BF.gw	0	1	-0.33
v__GW_DELAY.gw	30	450	74.01
v__GWQMN.gw	0	2	1.15
r__GW_REVAP.gw	0	10	4.08
v__ESCO.hru	0	1	-0.09
r__CH_N2.rte	0	3	2.39
r__CH_K2.rte	5	130	71.81
r__SOL_K().sol	-0.8	0.8	-0.19
r__SOL_BD().sol	-0.5	0.6	0.20
r__SOL_AWC().sol	-0.2	4	0.82

3.5 Model performance

As reported by Abbaspour *et al.* (2015), the objective function of the model was Nash-Sutcliffe Efficiency (NSE). The coefficient of determination (R^2) and percent bias (PBIAS) decide the strength of the models. The model performance was evaluated as follows using equations 1 – 3.

$$(\mathrm{NSE}) = 1 - \frac{\sum_{=i}^{n}(O_i - P_i)^2}{\sum_{=i}^{n}(O_i - O_{avr})^2} \quad \ldots 1$$

$$(R^2) = \left[\frac{\sum_{=i}^{n}(O_i - O_{avr})(P_i - P_{avr})}{\sum_{=i}^{n}(O_i - O_{avr})^2 \sum_{=i}^{n}(P_i - P_{avr})^2}\right]^2 \qquad \ldots 2$$

$$(PBIAS) = \left[\frac{\sum_{=i}^{n}(O_i - P_i) \times 100}{\sum_{=i}^{n}(O_i)}\right] \qquad \ldots 3$$

Where,
$O_i = i^{th} \, observed \, value,$
$O_{avr} =$
$average \, observed \, value \, of \, the \, entire \, study \, period,$
$P_i = i^{th} simulated \, value,$
$P_{avr} = average \, of \, simulated \, value.$

Table 3: Classification of statistic indices

NSE	PBIAS	R^2	Classification
0.75 -1.00	PBIAS ≤ ±10	>0.75 -0.75 - 1.00	Very Good
0.60 - 0.75	±10 - ±15	0.6 – 0.75	Good
0.36 - 0.60	± 15 - ±25	0.50 - 0.60	Satisfactory
0.00 - 0.36	±25 - ±50	0.25 - 0.50	Bad
NSE ≤ 0.00	PBIAS< ± 50	$R^2 \leq 0.25$	Inappropriate

Source: Almeida *et al.* (2018)

4.0 RESULTS AND DISCUSSIONS

4.1 Estimation of streamflow using SWAT-SUFI2 under ridging along the slope

Table 4 presents the calibration and validation of streamflow under BMPs. Figures 4 and 5 display the streamflow under ridge along the slope. The values of PBIAS were -4.5 and 20.5 for streamflow along the slope ridge during calibration and validation. The SWAT model also showed a better simulation with R-factors of 0.53 and 0.63. During calibration and validation, NSE values of 0.52 and 0.58 for streamflow along the slope ridges.

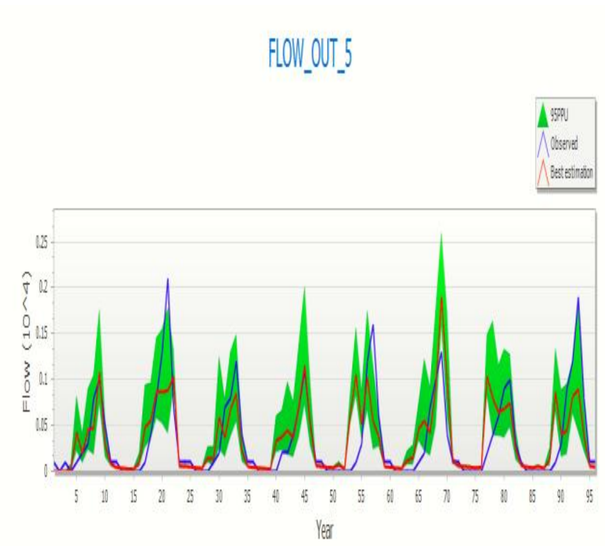

Figure 4: A monthly observed vs SWAT simulated streamflow for calibration (Jan. 2011 – Dec. 2018) in the Shiroro sub-basins under Ridge along the slope

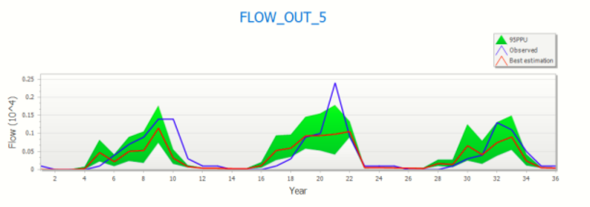

Figure 5: A monthly observed vs SWAT simulated streamflow for validation (Jan. 2019 – Dec. 2021) in the Shiroro sub-basins under Ridge along the slope

4.3 Estimation of streamflow using SWAT-SUFI2 under contouring

Figures 6 and 7 display the calibration and validation of streamflow under contouring. The values of PBIAS were -2.8 and -8.1 for streamflow under contouring during calibration and validation, which shows that the observed values are underestimated (Table 4). The SWAT model shows their variance in the observed data with R^2 of 0.58 and 0.65 during calibration and validation, but NSE values indicated a strong relationship between the simulated data and the observed data with 0.58 and 0.64 for streamflow under contouring.

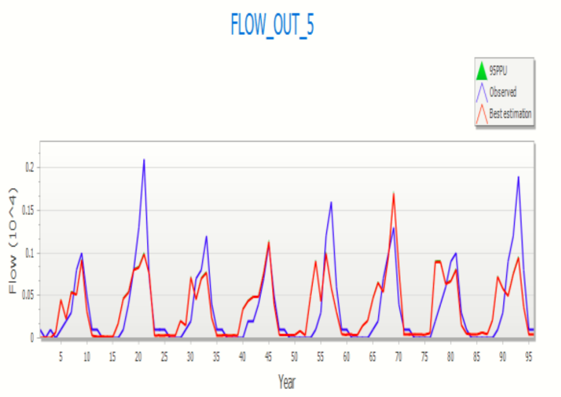

Figure 6: A monthly observed vs SWAT simulated streamflow for calibration (Jan. 2011 – Dec. 2018) in the Shiroro sub-basins under contouring

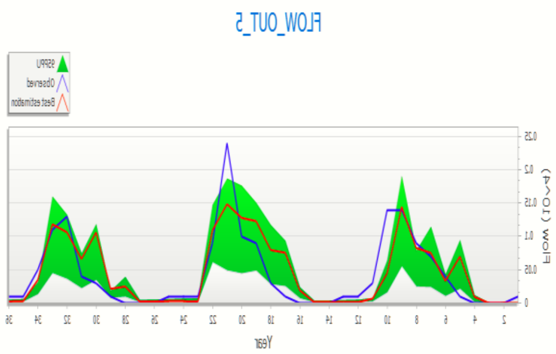

Figure 7: A monthly observed vs SWAT simulated streamflow for validation (Jan. 2019 – Dec. 2021) in the Shiroro sub-basins under contouring

4.4 Estimation of streamflow using SWAT-SUFI2 under strip cropping

Figures 8 and 9 display the calibration and validation of streamflow under strip cropping. The values of PBIAS were -2.7 and 1.3 during calibration and validation, which represents a good estimation of the observed data for streamflow under strip cropping (Table 4). The SWAT mod

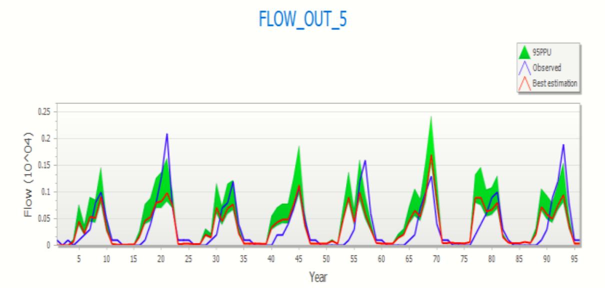

el also showed a good simulation with R^2 values of 0.58 and 0.65 during calibration and validation. NSE values of 0.58 and 0.65 for calibration and validation indicated strong proximity of the simulated data to the observed data for streamflow under strip cropping.

Figure 8: A monthly observed vs SWAT simulated streamflow for calibration (Jan. 2011 – Dec. 2018) in the Shiroro sub-basins under strip cropping

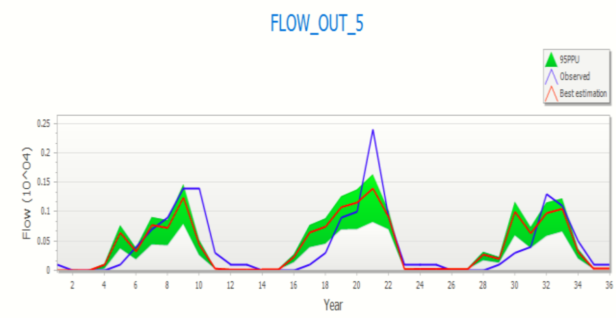

Figure 9: A monthly observed vs SWAT simulated streamflow for validation (Jan. 2019 – Dec. 2021) in the Shiroro sub-basins under strip cropping.

4.5 Estimation of streamflow using SWAT-SUFI2 under terracing

The calibration and validation of streamflow under terracing are shown in Figures 10 and 11. The values of PBIAS were -3.2 and 23.3 during calibration and validation (Table 4). The validation shows an underestimation of the observed data for streamflow under terracing. The SWAT model also showed a good simulation with R^2 values of 0.58 and 0.65 during calibration and validation. NSE values of 0.58 and 0.58 for streamflow terracing indicate a level of closeness between the simulated and the observed data.

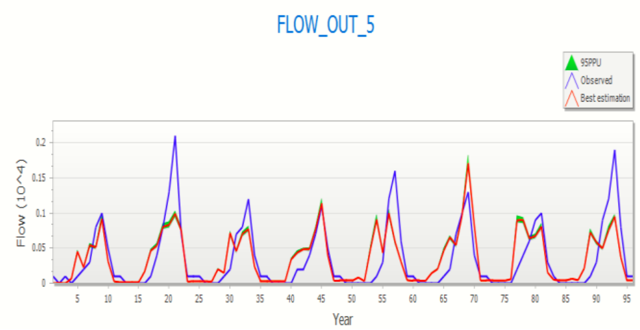

Figure 11: A monthly observed vs SWAT simulated streamflow for calibration (Jan. 2011 – Dec. 2018) in the Shiroro sub-basins under terracing

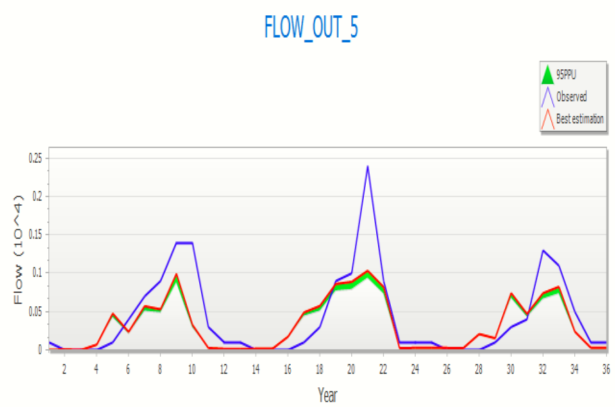

Figure 12: A monthly observed vs SWAT simulated streamflow for validation (Jan. 2019 – Dec. 2021) in the Shiroro sub-basins under terracing.

Table 4: Calibration and validation of streamflow

BMPs	Calibration and Validation of flow	NSE	P_{BIAS}	R^2	P-factor	r-factor
RALS	Calibration	0.52	-4.5	0.53	0.13	0.1
	Validation	0.58	20.5	0.63	0.28	0.47
CON	Calibration	0.58	-2.8	0.58	0.07	0.02
	Validation	0.64	-8.1	0.65	0.31	0.48
STR	Calibration	0.58	-2.7	0.58	0.13	0.19
	Validation	0.65	1.3	0.65	0.28	0.39
TER	Calibration	0.58	-3.2	0.58	0.09	0.07
	Validation	0.58	23.3	0.65	0.11	0.05

CONCLUSION

The SWAT model effectively simulated observed streamflow, demonstrating its reliability using SUFI2.

Notably, conservation practices such as terracing, contouring, and strip cropping resulted in modest increases in simulated streamflow. In contrast, non-conservation practices increase streamflow by 19%, and it is concluded that non-conservation practices around water bodies like the Shiroro Dam significantly increase streamflow and contribute to annual flooding. The implementation of contouring and strip cropping BMPs is expected to reduce flooding downstream by approximately 2 times, implying their potential benefits in mitigating flood risks by controlling runoff and preventing excessive water accumulation. There is a need for farmers to discourage non-conservation practices around water bodies like the Shiroro Dam, as they significantly increase streamflow and contribute to annual flooding.

REFERENCE

Abbaspour, K.C.; Rouholahnejad, E.; Vaghefi, S.; Srinivasan, R.; Yang, H.; Kløve, B. A (2015) continental-scale hydrology and water quality model for Europe: Calibration and uncertainty of a high-resolution large-scale SWAT model. *J. Hydrol.* 2015, *524*, (pp 733–752)

Abbaspour, K.C;Vaghefi, S; Srinivasan, R. (2017). A guideline for successful calibration and uncertainty analysis for soil and water assessment: a review of papers from the 2016 International SWAT Conference, https://doi.org/10.3390/w10010006 .

Adeogun, A., Ganiyu, H., Okunade, A., Oseni, A. (2022) modelling the impacts of selected watershed management strategies on sediment reduction upstream of Shiroro dam, Nigeria (Vol 28) Do 10.29081/jetsv2814.001 journal of engineering studies and research.

Bera, S., & Maiti, R. (2021). Assessment of water availability with SWAT model: A study on Ganga river. *Journal of the Geological Society of India*, *97*(7), 781-788.

Daramola, J, Ekhwan, T. M, Mokhtar, J., Lam, K.C., Adeogun, G.A., Estimating sediment yield at Kaduna watershed, Nigeria using soil and water assessment tool (SWAT) model, Heliyon 5 (7) (2019) e02106.

Eze, J. N. (2004). Vulnerability & Adaptation to Climate Variability & Extremes: A Case Study of Flooding in Niger State, Nigeria

Ezugwu, C.N., (2013). Sediment deposition in Nigeria reservoirs: impacts and control measures. Innov. Syst. Des. Eng. 4 (15), 54–62.

Fan, Majie. "Stream Flow: Understanding its Measurement, Characteristics, Factors and Importance." H*ydrol Current Res* 14 (2023): 460.

Food and Agricultural Organization FAO, (2009). http://www.fao.org/faostat/en/#home. (Accessed 4 August 2018).

Himanshu S.K., Pandey A, Yadav B, Gupta A. (2019). "Evaluation of best management for sediment and nutrient loss control using SWAT model" Journal of Soil & Tillage research journal. V. 192, p. 42-58.

Kushwaha, Akansha, Jain M K. 2013. Hydrological Simulation in a Forest Dominated Watershed Himalayan Region using SWAT Model. J. Water Resources Management, Springer, Vol.27: 3005 – 3023. (DOI: 10.1007/s11269-013-0329-9).

Kuti, I. A. and. Ewemoje, T. A. (2021) Modelling of sediment yield using the soil and water assessment tool (SWAT) model: A case study of the Chanchaga Watersheds, Nigeria *Scientific African 13 e00936.*

Krause, P., Boyle, D. P., & Bäse, F. (2005). Comparison of different efficiency criteria for hydrological model assessment. *Advances in Geosciences, 5,* (pp 89-97).

Pandey A, Himanshu SK, Mishra SK, Singh VP (2016) Physically based soil erosion and sediment yield models revisited. CATENA 147:595–620

Song, X.; Zhang, J.; Zhan, C.; Xuan, Y.; Ye, M.; Xu, C. Global sensitivity analysis in hydrological modeling: Review of concepts, methods, theoretical framework, and applications. *J. Hydrol.* 2015, *523*, (pp 739–757).

PRODUCTION AND CHARACTERISATION OF COCOA POD HUSK AND BANANA PEEL ACTIVATED CARBON USING CHEMICAL IMPREGNATION (ZINC CHLORIDE) FOR REMOVAL OF HEAVY METALS FROM SURFACE WATER

Abdulahi Kyuata[1] Ibrahim Abayomi Kuti[2] and John Jiya Musa[3]
[1]Kontagora Irrigation Scheme, Upper Niger River Basin Development Authority, Minna, Niger State.
[2]Department of Agricultural and Bioresources Engineering, Federal University of Technology Minna, Niger State.
[3]Department of Agricultural and Bioresources Engineering, Federal University of Technology Minna, Niger State.
Corresponding author email: kyautaabdullahi30@gmail.com

ABSTRACT

The agricultural wastes cause environmental pollution. In view of this, the study produced and characterised cocoa pod husk and banana peel activated carbon (CPH and BPAC) differently using zinc chloride to remove heavy metals in surface water. The samples were characterised using Brunauer-Emmett-Teller (BET) and Barrett-Joyner-Halenda (BJH) methods. A mixture and optimal design were used to optimise the mixture of CPH and BPAC. Nine (9) surface water samples were collected from the Garatu, Kataeregi, and Gadayeregi, where mining activities were conducted along river banks. The surface water samples were analysed using standard methods. The results indicated that the surface areas for impregnated CPH and BPAC, as determined by BET, were 762.775$m^2g^{-1}$and 678.415m^2g^{-1}, respectively, while their Dubinin-Radushkevich micropore volumes were 0.272$ccg^{-1}$and 0.273 ccg^{-1}, respectively, implying that CPH and BPAC exhibited a higher adsorptive capacity. The results included the concentrations of Lead, Chromium, and Cadmium, ranging from 0.24 - 0.55,0.24 - 0.55, and 1.55 to 3.12, were very high in the water samples when compared to WHO standard, implying that Lead, Chromium, and Cadmium pose significant health risks. Therefore, the CPH and BPAC (50, 50) removed Nickel and Zinc, implying that these heavy metals were within acceptable levels of WHO limits. The study concluded that the CPHAC (50%) and BPAC (50%) is the best for removing nickel and zinc in surface water. Future studies should use the composition ratio of BPAC (60%) and CPHAC (40%) to remove lead, chromium, and cadmium in surface water.

Keywords: *cocoa husk pod, banana peel, chemical impregnation-zinc chloride, activated carbon, heavy metal and surface water.*

1. INTRODUCTION

Mining activities also interfere with either surface or groundwater sources. These waters have been diverted from either river or stream into mining wells, which has affected the river regime (Dukiya, 2013). Additionally, the digging and washing of mined minerals find their way into surface water, causing increased accumulation of heavy metals. Heavy metal contamination in surface water is a significant environmental concern arising from various sources, including industrial, agricultural, and urban activities (Zhang et al., 2023; Aziz et al., 2023). This pollution is a global issue due to the widespread presence of toxic heavy metals in water bodies. This pollution is a global issue due to the widespread presence of toxic heavy metals in water bodies (Zhang et al., 2023). According to Zhang et al. (2023), common heavy metal pollutants include arsenic (As), cadmium (Cd), chromium (Cr), copper (Cu), lead (Pb), mercury (Hg), Nickel (Ni), and zinc (Zn). These metals are found in the earth's crust and are non-biodegradable. Some heavy metals, such as copper, iron, manganese, molybdenum, selenium, and zinc, are essential in small quantities but can be toxic at higher concentrations. Other heavy metals, like lead, cadmium, and mercury, are toxic even at low concentrations. These contaminants pose severe health risks, including neurological disorders, organ damage (such as liver and kidney damage), skin lesions, and cancer (Zhang et al., 2023).

Despite the availability of various water treatment methods, many conventional techniques, such as Ion exchange and membrane filtration techniques (reverse osmosis and nanofiltration) and advanced oxidation processes (Lubal, 2024), are often expensive and energy-intensive. These methods can generate secondary waste or prove inefficient in removing low concentrations of heavy metals. Therefore, there is a pressing need for affordable, sustainable alternatives for heavy metal removal from contaminated mine water sources using adsorption (activated carbon and biochar).

Cocoa and banana production have been a significant source of economic development in South-West Nigeria and other parts of Nigeria, contributing to the country's economy (Biney, 2017). However, the increase in productivity can lead to higher rates of pollution due to the waste generated by these activities (Velázquez-Araque, 2023; Vásquez et al., 2019). A variety of wastes, such as cocoa pod husk and banana peels, are abundantly generated in large quantities and often abandoned in field sites, littered in the surroundings, constituting foul odours, breeding grounds for pathogenic micro-organisms and environmental pollutants.

Activated carbon (AC) is a product derived from charcoal or mineral with physicochemical properties that make it a suitable filter medium in different industrial, medicinal, environmental remediation, food, and commercial applications (Velázquez-Araque, 2023). Because of its high cellulosic and hemicellulosic content, there are two types of activation techniques for AC: chemical activation and physical activation (Prauchner and Rodríguez-Reinoso, 2012; Macia-Agullo et al., 2004). While physical activation employs steam, air, CO2, or a mixture of those as an activation agent, chemical activation uses chemicals such as ZnCl2, H3PO4, and KOH (Cruz et al., 2012). Chemical activation, on the other hand, has a few advantages over physical activation: it yields much higher activated carbons, uses temperatures lower than pyrolysis, usually only needs one step, and produces activated carbons with extremely high surface areas and well-developed microporosities. Additionally, the activated carbons produced significantly reduce the mineral matter content.

Few studies used AC (adsorption) to remove heavy metals from groundwater, while others did not apply it as a filter medium. Cruz et al. (2012) employed cocoa pod husks from activated carbon to remove arsenic (As) in groundwater pollution and discovered that AC from cocoa pod husks can absorb up to 80% of arsenic in less than an hour. However, the research did not vary the percentage of cocoa pod husk and banana prior to ZnCl2 impregnation to establish the optimal biomass for the removal of arsenic in groundwater. In addition, Velázquez-Araque et al. (2023) produced activated carbon (AC) from cocoa pod husks and banana peels prior to phosphoric acid (H_3PO_4) and sulfuric acid (H2SO4) impregnation. This study found that cocoa husk pod and 50 % concentration of sulfuric acid solution as an activating agent, making it highly suitable to be used as a filter medium. However, this research did not vary the percentage of cocoa pod husk and banana peels prior to phosphoric acid (H3PO4) and sulfuric acid (H2SO4) impregnation to determine optimal biomass that will be suitable for the removal of heavy metals in mine water. In this research, the percentage of cocoa pod husk and banana peels was varied prior to ZnCl2 impregnation to determine its effect on the quality of the activated carbon produced, aiming to find an optimal biomass for effective AC production from cocoa pod husks and banana peels, which will remove heavy metals in mine water.

Varying the percentage of cocoa pod husk and banana peels helps determine the best proportion of activated carbon. Different proportions of cocoa pod husk and banana peel can significantly influence the chemical composition and physical characteristics of the biomass, which in turn affects the efficiency of the ZnCl2 activation process. Moreover, varying the biomass composition can help tailor the final product for specific applications, such as improving its adsorption capabilities or combustion properties. The research aims to establish the optimal biomass from cocoa pod husks and banana peels for effective AC production. The variation in percentages of cocoa pod husk and banana peel prior to ZnCl2 impregnation would give not only the optimal biomass but also a strategic approach to enhancing the quality and performance of activated carbon derived from agricultural waste.

2.0 METHODOLOGY

2.1 Description of the study area

Location	Latitude	Longitude
Garatu	9.483202	6.439378
Kataeregi	9.365477	6.165388
Gadayeregi	9.387992	6.34921

2.2 Materials

The materials used for this study include cocoa pod husk, banana peel, water sample, distilled water, $Zncl_2$ and Liquid nitrogen. The equipment used for this study includes a Muffle furnace (model number: HSX-2-6-13 and serial number: 20220412), Electronic weighing balance (Metlab electronic compact scale, SF-400C), Ultraviolet spectrophotometer (Jenway, Model 6300); Cutlass; Porosimeter (ASAP 2020 model from micrometric); Oven dryer (model number: PBS118SF and serial number: 94L234); Buhr mill (model number: XM0240X90 and year: June 2022); Crucible; Oven (hot air oven, drier box AX-OV73); Atomic Absorption Spectrometry (Jenway, Model PFP7); Nova 4200e (model number:1413052102)

2.3 Preparation of Activated Carbon

Cocoa pod husks (CPH) and banana peels (BP) were sun-dried, reduced to smaller sizes (Plate I), and washed with distilled water to remove external waste particles. The washed cocoa pod husk and banana peel pieces were dried in an oven (model number: PBS118SF and serial number: 94L234) at 105^0C for 24 hours to remove moisture content (fig1).

Figure 1A and B Pieces of cocoa pod husk and banana peel during sun-dried and oven-dried

CPH and BPAC were subjected to a carbonisation process at 350^{0}C in the muffle furnace, as shown in Figure 2 (Velázquez-Araque *et al.*, 2023; Rangari and Priyanka, 2017).

Figure 2: Carbonisation of cocoa pod husk and banana at the Muffle furnace

The sample was later crushed to sizes of 0.25mm and 0.5mm (Figure 3 A and B) with a buhr mill (model number: XM0240X90 and serial number: 80220452).

Figure 3 A and B: Crushed cocoa pod husk and banana peel before impregnation

The crushed samples were divided into two portions and accurately weighed 50 grams each. The first sample was non-impregnated, and the second sample was impregnated with sulfuric acid of 10% concentration level for 24 hours until the mixed sample turned into a paste to the level of activation carbon properties as shown in Figure 4 A and B (Kuti *et al.*, 2018; Rangari and Priyanka, 2017). The percentage of cocoa pod husk and banana peels varied after ZnCl2 impregnation to determine its effect on the quality of the activated carbon, which has not been conducted before in the literature. One molar of zinc chloride was used for the impregnation.

Figure 4. A and B: Impregnation of cocoa pod husk and banana peel with Zinc Chloride ($ZnCl_2$)

2.4 Characterisations of Activated Carbon

The Brunauer- Emmet- Teller theory (BET) was used to determine the surface area of the activated carbon produced from cocoa pod husk and banana peel according to Chen *et al.* (2018) and Rouquero *et al.* (2013), respectively. The samples were degassed at 523^{0}C for 3 hours for moisture and removal. The degassed samples were then analysed for physisorption of the adsorbate (nitrogen) by the adsorbent in a liquid nitrogen environment on the surface (Kariim et al., 2015).

2.5 Data analysis

The surface area of impregnated CPH and BPAC were determined using the BET method with Nova 4200e (Kariim et al., 2015). The equipment analysed and generated results in descriptive statistics such as mean values and correlation coefficients.. The removal efficiency was determined as followed:

$$Removal\ Efficiency\ (\%) = \frac{(C_i - C_{f)}}{C_i} \times 100$$

where C_i and C_f represent the initial and final concentration of heavy metals.

3.0 RESULT AND DISCUSSIONS

3.1 Characterisation of Activated Carbon from Cocoa Pod Husk and Banana Peels

Cocoa pod husk (CPH) and Banana peel (BPAC) with Zinc Chloride acid were characterised by Nitrogen gas analysis at 250^{0}C. Appendices I and II showed multi-point BET plots for CPH and BPAC with Zinc Chloride acid. Also, the results showed linear and nonlinear, indicating correct and incorrect BET plots for both CPH and BPAC with Zinc Chloride acid. The CPH and BPAC impregnated with (ZnCL2) have a correlation coefficient and slope values of 0.999297 and 2.936, then 0.995275 and 3.933, respectively. Furthermore, Appendices I and II have positive constant C for CPH (2.801) and BPAC (4.277).   The Multi-BET surface area for the CPH and BPAC with Zinc Chloride acid had a mean of 762.775 m^{2}g, 678.415m2/g, implying a significant difference in Multi BET area obtained in different relative pressure ranges (Table 1). Its Langmuir surface area also had a mean of 14635.233 m^{2}g(CPH) and 2547.965m^2/g(BPAC) (Table 1), implying that the CPH and BPAC with Zinc Chloride acid had a large surface area under the BET and Langmuir method. The curves sharply increase at low relative pressure, showing a high adsorptive capacity for CPH and BPAC impregnated with Zinc Chloride acid. This finding aligns with related studies (Kuti *et al*., 2018a).

The Dubinn-Radushkevic Method **(**DR) micropore pore volume and average pore width for CPH and BPAC impregnated with Zinc Chloride acid ($ZnCl_2$) were 0.272cc/g, 6.503nm and 0.273cc/g and 6.006nm, respectively. In comparison, the values for CPH and BPAC with Zinc Chloride are shown in Table 1. This finding is evidenced by a remarkable increase of 36.25% in the Langmuir surface area, as shown in Table 1. These results are consistent with related studies (Kuti et al., 2018a). However, Kuti et al. (2018) utilised bamboo as a precursor with different chemical activation methods, and their findings indicated that Zinc Chloride acid treatment resulted in a higher surface area (Langmuir). Similarly, agricultural waste (bamboo) had a higher surface area than carbons activated with zinc chloride (Ademiluyi et al., 2012). The correlation between the two samples is positive and very high. The Barrett-Joyner-Halenda surface area, pore volume, and pore diameter were like the Multi-BET surface area (Table 1). However, the micropore analysis using the Dubinin-Astakhov (DA) method had the highest pore volume, followed by the BJH pore volume (Table 1). The study revealed that the micropore Analysis (Dubinin-Astakhov (DA) method is preferred over other methods in terms of pore volume (Sdanghi et al., 2020). A study conducted by Velázquez-Araque*et al*. (2023) revealed that the CPH and BPAC had the highest surface area of 762.775 m^{2}g, with a 50% Zinc Chloride acid solution and aligns with the finding of this study, although with 10% Zinc Chloride acid. Cruz *et al*. (2012) also discovered that the highest surface area obtained for Zinc Chloride that removed heavy metals from the water was 762.775 m^2g; similarly, the adsorption efficiency of cocoa pod husk biochar for heavy metals ranged from 99.97% to 99.99% (Abbey et al., 2023), implying that CPH had a higher affinity for heavy metals removal. The activated carbon from cocoa pod husk and banana peel removed heavy metals.

Table 1: Textural porous characteristics of cocoa pod husk (CPH) and banana peel (BP) activated carbon using ($ZnCl_2$)

Characteristics	Impregnated Cocoa pod husk with Zinc Chloride ($ZnCl_2$)	Impregnated Banana Peel With Zinc Chloride ($ZnCl_2$)
Multi-point BET surface area (m^2/g)	762.775	678.415
DA micropore volume (cc/g)	0.678	0.618
DA pore diameter (nm)	3.000 e^{+00}	2.860 e+00
BJH surface area (m^2/g)	789.483	806.347
BJH pore volume (cc/g)	0.389	0.391
BJH pore diameter (nm)	2.105	2.115
Langmuir surface area (m^2/g)	14635.233	2547.965
DR micropore volume (cc/g)	0.272	0.273
DR micropore surface area (m^2/g)	765.718	767.118
DFT pore volume (cc/g)	0.196	0.210
DFT surface area (m^2/g)	161.766	176.707
DR Absorption energy (KJ/mol)	3.998	4.329
DR average pore width (nm)	6.503	6.006

Note: Brunauer-Emmett-Teller (BET), Barrett-Joyner-Halenda (BJH), Dubinn-Radushkevic Method (DR), Dubinin-Astakhov (DA), Density Functional Theory (DFT).

3.2 Removal of Heavy Metals from Surface Water using Cocoa Pod Husk and Banana Peel Activated Carbonin Selected Study Area

Table 2 presents the removal rate of heavy metals in surface water under different compositions of cocoa pod husk and banana activated carbon in selected study areas. The results showed the removal rates of heavy metals across different locations and compositions of CPH and BP. The highest removal rates were observed for Nickel (Ni) at Garatu, where a composition of 50:50 CPH and BP achieved an impressive 97% removal rate. Similarly, Zinc (Zn) removal was maximised at Kataeregi with the same 50:50 composition, reaching a removal rate of 94%. In Garatu, the cocoa pod husk and banana-activated carbon consistently demonstrated higher removal rates for Ni and Zn compared to Kataeregi and Gadaeregi.

In contrast, the cocoa pod husk and banana-activated carbon removed Zn and Lead (Pb), while Gadayeregi showed a notable efficiency in removing Cadmium (Cd). The results also showed that CPH and BP-activated carbon (50,50 composition) had a minimum removal rate of 45% for zinc. A similar trend was observed for CPH and BP-activated carbon (80,20 and 65,35), where their minimum removal rates were 14% (Zinc) and 15% (Chromium). The effect of composition on removal efficiency was another critical factor. Generally, as the proportion of CPH increased relative to BP, the removal efficiency decreased. However, there were exceptions to this trend. For instance, at Kataeregi, the removal of Zn remained effective even with varying compositions, indicating that specific metal removals can be less sensitive to changes in CPH and BP ratios under certain conditions.

Table 2: Removal rate of heavy metals in surface water in selected study area

Sample Locations	CPH and BP	Pb (%)	Cr (%)	Cd (%)	Cu (%)	Zn (%)	Ni (%)
A	50,50	86	80	81	79	88	97
A	65,35	61	45	38	68	75	59
A	80,20	56	24	52	53	62	53
B	50,50	80	69	83	70	94	80
B	65,35	70	62	60	59	87	47
B	80,20	62	57	43	33	89	39
C	50,50	65	76	96	68	45	81
C	65,35	29	15	65	53	17	54
C	80,20	41	32	58	56	14	27

3.3 Determination of the optimal biomass for effective Activated Carbon production from cocoa pod husks and banana peels

The mean concentrations of heavy metals varied across different composition ratios. For Lead (Pb), the lowest concentration was observed at a 50:50 composition ratio (0.08 ppm), while the highest concentrations were found at the 80:20 and 65:25 ratios (0.19 ppm and 0.18 ppm, respectively). Chromium (Cr) showed its highest concentration at the 80:20 ratio (1.31 ppm) and its lowest at the 50:50 ratio (0.54 ppm). Cadmium (Cd) concentrations were consistent at 0.06 ppm for both the 80:20 and 65:25 ratios but significantly lower at 0.02 ppm for the 50:50 ratio. Copper (Cu) had its highest concentration at the 80:20 ratio (0.13 ppm) and its lowest at the 50:50 ratio (0.07 ppm). Zinc (Zn) concentrations were highest at the 80:20 ratio (0.58 ppm), decreasing to 0.36 ppm at the 50:50 ratio. Lastly, Nickel (Ni) concentrations decreased from 0.10 ppm at the 80:20

ratio to 0.03 ppm at the 50:50 ratio. This study discovered that the 50:50 composition ratio resulted in the lowest concentrations of all heavy metals tested.

Table 3: Mean concentration of heavy metals using cocoa pod husk and banana peel activated carbon under different compositions in the selected study area

Ratio	Pb (ppm)	Cr (ppm)	Cd (ppm)	Cu (ppm)	Zn (ppm)	Ni (ppm)
80,20	0.19	1.31	0.06	0.13	0.58	0.10
65,25	0.18	1.20	0.06	0.11	0.55	0.08
50,50	0.08	0.54	0.02	0.07	0.36	0.03

Table 4 presents the treatment of heavy metal in surface water using cocoa pod husk and banana peel-activated carbon. Comparing the results with the WHO standard, as shown in Table 1, the study observed that nickel was below the limits (0.07), followed by zinc (3). The remaining heavy metals were above the WHO standard.

Table 4: Treatment of heavy metals in surface water using cocoa pod husk activated (50%) and banana peel activated carbon (50%)

Sites	Pb (ppm)	Cr (ppm)	Cd (ppm)	Cu (ppm)	Zn (ppm)	Ni (ppm)
SL1	0.05	0.39	0.03	0.04	0.04	0
SL2	0.11	0.97	0.02	0.07	0.19	0.04
SL3	0.09	0.37	0.01	0.11	0.78	0.04

Note: SL1: Garatu; SL2: Kataeregi; SL3: Gadayeregi

These findings align with an existing study, which reported that Chromium levels were higher than the safe limit of 0.141 mg/l in the water hand pump samples at Gupta Gate, Shivnagar (Tripathi and Chaurasia, 2020). The contamination level of cadmium in the surface water was high in the selected area, ranging from 1.55 to 3.12. This outcome aligns with a previous study (Panwar and Ahmed, 2018), which reported that a sample of groundwater had a level up to 0.28 mg/l, which was above the safe level standard. These findings imply that lead, chromium, and cadmium pose significant health risks, including kidney damage, bone disorders, and increased cancer risk (Bouida et al., 2022; Sholehhudin et al., 2021). The concentrations of the heavy metals are linked to mining activities.

The Cocoa pod husk activated with Zinc Chloride ($ZnCl_2$) had a surface area of 762.775 m^2/g, while the surface area for the banana peel was 678.415 m^2/g. This finding aligns with an existing study (Velázquez-Araque et al., 2023), which reported that activating cocoa pod husk and banana peel with sulphuric acid had a mean of 600 and above (m^2/g) is appropriate.

The study revealed that the removal of Zn remained effective even with varying compositions of cocoa pod husk and banana peel activated carbon for different compositions: 80,20, 50,50, and 65, 35. There is little or no information about the suitable composition of cocoa pods and banana peel activated for the removal of nickel and zinc. Therefore, the cocoa pod husk and banana peel activated carbon (50,50) removed Nickel and Zinc.

4.0 CONCLUSION

The study characterised cocoa pod husk and banana peel and activated them with zinc chloride for the removal of heavy metals in surface water near mining activities in the selected study area. The results discovered that the surface water samples contain high concentrations of lead, chromium, and cadmium, posing serious health risks to consumers. The BET surface area also showed that cocoa pod husk activated with zinc chloride has a higher surface area compared to banana peel, which could potentially enhance its adsorption capabilities. Findings from this study showed that the removal of zinc remained effective across varying compositions, indicating its robustness in different conditions. The optimal biomass composition for the removal of heavy metals was 50 percent cocoa pod husk and banana peel, and the level of its removal rate was high. In addition, the correlation coefficient revealed a positive and strong relationship between the percentage of cocoa pod husk and heavy metal concentrations after treatment, while a negative correlation was observed with banana peel. These findings suggest that banana peel may be more effective in reducing heavy metal levels.

Furthermore, the study found that nickel and zinc levels were within acceptable limits after treatment and concluded that the removals of nickel and zinc were superb. A composition ratio of cocoa pod husk (50%) and banana peel (50%) is recommended to remove nickel and zinc from gold mining wastewater. It is also recommended that future studies should use the composition ratio of banana (60%) and cocoa pod husk (40%) to optimally remove lead, chromium, and cadmium in gold mining surface wastewater.

REFERENCES

Aziz, K. H. H., Mustafa, F. S., Omer, K. M., Hama, S., Hamarawf, R. F., & Rahman, K. O. (2023). Heavy metal pollution in the aquatic environment: efficient and low-cost removal approaches to eliminate their toxicity: a review. RSC advances, 13(26), 17595-17610.

Biney, K. A. (2017). Cocoa Production Trends in South-West, Nigeria. PhD thesis submitted to the University of Lagos, Akoka.

Chen, Q., Yao, Y., Li, X., Lu, J., Zhou, J., & Huang, Z. (2018). Comparison of heavy metal removals from aqueous solutions by chemical precipitation and characteristics of precipitates. *Journal of water process engineering*, *26*, 289-300.

Cruz, G., Pirilä, M., Huuhtanen, M., Carrión, L., Alvarenga, E., &Keiski, R. L. (2012). Production of activated carbon from cocoa (Theobroma cacao) pod husk. *J. Civ. Environ. Eng*, *2*(2), 1-6.

Dukiya J. J. (2013). The environmental implication of illegal mining activities in Nigeria, a case study of Pandogari and BarkinLadi/Buruku surface mines in Niger/plateau states." Journal of Humanities and Social Sciences 13.5 (2013): 13-19.

Kariim, I., A. S. Abdulkareem, O. K. Abubakre, M. T. Bankole, & J. O. Tijani. 2015. Studies on the suitability of alumina as bimetallic catalyst support for MWCNTs growth in a CVD reactor. *International Engineering Conference held at Federal University of Technology Minna*, on September

Kuti, I. A., Adabembe, B. A., Adeoye, P. A., Musa, J. J., Animashaun, I. M., & Issa, M. O. (2018). Production and characterisation of bamboo activated carbon using different chemical impregnations for heavy metals removal in surface water.

Lubal, M. J. (2024). Health Effects of Heavy Metal Contamination in Drinking Water. Uttar Pradesh Journal of Zoology, 45(10), 16-25.

Maciá-Agulló, J. A., Moore, B. C., Cazorla-Amorós, D., & Linares-Solano, A. (2004).Activation of coal tar pitch carbon fibres: Physical activation vs. chemical activation. Carbon, 42(7), 1367-1370.

Prauchner, M. J., & Rodríguez-Reinoso, F. (2012). Chemical versus physical activation of coconut shell: A comparative study. Microporous and Mesoporous Materials, 152,163-171.

Rangari, P. J., & Chavan, P. (2017). Preparation of activated carbon from coconut shell. *IJIRSET, 6*(7), 1-8.

Rouquerol, J., Rouquerol, F., Llewellyn, P., Maurin, G., & Sing, K. (2013). *Adsorption by powders and porous solids: principles, methodology and applications*. Academic press.

Vásquez, C., Calva, J., Morocho, R., Donoso, D. A., & Benítez, Á. (2019). Bryophyte communities along a tropical urban river respond to heavy metal and arsenic pollution. *Water*, *11*(4), 813.

Velázquez-Araque, L., Chávez, A. O., & Calle, M. C. (2023). Production of activated carbon from cocoa pod husks and banana peels using H3Po4 and H_2SO_4 as activating agents. 31st European Biomass Conference and Exhibition, 5-8 June 2023, Bologna, Italy.

Zhang, P., Yang, M., Lan, J., Huang, Y., Zhang, J., Huang, S., ... & Ru, J. (2023). Water quality degradation due to heavy metal contamination: Health impacts and eco-friendly approaches for heavy metal remediation. Toxics, 11(10), 828.

Zia, Z. (2022). Synthesis *and characterisation of low-cost biopolymer/mineral composite systems* and evaluation of their potential application for heavy metal removal (Doctoral *dissertation, The* University *of Waikato).*

Development of Pulverizing Machine for Pharmaceutical Industries

*Ugwunna, A. K.[1]; Olugboji, O. A.[2]; Awotoye, B. A[3]
[1] Department of Mechanical Engineering Federal University of Technology, Minna
[2] Department of Mechanical Engineering Federal University of Technology, Minna
[3] Department of Mechanical Engineering Federal University of Technology, Minna
*Corresponding author email: ugwunnaazuka@gmail.com

ABSTRACT

This project focuses on the design, fabrication, and evaluation of a pulverizing machine specifically tailored for pharmaceutical industries in Nigeria. The hammer mill, made from stainless steel, was chosen due to its high processing capacity and ability to handle various dry materials. Stainless steel was selected for its corrosion resistance, strength, and durability, ensuring compliance with pharmaceutical hygiene standards and providing long-lasting performance. The pulverizer consists of essential components including a high-speed motor, hammers, a sieve, and a suction fan for efficient dust control and heat prevention. The machine was fabricated using locally sourced materials at a cost of #200,000, significantly lower than the cost of imported equivalents. Performance tests were conducted using maize, guinea corn, and millet, demonstrating consistent particle sizes of 400µm-600µm across crops. The results showed that the machine performed reliably, with fine particle output and minimal variations in mass loss and processing time. Although variations in weight changes were observed, particularly with millet, the hammer mill proved to be efficient, achieving uniform grinding with minimal energy consumption. The study concludes that the locally fabricated pulverizer, made from stainless steel, is cost-effective, durable, and suitable for pharmaceutical grinding processes, with potential for optimization and further development, including solar-powered operation to address energy supply challenges in Nigeria.

Keywords: *Corrosion resistance, Fabrication, Hammer mill, Pharmaceutical industries, Pulverizing machine, Stainless steel*

1 INTRODUCTION

A pulverizer is a machine designed to crush, grind, or shred materials into smaller particles through repeated hammering. These machines have a wide range of industrial applications, including use in agriculture, where they mill grain into coarse flour for livestock feed, in fruit juice production, where they help extract juice by breaking down fruit fibers, and in recycling industries, where they grind used shipping pallets into mulch. The grinding process has been utilized since ancient times, dating back to the Stone Age, and continues to be an essential operation in modern industries due to its numerous advantages. Grinding is widely employed to increase the reactivity, solubility, and homogeneity of solid materials, making them more suitable for various applications (WU Z *et al.*, 2012).

Controlling particle size is crucial in different industries, as it directly impacts the performance and quality of the final product. In the pharmaceutical industry, for instance, the particle size of active pharmaceutical ingredients (APIs) and excipients must be precisely maintained to ensure proper dissolution rates and solubility. An improper particle size distribution can lead to reduced drug efficacy or unpredictable release rates (Cerdeira AM *et al.*, 2010; Merisko-Liversidge E & Liversidge GG, 2011). Similarly, in the mining and mineral processing sector, controlling particle size enhances the efficiency of ore concentration, allowing metals to be more effectively extracted from raw mineral ores (Chemjea TW *et al.*, 2004). A well-regulated grinding process ensures that the ore particles are broken down to the optimal size, improving the efficiency of further separation and refining processes.

Beyond simple size reduction, grinding has recently been utilized in the synthesis of advanced materials, taking advantage of the mechanical forces generated during the process. In material science and engineering, mechanical grinding helps modify material properties, create new structures, and enhance performance characteristics for specialized applications. This approach is being explored for improving catalysts, enhancing fuel cell efficiency, and even developing high-performance composite materials.

The size reduction process depends on several material properties, including hardness, toughness, moisture content, abrasiveness, and thermal sensitivity. Grinding and cutting are common methods for reducing the size of solid materials, while emulsification and atomization are used for liquids. There are various types of size-reduction machines designed for specific applications, and their efficiency is influenced by factors such as feed size, final particle size, energy consumption, and material handling properties. Ensuring an optimal grinding process requires a deep understanding of these factors to achieve desired particle size distribution while maintaining efficiency.

Despite advancements in grinding technology, the understanding of grinding phenomena remains challenging due to the complex interactions of particles, mechanical forces, and fluid movements within the system. In recent years, researchers have attempted to analyze grinding processes using numerical simulation techniques, which help model the motion of particles and the forces acting on them. However, one of the major challenges in numerical simulation is accurately predicting particle breakage mechanisms. Although many studies have focused on single-particle breakage, there is still a lack of comprehensive models that can simulate overall grinding behavior in an industrial setting.

To overcome these limitations, ongoing research is focused on developing novel simulation methods that can integrate both single-particle breakage and bulk grinding phenomena. Such advancements will enhance the efficiency, precision, and predictability of grinding processes across various industries, ensuring better control over particle size distribution and improving material processing. Understanding and optimizing these processes will have significant implications in fields ranging from pharmaceuticals and materials science to mining and manufacturing.

2 METHODOLOGY

This section outlines the procedures and methods used in the research, including the design, fabrication, and performance evaluation of the pulverizer. The methodology includes machine description, materials selection, design analysis, fabrication process, testing procedures, and data analysis.

2.1 RESEARCH DESIGN

The study follows an experimental research approach, involving the design, fabrication, and performance evaluation of a pulverizer. The research process consists of four key phases:

i. Conceptual Design and Analysis – Reviewing existing pulverizer designs, identifying limitations, and developing an improved design.
ii. Material Selection and Fabrication – Choosing appropriate materials based on strength, durability, and corrosion resistance, followed by the machine's fabrication.
iii. Performance Testing – Conducting tests to evaluate the efficiency, throughput, and operational reliability of the pulverizer.
iv. Data Collection and Analysis – Measuring key performance parameters, including particle size distribution, energy consumption, and throughput rate.

2.2 DESIGN AND FABRICATION PROCESS

The pulverizer was designed to operate based on the principle of impact and attrition. The hammer mill mechanism was selected for its high efficiency in pulverizing different dry materials. The design process included:

- Structural Design: CAD software (SolidWorks) was used to design and simulate the components to ensure structural integrity.
- Material Selection: Materials were chosen based on strength, durability, heat resistance, and corrosion resistance. The materials used for various components are listed in Table 3.1.
- Fabrication Steps:
  i. Cutting and shaping of stainless-steel sheets for the pulverization unit.
  ii. Welding and assembly of frame components using medium-carbon steel.
  iii. Installation of hammers, rotors, and bearings.
  iv. Mounting the electric motor, belt system, and fan assembly.
  v. Assembly of the cyclone system for dust control and improved efficiency.

2.3 PERFORMANCE EVALUATION

The fabricated pulverizer was tested for efficiency using the following parameters:

i. Throughput Rate (kg/hr): Measured by determining the weight of processed material over time.
ii. Particle Size Distribution: A sieve analysis was conducted to evaluate the uniformity of the output.
iii. Energy Consumption: The power input of the 3.69 kW electric motor was recorded during operation.
iv. Operational Efficiency: The effectiveness of the suction fan in preventing clogging and heat buildup was observed.

2.4 SAFETY AND MAINTAINABILITY CONSIDERATION

i. Safety measures such as protective enclosures for the cutting blades and insulated heating coils were incorporated to prevent hazards.
ii. The machine was designed for easy maintenance, with bolts and nuts facilitating the replacement of parts like the heating coil, motor, and rotor.

2.5 DATA COLLECTION AND ANALYSIS

i. Experimental data were recorded, tabulated, and analyzed statistically.
ii. Results were presented using graphs, tables, and charts to evaluate machine performance.

2.6 DESIGN ANALYSIS FOR SMALL HAMMER MILL

2.6.1 Determination of shank diameter of bolts connecting the Coupler to disc-1

This is given by

$$\sigma_b = \frac{F}{A} \qquad 1$$

Where σ_b is bearing stress
F is force acting on shank
A is bearing area on disc-1
But

$$A = dt \qquad 2$$

Where d is diameter of shank
t is the thicknes of disc-1, Therefore,

$$\sigma_b = \frac{F}{dt}$$

$$d = \frac{F}{\sigma_b t} \qquad 3$$

But $F = 125\ N, t = 2\ mm, \sigma_b = 20\ N/mm^2$, then

$$d = \frac{125}{20 \times 2}$$

$$\boldsymbol{d = 3.13\ mm}$$

Based on the above result, the M4 bolt size of root diameter of 3.16mm is selected

2.6.2 DETERMINATION OF TORQUE ON SHAFT

Torque on the motor shaft is given by the relation

$$T = 2Fr \qquad 4$$

Where F is force on each coupler bolt
r is coupler bolt distance form shaft center
but $F = 123\ N, r = 0.02\ m$, therefore,

$$T = 2 \times 123 \times 0.02$$

$$\boldsymbol{T = 4.92\ Nm}$$

2.6.3 POWER TO DRIVESHAFT

The power to drive shaft is determined from the given relation

$$P = T\omega \qquad 5$$

$$\omega = \frac{2\pi N}{60} \qquad 6$$

$$P = \frac{2\pi NT}{60} \qquad 7$$

Where N is speed of electric motor in rpm.
Having N as 1400 rpm, then

$$P = 2\pi \times 1440 \times 4.92/60$$

$$\boldsymbol{P = 742.0\ W}$$

Based on the above result, a 1HP (746 W) Electric motor is selected

2.6.4 DETERMINATION OF THICKNESS OF STRIKER

Let the force acting per unit length of hammer be q.

$$q = \frac{F_s}{l} \qquad 8$$

Taking the length of the striker to be 55 mm and resultant force on hammer as 61.83 N, then

$$q = \frac{61.83}{55}$$

$$q = 1.124\ N/mm$$

Considering the striker as a cantilever, the following expression holds

$S = \frac{M_{max}}{\sigma_{all}}$, Gere, J, 2006 9

Where S is sectional modulus
M_{max} is maximum bending moment
σ_{all} is allowable stress
If b is the breadth of the striker and h is its thickness, then

$$S = \frac{bh^2}{6} \qquad 10$$

Equating 9 and 10 gives

$$\frac{M_{max}}{\sigma_{all}} = \frac{bh^2}{6} \qquad 11$$

But for a cantilever,

$$M_{max} = \frac{qL^2}{8} \qquad 12$$

$$\frac{qL^2}{\sigma_{all}} = \frac{4bh^2}{3}$$

$$h = \sqrt{\frac{3qL^2}{4b\sigma_{all}}} \qquad 13$$

When L = 55mm, b = 10 mm and $\sigma_{all} = 30\ Nmm^2$, then

$$h = \sqrt{\frac{3 \times 1.124 \times 55^2}{4 \times 10 \times 30}}$$

$$h = \ 2.9\ mm$$

2.6.5 SHANK DIAMETER OF BOLT CONNECTING THE STRIKER TO DISC-1 AND DISC-2

Recalling equation 3 where F is now centrifugal force, F_c

$$d = \frac{F_c}{\sigma_b t} \qquad 14$$

$$F_c = m\omega^2 r \qquad 15$$

$$d = \frac{m\omega^2 r}{\sigma_b t} \qquad 16$$

but

$$\omega = \frac{2\pi N}{60} \qquad 17$$

Where m is mass of striker
ω is angular velocity
r is distance from origin

Taking $m = 0.03\ kg,\ r = 0.06\ m, t = 0.002\ m, \sigma_b = 20\ MPa$

$$\omega = \frac{2 \times 3.142 \times 1440}{60}$$

$$\omega = 150.816\ rad/s$$

$$d = \frac{0.03 \times 150.816^2 \times 0.06}{20 \times 10^6 \times 0.02}$$

$$d = 0.002\ m$$

2.6.6 DETERMINATION OF CENTRIFUGAL FAN PARAMETERS

As the striker hammers on materials in the chamber it also functions as a centrifugal fan. Hence the need to analyze it as one of such.
Generally, the tangential velocity for centrifugal fan is:

$$u = \omega r$$

Therefore, tangential blade velocities at inlet and outlet respectively are given by:

$$u_1 = \omega r_1\ ;\ u_2 = \omega r_2 \qquad 18$$

Where r_1 = radius of inlet cylinder surface

r_2 = radius of outlet cylinder surface

ω =Angular Velocity

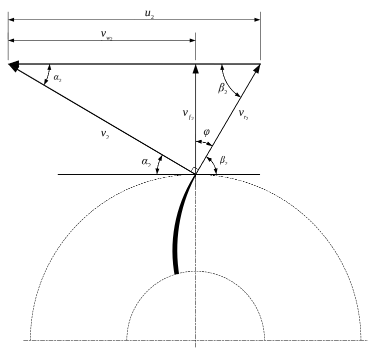

Figure 1: Free body diagram for the impeller blade

Applying continuity equation to the inlet and outlet for the mass flow rate$\dot{m}$ gives

$$\dot{m} = 2\pi r_1 \rho_1 b_1 v_{f1} = 2\pi r_2 \rho_2 b_2 v_{f2}$$ J. M. Gasiorek, 2000

Where:b_1 = Impeller width at inlet

b_2 = Impeller width at outlet

ρ_1= density of air at inlet

ρ_2= Density of air at outlet

v_{f1}= Velocity of flow at inlet

v_{f2}=Velocity of flow at outlet

For incompressible flow

$$m = r_1 b_1 v_{f1} = r_2 b_2 v_{f2} \qquad 19$$

Assumptions;

1. For inlet, absolute velocity, V is radial. Therefore
$V = v_{f1}, v_w = 0, \alpha_1 = 90^0$

Where v_{w1} is velocity of whirl at inlet,

α_1 is angle that absolute inlet velocity make with tangent.

2. Blade angle at inlet,β is such that the blade meets the relative velocity tangentially.
3. Fluid leaves impeller with a relative velocity tangential to the blade at outlet.

Theoretical head is given by Euler's equation

$$H_{th} = \frac{u_2 v_{W2} - u_1 v_{W1}}{g} \quad 20$$

Where H_{th} istheoretical head

$V_{w1}$is Tangential component of absolute fluid velocity an inlet. Also, known as velocity of whirl. But vω1 = 0, Therefore,

$$H_{th} = \left(\frac{U_2 V_{\omega 2}}{g}\right) \quad 21$$

Volume of flow Q is given as

$$Q = v_{f2} A_2$$

$$A_2 = 2\pi r_2 b_2$$

$$Q = 2 v_{f2} \pi r_2 b_2 \quad 22$$

Where $A_2$is area of outlet cylinder surface

Torque on shaft is given as

$$T = \frac{Q \rho v_{\omega 2} r_2}{g} \quad 23$$

Where ρ is density of air and $g$is acceleration due to gravity

Therefore, power required to drive fan is given as

$$P = T\omega \quad 24$$

But from figure 1

$$\alpha_2 = 180 - 90 - \beta_2 \quad 25$$

$$\varphi = 180 - 90 - \beta_2 \quad 26$$

$$\frac{v_{r2}}{Sin\alpha_2} = \frac{u_2}{Sin90}; v_{r2} = \frac{u_2 Sin\alpha_2}{Sin90} \quad 27$$

$$\frac{v_{f2}}{Sin\beta_2} = \frac{v_{r2}}{Sin90}; v_{f2} = \frac{v_{r2} Sin\beta_2}{Sin90} \quad 28$$

$$\frac{v_{\omega 2}}{Sin(90-\varphi)} = \frac{v_{f2}}{Sin\alpha_2}; v_{\omega 2} = \frac{v_{f2} Sin(90-\varphi)}{Sin\alpha_2} \quad 29$$

Considering equations 17 to29 when

r1 = 0.03 m, r2 = 0.05 m, $b_1 = b_2 = 0.02\ m$, β_2 = 60,$\omega = 150.816\ rad/s$

$$u_1 = \omega r_1$$

$$= 150.816 \times 0.03$$

$$u_1 = 4.5245\ m/s$$

$$u_2 = \omega r_2$$

$$= 150.816 \times 0.05$$

$$u_2 = 7.5408\ m/s$$

$$\alpha_2 = 180 - 90 - \beta_2$$

$$= 180 - 90 - 60$$

$$\alpha_2 = 30°$$

$$\varphi = 30°$$

$$v_{r2} = \frac{u_2 Sin\alpha_2}{Sin90} = \frac{7.5408 \times Sin30}{Sin90}$$

$$v_{r2} = 3.7704\ m/s$$

$$v_{f2} = \frac{v_{r2} Sin\beta_2}{Sin90} = \frac{3.7704 \times Sin60}{Sin90}$$

$$v_{f2} = 3.2653\ m/s$$

$$v_{\omega 2} = \frac{v_{f2} Sin(90-\varphi)}{Sin\alpha_2} = \frac{3.2653 \times Sin(90-30)}{Sin30}$$

$$v_{\omega 2} = 5.6556\ m/s$$

Considering equation 5, the theoretical head is given by

$$H_{th} = \frac{u_2 v_{W2}}{g}$$

$$\frac{7.5408 \times 5.6556}{9.81}$$

$$H_{th} = 4.3474\ m$$

The volume of flow is given by equation 22

$$Q = v_{f2} 2\pi r_2 b_2$$

$$= 2 \times 3.142 \times 0.05 \times 0.02$$

$$Q = 0.0205\ m^3/s$$

Using equations 23 and 24, the Torque and power respectively for blowing out air by the fan are given.

$$T = \frac{Q\rho v_{\omega 2} r_2}{g} = \frac{0.0205 \times 1.23 \times 5.6556 \times 0.05}{9.81}$$

$$T = 0.0007\ Nm$$

$$P = T\omega = 0.0007 \times 150.816$$

$$P = 0.1097\ W$$

3 RESULTS AND DISCUSSION

The designed hammer mill was successfully fabricated using locally sourced materials at a cost of 200,000 Naira. The cost of acquiring a hammer mill of equivalent capacity from foreign sources such as China and Europe range between 900,000 and 3,500,000 Naira. Significant design parameters as calculated are shown in Table 1. The fabricated hammer mill was tested by using it to pulverize various quantities of dried Maize, Guinea Corn and Millet. The performance evaluation of the machine is across maize, Guinea Corn and millet are shown in Table 2, 3, 4 below which was carried out based on three key operational output which include:

i. Particle size of pulverized material
ii. Mass of the material (kg)
iii. Duration of pulverization (min)

TABLE 1: RESULT OF CALCULATED PARAMETERS

Parameters	Symbol	Value	Unit
Centrifugal force exerted by the hammer	C.F	3473	N
Shaft Speed	N_2	2880	rpm
Diameter of main shaft	d	40	Mm
Length of Belt	L	1235	mm
Belt Contact Angle	B	3.48	^{o}c
Angle of wrap between belt and pulley	A	199.2	^{o}c
Tension in the slack side of belt	T2	194	N
Tension in the tight side of belt	T1	464	N
Power transmitted to the shaft	P	7460	W
Weight of hammer	W_{hammer}	1.25	N
Diameter of hammer shaft	D	15	mm
Weight of hammer shaft	Ws	0.243	N
Bending force of blade	Fb	101.7	N
Maximum bending moment of blade	Mb (max)	2034	Nmm
Total surface area of material of cyclone	Ats	1.2	M2
Volume of cyclone	Vc	0.064	M3

3.1 DATA REPRESENTATION OF HAMMER MILL CROPS

3.1.1 PULVERIZED MAIZE

TABLE 2. HAMMER MILL TEST RESULTS USING MAIZE

Trials	Mass of Maize before grinding (kg)	Mass of Maize after grinding (kg)	Time Taken (min)	Particle Size Remark
1	7	6.5	16	Fine (400µm-600400µm)
2	7	6.9	14	Fine (400µm-600400µm)
3	7	6.8	15	Fine (400µm-600400µm)
4	7	6.6	13	Fine (400µm-600400µm)
Average	7	6.7	14.5	Fine (400µm-600400µm)

The table above shows the results obtained from the operation carried out by the pulverizer. The results show that the hammer mill effectively grinds maize to a consistent particle size of 400µm to 600µm, with minimal variation in mass loss and grinding time across trials. The system demonstrates reliable and consistent performance, making it suitable for applications requiring fine grinding of maize. The slight variations in mass and time are within acceptable ranges, underscoring the mill's efficiency and effectiveness in processing maize.

3.1.2 PULVERIZED GUINEA CORN

TABLE 3: HAMMER MILL TEST RESULT USING GUINEA CORN

Trials	Mass of Guinea Corn before grinding (kg)	Mass of Guinea Corn after grinding (kg)	Time taken (min)	Particle Size Remark
1	5	4.8	15	Fine (400µm-600400µm)
2	5	4.7	14	Fine (400µm-600400µm)
3	5	4.9	16	Fine (400µm-600400µm)
4	5	4.5	15	Fine (400µm-600400µm)
Average	5	4.725	15	Fine (400µm-600400µm)

The hammer mill demonstrated consistent performance in grinding 5 kg of Guinea Corn per trial, with an average mass loss of 5.5% due to fine particle generation and dust. The grinding time ranged from 14 to 16 minutes, averaging 15 minutes, indicating stable operation. The particle size of the ground material remained within the 400µm to 600µm range, suitable for applications like animal feed production. Overall, the system exhibited reliability, efficiency, and uniform performance across all trials.

3.1.3 PULVERIZED MILLET

TABLE 4: HAMMER MILL TEST RESULT USING MILLET

Trials	Mass of Maize before grinding (kg)	Mass of maize after grinding (kg)	Time Taken(min)	Particle Size Remark
1	5	5.2	14	Fine (400µm-600400µm)
2	5	5.6	16	Fine (400µm-600400µm)
3	5	5.8	15	Fine (400µm-600400µm)
4	5	5.7	17	Fine (400µm-600400µm)
Average	5	5.575	15.5	Fine (400µm-600400µm)

The hammer mill trials for millet grinding showed consistent performance in particle size (400–600µm) and grinding time (14–17 minutes, averaging 15.5 minutes). However, an unusual increase in mass after grinding (5.2–5.8 kg from an initial 5 kg) suggests potential measurement errors or anomalies in the setup. Possible causes include moisture absorption, weighing scale calibration issues, or residual accumulation. While the grinding process was efficient, further investigation or repeated trials with careful measurement are recommended to verify the results.

3.1.4 AVERAGE PULVERIZED CROPS

The results indicate that all crops achieved a fine particle size between 400µm and 600µm, demonstrating the hammer mill's capability to produce a uniform grind across different materials. The milling time remained consistent, ranging from 14.5 to 15.5 minutes, suggesting similar efficiency for maize, guinea corn, and millet. Weight changes varied among the crops—while maize and guinea corn exhibited weight losses, millet showed a notable weight gain, pointing to potential differences in moisture content and physical properties post-milling. These variations highlight the need for further investigation into crop-specific milling conditions. Overall, the hammer mill effectively grinds diverse crops to fine particle sizes suitable for various applications, though factors such as moisture content and hardness influence milling outcomes.

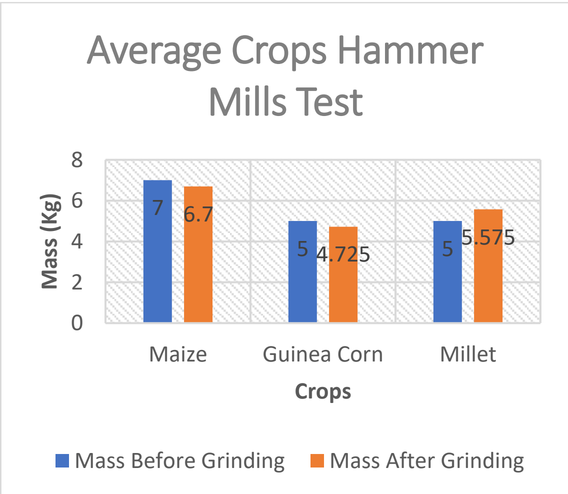

Figure 2: Graphical Representation of Hammer Mills Test Mass (Kg) against Crops.

3.2 SUMMARY OF DISCUSSION OF RSULT

The particle size distribution analysis of the hammer mill output confirms that the machine produces only fine particles for both tested grains. This affirms the effectiveness of the integrated mechanical separator, which ensures that only particles meeting the desired specifications are retained in the final output. Additionally, incorporating a feedback mechanism allows uncrushed and coarse materials to be recirculated into the crushing chamber for further fracturing. This feature enhances the machine's efficiency by ensuring the production of high-quality, fine-grained products suitable for processing solid minerals and agricultural materials.

Furthermore, the fabricated hammer mill is designed to be compact, making it suitable for production environments with limited workspace. The elimination of the sieve screen and separation chamber contributes to its reduced size, distinguishing it from previous models such as the hammer mill developed by Nasir (2005), which included a sieve screen, and the one designed by Ebunilo *et al*. (2010), which featured a separation chamber. These modifications not only optimize space utilization but also improve the overall performance and usability of the machine.

4 CONCLUSION

The study highlights the significant impact of moisture content on the grinding efficiency, throughput capacity, and particle size distribution of corncobs and corn. Higher moisture levels resulted in coarser particle sizes and improved throughput but also led to increased energy consumption. In contrast, lower moisture levels produced finer particles at the cost of reduced throughput. Additionally, the frictional heat generated during grinding caused moisture loss, which must be accounted for in mass balance calculations.

The grinding process using a hammer mill is inherently complex due to the random movement of materials within the milling chamber. While sieve dimensions strongly influence particle size distribution, feeding flow plays a lesser role. Optimizing this process remains a challenge, necessitating further research to enhance efficiency, minimize energy consumption, and achieve consistent grinding performance.

REFERENCES

Cerdeira AM, Mazzotti M, Gander B. Miconazole nanosuspensions: Influence of formulation variables on particle size reduction and physical stability. Int. J. Pharm.2010;396:210-218.

Chenjea TW, Simbib DJ, Navara E. Relationship between microstructure, hardness, impact toughness and wear performance of selected grinding media for mineral ore milling operations. Mater. Des. 2004;25:11-18.

Ebunilo.P.O, Obanor A.O and Ariavie, G.O. (2010). Design and Preliminary Testing of a Hammer Mill with End-Suction Lift Capability Suitable for Commercial Processing of Grains and Solid Minerals in Nigeria. International Journal of Engineering Science and Technology Vol. 2(6), 2010, 1581-1593

Merisko-Liversidge E, Liversidge GG. Nanosizing for oral and parenteral drug delivery: A perspective on formulating poorly water-soluble compounds using wet media milling technology. Adv. Drug Delivery Rev. 2011;63:427-440.

Nasir, A. (2005). Development and Testing of a Hammer Mill. AU J.T. 8(3): 124-130.

Probst, K.V., Ambrose, R.P.K., Pinto, R.L., Bali, R., Krishnakumar, P., Ileleji, K.E., 2013. The effect of moisture content on the grinding performance of corn and corncobs by hammermilling. American Society of Agricultural and Biological Engineers, 56(3), 1025-1033, https://core.ac.uk/download/pdf/18529159.pd

Wu Z, Fang B, Bonakdarpour A, Sun A, Wilkinson DP, Wang D. WS2 nanosheets as a highly efficient electrocatalyst for hydrogen evolution reaction. Appl. Catal., B.2012;125:59-66.

/

Optimization of Microbial-Induced Calcite Precipitate - Zeolite Stabilisation of Silt-Sand Soil for Geotechnical Application Using Response Surface Methodology

Murtala Hassan Mohammed[1] Musa Alhassan[2] Mustapha Mohammed Alhaji[3] Taiye Elisha Adejumo[4]
[1] Department. of Civil Engineering, Modibbo Adama University Yola Adamawa, Nigeria
[2] Department. of Civil Engineering Federal University of Tech. Minna, Niger, Nigeria
[3] Department. of Civil Engineering Federal University of Tech. Minna, Niger, Nigeria
[4]Department. of Civil Engineering Federal University of Tech. Minna, Niger, Nigeria
*Corresponding author email: hmurtala@mau.edu.ng

ABSTRACT
Microbially-Induced Calcite Precipitation (MICP) is an innovative soil improvement technique in geotechnical engineering, that deals with microbiological activity to enhance soil properties. Studies conducted using the techniques have shown its potentials in geotechnical engineering applications. However, the ammonia generated as by-product during the MICP process limits its broader application. This study aims to optimize the MICP input parameters to minimize the ammonia generation, by incorporating zeolite, using Response Surface Methodology (RSM) for design of experiment. Urease positive bacteria (Lysinibacillus fusiformis) was isolated, characterized and identified to specie level using biochemical and molecular DNA test, which was then used for the MICP treatment. Series of laboratory experiments were conducted, varying pH, zeolite content, bacterial suspension density, cementation reagent concentration, and compactive effort. These input variables were optimized to improve shear strength, reduce permeability, and lower the ammonia production. The results demonstrated the effectiveness of using Lysinibacillus fusiformis as a urease producing bacteria for MICP and the potential of incorporating zeolite into the process, which significantly improves soil strength, decrease permeability, and reduce the production of excess ammonia. Thus, the optimized MICP process with zeolite presents an effective sustainable solution for reducing ammonia, while enhancing the geotechnical properties of silt-sand soil.

Keywords: *Ammonia Reduction,* Lysinibacillus fusiformis, RSM, Silt-Sand, Zeolite

1 INTRODUCTION

Microbial induced carbonate precipitation has been attracting researchers in many fields due to its sustainable and environmentally friendly nature (De Muynck *et al.*, 2010; Dejong *et al.*, 2013; Su *et al.*, 2022) when applied to soil it can reduced permeability, improve mechanical properties and mitigate harmful element pollution (Warren *et al.*, 2001; Xue *et al.*, 2022). Most researchers use urea hydrolysis pathway to fulfill MICP process (DeJong, Fritzges and Nüsslein, 2006). In this pathway urea is decomposed to CO_3^{2-}/HCO_3^- and NH_4^+ (pH increase) by urease of urea catalytic bacteria (Hammes *et al.*, 2003). Utilization of MICP is limited by the byproduct ammonia NH_3/NH_4^+ .High-strength ammonia is pollutant that can accelerate eutrophication, deplete dissolved oxygen, and be toxic to aquatic life in water bodies (Karadag *et al.*, 2006) therefore the byproduct ammonia limits the wide application of the MICP technique. There are several biological procedures that can lead to calcite precipitation, however, hydrolysis of urea is the most preferred because the mechanism is straight forward and can produce up to 90% chemical conversion efficiency of precipitated amount of calcite in less than 24 hours (Al-Thawadi, 2008; Mujah, Shahin and Cheng, 2017). Granular soils are good candidate soils for MICP because of their geometric compatibility that enables the bacteria to freely move through the pore spaces of the soil during which bio-cementation and bio-clogging processes result in strength gain and reduction in void of the treated soil (Moravej *et al.*, 2018). Silt-sand is one of such soil types.

Silt-sand is one of the soil groups that are regarded as problematic. This is because, in most cases, they do not meet specifications for engineering applications, and therefore requires some modifications. This study focusses on adding zeolite to MICP treatment variables and optimizing MICP process factors to reduce excess ammonia generated during MICP process of silt-sand, evaluating the response in geotechnical properties improvement of silt-sand when stabilised trough MICP with zeolite using Response Surface Methodology (RSM).

2 MATERIALS AND METHOD

2.1 MATERIALS

The soil used in this study is a silt-sand soil. This soil was characterized form soil collected from three (3) trial pit in Girei local government area Adamawa state. Disturbed samples were collected, packaged, labelled and transported to Civil Engineering laboratory of Modibbo Adama University for geotechnical soil investigation similarly the bacteria used was isolated in the laboratory from natural soil. The bacteria were identified and characterized using standard microbiological techniques that is biochemical confirmatory test and molecular identification, and their purity and viability were confirmed before using in the experiments. Design expert® software version 13 was used to generate experimental design and carry out data analysis. The software allows for the design of experiments and analysis of data using response surface methodology.

2.2 EXPERIMENTAL DESIGN

Response surface methodology was used to investigate the effect of independent variables which including bacterial suspension density, cementation reagent concentration, pH, compactive effort and zeolite on response variable (erodibility, permeability, ammonia content). Experimental Design was developed using expert design software version 13.0.1.0 for studying the interaction between different combinations of bacterial suspension density, cementation reagent concentration, pH, compactive effort and zeolite. The response variables were measured in a factorial design with the range and levels of the input variables determined based on experimental tests. RSM design with coded and un-coded levels developed with D-optimal (custom) design is presented in table 1. D-optimal design type and quadratic model were used to design the experiment. Thirty-one treatment were randomly performed according to D-optimal custom design. Real levels of the in-depended variables were coded based on the equation

$$Z = \frac{Z_{real} - Z_o}{\Delta Z} \quad (1)$$

were

Z: Actual value of the factor

Z_{real}: Actual (real-world) value of the factor

Z_o: Center point (mid-point of the real factor level in design)

ΔZ: Step size (half the range of the real factor levels)

Table 1 In-depended Variables with their corresponding levels for MICP Stabilisation of Silt-sand and based on D-optimal (custom) design.

Factor	A	B	C	D	E
Name	Bacteria	Cementation reagent	pH	Zeolite	Compactive effort
Type	Numeric	Numeric	Numeric	Numeric	Categoric
Sub type	Discrete	Discrete	Discrete	Discrete	Nominal
Minimum	1.500E+09	0.5000	3.50	2	BSH
Maximum	3.500E+09	1.0000	9.50	10	
Coded low	-1 ↔ 1500000000.00	-1 ↔ 0.50	-1 ↔ 3.50	-1 ↔ 2.00	BSL
Coded high	+1 ↔ 3500000000.00	+1 ↔ 1.00	+1 ↔ 9.50	+1 ↔ 10.00	WAS

2.2.1 MICP Specimen Preparation.

3000g of the soil was thoroughly mixed with zeolite and liquid containing soil pH buffer of wet optimum moisture content (OMC) containing 1/3 of its pore volume as the bacteria suspension density. And the mixture was compacted to BSH, BSL and WAS respectively. The compacted specimens were permeated with 2/3 of their pore volume of the cementation reagent under gravity in three 24 hours' circles intervals each to initiate and facilitate the MICP process. Following design of experimental, the concentration of all the input factors were varied according to experimental design. The soil was then cured for 72h before strength determination.

2.2.3 Data Analysis

The data obtained from the experiments was analyzed using the statistical software Expert Design Software version 13. The response surface methodology was used to investigate the relationship between the input variables and the measured responses of the MICP treated silt-sand soil. The optimal bacterial suspension density, cementation reagent concentration, pH, zeolite and the Compactive effort of MICP treated silt-sand soil was determined by identifying the maximum or minimum values of the response surface. In addition, the statistical significance of the effects of each input variable on the measured responses was evaluated using analysis of variance (ANOVA) and regression analysis.

3 RESULT AND DISCUSION

3.1 MATERIAL CHARCTERIZATION

The particle size distribution of the natural soil obtained by standard sieve test is presented in figure 1, the soil has 97.5% passing 2mm and 15.2% passing 0.075mm, the sample met the geometrical compatibility requirement for MICP soil (Sand: 0.075 mm – 2 mm, Silt: 0.002 mm – 0.075 mm). The soil was classified as Non-plastic silt-sands (NSM) described as Non-plastic silty sands, poorly graded sand-silt mixture using modified Unified Soil Classification system chart.

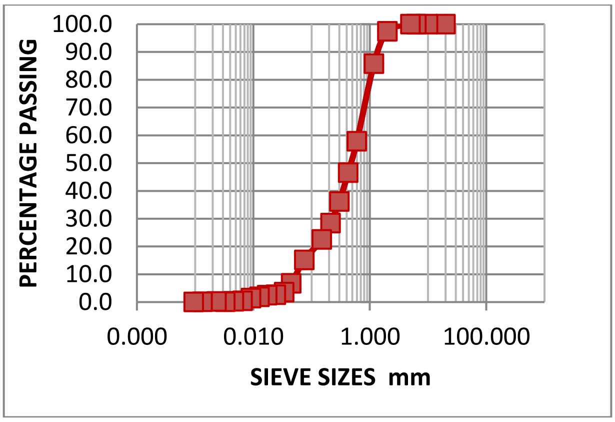

Figure 1 Particle Size Distribution Curve for Soil use for Soil used in the Study

3.2 MODEL FITTING

The responses for the influence of independent factors of MICP stabilized silt sand (bacteria concentration x_1, cementation reagent x_2, pH x_3, zeolite x_4 and compactive effort x_5) were predicted by the model equations. Coefficients of polynomial equation were computed from experimental data to predict the values of the response variable. Regression equations for each response variable, as obtained from response surface methodology were presented in Equations. 2, 3 and 4 respectively. Statistical analysis results of (ANOVA) indicates that the experimental data can best be represented with quadratic polynomial model with coefficient of determination R-square values of 0.8679, 0.8918 and 0.8643 for permeability, erodibility and ammonia content respectively, lack of fit was insignificant as the ($p \leq 0.05$) relative to pure error for all variables is less than 0.05, which shows that our model is statistically accurate. Table 2 present the model prediction error analysis, the predicted R^2 of 0.537, 0.5648 and 0.5141 are closer to the adjusted R^2 of 0.7170, 0.7628 and 0.7091for permeability, erodibility and ammonia content respectively as their differences is less than 0.2, also adequate precision of 12.2183, 10.5423 and 13.0213 for the permeability, erodibility and ammonia content is greater than 4 indicating that signal to noise ratio is desirable implying that the model can be used to navigate the design space.

Table 2 Model Fit Statistics and Prediction Accuracy

Fit Statistics	Permeability	Erodibility	Ammonia Content
Std. Dev.	3.049E-06	3.61	94.78
Mean	8.795E-06	23.1	641.45
C.V. %	34.76	15.35	14.78
R²	O.8679	0.8918	0.8643
Adjusted R²	0.7170	0.7628	0.7091
Predicted R²	0.537	0.5648	0.5141
Adequate Precision	12.2183	10.5423	13.0213

$$\boldsymbol{permeabilit} = +7.069X10^{-6} - 4.221X10^{-7}x_1 + 2.079X10^{-7}x_2 + 1.085X10^{-7}x_3 - 3.378X10^{-7}x_4 + 3.051X10^{-6}X_5[1] - 1.273X10^{-6}x_5[2] + 1.914X10^{-6}x_1x_2 + 3.734X10^{-6}x_1x_3 + 3.296X10^{-6}x_1x_5[1] - 5.145X10^{-6}x_1x_5[2] + 3.533X10^{-6}x_2x_3 - 5.146X10^{-6}x_2x_4 - 3.676X10^{-6}c_3x_4 + 3.839X10^{-6}x_3x_5[1] + 1.234X10^{-6}x_3x_5[2] + 3.059X10^{-6}x^2{}_3 \quad (2)$$

$$\boldsymbol{erodibility} = 23.106746039 - 0.3377333790776x_1 - 1.5578946164553x_2 - 0.39840698056329x_3 + 3.9074417026593x_4 + 4.0193588380924x_5[1] + 1.449430264647x_5[2] + 4.8053226116126x_1x_2 + 2.7896372750313x_1x_4 - 1.1127895553889x_2x_5[1] + 6.1903143356748x_22_5[2] - 5.7262417306138x_3x_4 - 9.5669241110838x_3x_5[1] + 3.4864529196912x_3x_5[2] - 8.9655122710829x^2{}_1 + 4.7650626273941x^2{}_2 + 3.567064265287x^2{}_4 \quad (3)$$

$$\boldsymbol{Amonia\ content} = 399.72330993848 - 76.20063188012x_1 + 61.3417444431389x_2 + 18.021404708982x_3 - 37.695537429494x_4 + 43.227153215702x_5[1] + 2.3920171362371x_5[2] - 125.61134610225x_1x_2 - 127.85331261958x_1x_4 - 130.22448790494x_1x_5[1] + 91.004216950547x_1x_5[2] + 91.761480428973x_2x_3 + 144.53198305631x_2x_5[1] - 312.06770124088x_2x_5[2] + 49.2271077420577x_4x_5[1] - 171.16115129125x_1x_5[2] + 313.55373782212x^2{}_1 \quad (4)$$

3.3 EFFECT OF MICP INDEPENDENT FACTORS ON PERMEABILITY OF MICP TREATED SILT-SAND

Figure 2(A) illustrate the influence of the concentration of Lysinibacillus fusiformis and cementation reagent concentration on permeability of MICP treated silt-sand soil. It can be observed that increase in both concentration of Lysinibacillus fusiformis and cementation reagent concentration leads to reduction in permeability, it can be inferred that at higher concentration of Lysinibacillus fusiformis more urease enzyme was produced and as the cementation reagent increase from 0.5 to 1mole there is sufficient urea and calcium that combine with the urease enzyme produced and precipitate calcium carbonate which in turn filled the pore spaces, there by clogging the soil and reduced permeability. Soon *et al.*,(2014) stated that for effective MICP treatment the preference concentration of cementation reagent should lies between 0.5-1.0 mol. Figure 2(B) show the combine effect of the Lysinibacillus fusiformis and soil pH on the permeability of MICP treated silt-sand soil. A saddle shape nature of the 3D surface plot shows upward curve in the direction of increasing soil pH indicating increase permeability and a downward curve in the direction of increasing concentration of Lysinibacillus fusiformis indicating decrease permeability it can be noticed that the optimal pH is located in the region were the soil pH is slightly acidic to basic at higher concentration of Lysinibacillus fusiformis, the reduction in permeability can be attributed to formation of uniform calcite which form during the MICP process as a result of change in the pH of the environment which favors the urease activities of Lysinibacillus fusiformis. Study from Liu, Li and Li, (2021) reveal that MICP process is favored in initial pH environment of 6.5–9.3 (neutral to basic condition). Figure 2(C) illustrate the combine effect for the interaction between Lysinibacillus fusiformis and zeolite, as indicated by the near flat surface of the 3D plot the relationship between Lysinibacillus fusiformis and soil pH is assume to be linear i.e. increase in both factors increase the permeability and the region of interest is located at the point where concentration of Lysinibacillus fusiformis is in the range 2.5E+09 - 3.0E+09cell/mL at higher zeolite content. Su and Yang, (2021) conducted a research on improving MICP technique with zeolite and found out that strength gain is positively correlated with zeolite dosage, in their study they use zeolite dosage of 0-10g and found the optimal zeolite dosage to be10g which is similar to the prediction of higher zeolite dosage of 10g in this study

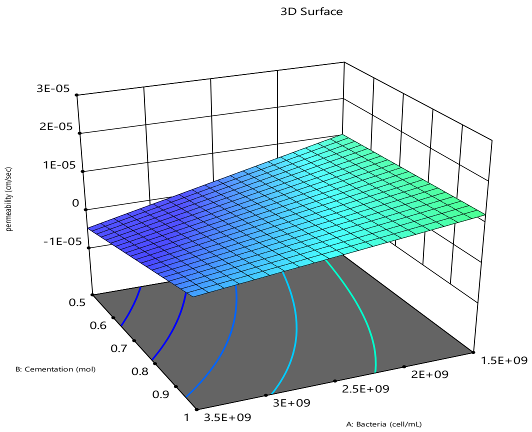

A

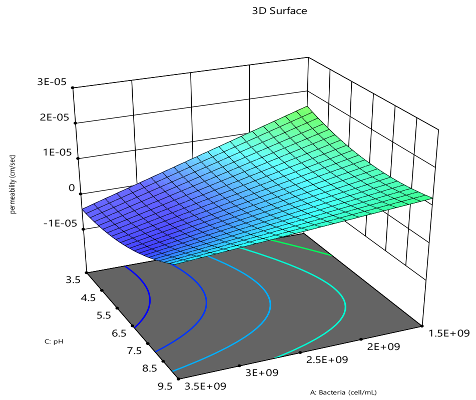

B

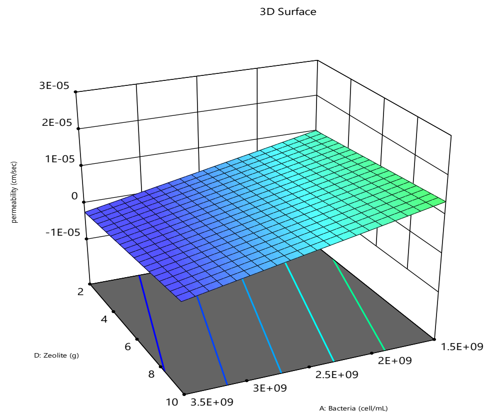

C

Figure 2 Response Surface plot of interaction between (A) Bacteria and Cementation reagent, (B) Bacteria and soil pH, (C) Bacteria and Zeolite for permeability.

3.4 EFFECT OF MICP INDEPENDENT FACTORS ON ERODIBILITY OF MICP TREATED SILT-SAND

Figure 3 (A) present the surface plot of the effect of Lysinibacillus *fusiformis* bacteria and cementation reagent solution on erodibility of MICP treated silt-sand, the interaction between Lysinibacillus *fusiformis* and cementation solution exhibit a nonlinear relationship as indicated by convex nature of the plot. This pattern typically suggests that factor level low or high are less favorable and there exist a mid-range where erodibility can be maximized. At this point it is expected that Lysinibacillus *fusiformis* produced effective urease enzymes that combined with calcium from supply cementation solution and precipitated effective calcite with bind the soil together and resist soil loss due to resist soil movement. Study of Montoya, Do and Gabr, (2018) suggest that erodibility of MICP treated sand is affected by change in cementation level as a result of precipitated calcite. Figure 3 (B) depict the surface plot for the combine influence of Lysinibacillus *fusiformis* bacteria and soil pH on erodibility of MICP treated silt-sand, the plot suggest a nonlinear relationship between Lysinibacillus *fusiformis* and soil pH which was indicated by the concave curved nature of the surface plot, it can be observed that from the initial point erodibility increase with increasing both factor level which continuous until a region is reach within the deign space where any further increase in factor level leads to decrease in the erodibility value this region is consider as the region of optimality and upon amplifying the contour plot this region is predicted to be in the range of 6.5-9.5 pH and 2E+09-3E+09cell/mL Lysinibacillus *fusiformis* bacteria concentration. Do, Montoya and Gabr, (2020) found that erodibility of MICP treated sand reduced with increasing cementation level. Figure 3 (C) illustrate the effect of interaction between Lysinibacillus *fusiformis* bacteria and zeolite on erodibility of MICP treated silt-sand, the interaction between Lysinibacillus *fusiformis* bacteria zeolite follow similar pattern with the interaction between Lysinibacillus *fusiformis* bacteria and soil pH as indicated by the concave nature of the surface plot, this suggest that mechanism of interaction between Lysinibacillus *fusiformis* bacteria and zeolite for the erodibility of MICP treated silt-sand is as explain above.

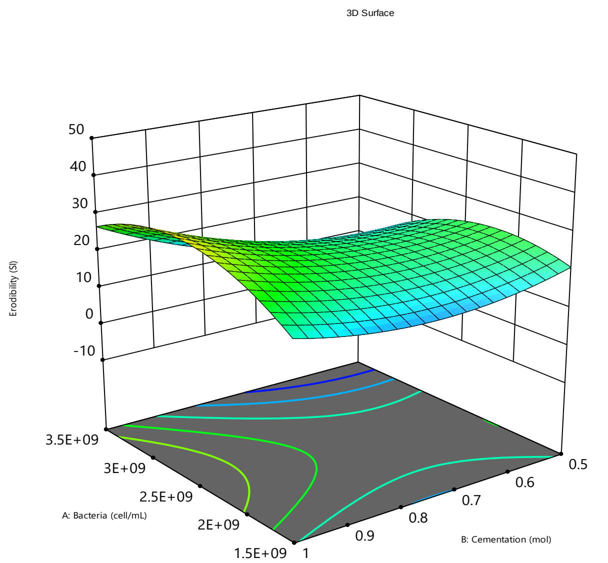

A

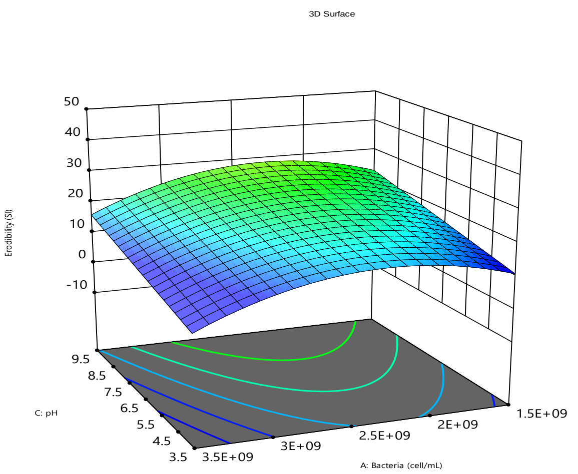

B

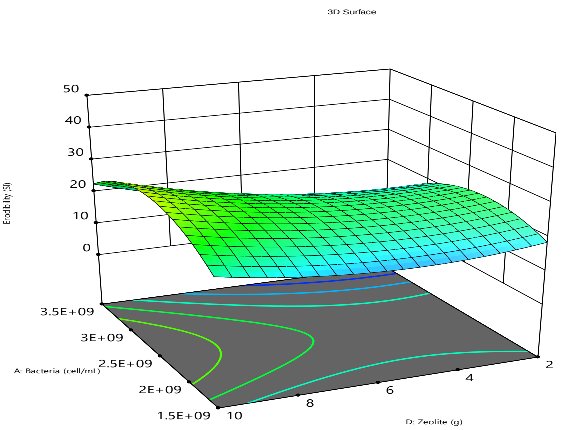

C

Fig. 3 Response Surface plot of interaction between (A) Bacteria and Cementation reagent, (B) Bacteria and soil pH, (C) Bacteria and Zeolite for erodibility

3.5 EFFECT OF MICP INDEPENDENT FACTORS ON AMMONIA CONTENT OF MICP TREATED SILT-SAND

Figure 4 (A), illustrate the combine influence of Lysinibacillus *fusiformis* and cementation reagent on ammonia reduction of MICP treated silt-sand the curvature nature of the surface plot suggests a nonlinear relationship implying that the response does not increase linearly with either factors, the color transition from lowest ammonia generated (blue region) to the highest ammonia generated (red region) indicate how changes in factor level influence the response. Thus, moving from lower Lysinibacillus *fusiformis* and cementation reagent concentration (blue) to higher concentration (red) ammonia reduction improve significantly. The optimal ammonia reduction is located in the red region where concentration of both factors is high. The red zone at the top of the curve signify the highest ammonia reduction achieved within the tested parameters, this suggest that the optimal combination of Lysinibacillus *fusiformis* and cementation reagent for effective ammonia reduction is located in the red zone. The interaction between Lysinibacillus *fusiformis* and zeolite follow the same trend as can be observed in Figure 4 (A). Similarly, the effect of Lysinibacillus *fusiformis* and soil pH is illustrated in Figure 4 (C), the surface plot exhibits a relatively flat and slightly slope pattern which indicate that ammonia reduction may not be highly sensitive to changes in the two factors level (Lysinibacillus *fusiformis* and pH), it can be observed from the color gradient that ammonia levels decrease with increasing Lysinibacillus *fusiformis* and pH concentration but the changes appear to be gradual and not rapid implying that the interaction is moderate. The gradual improvement in ammonia reduction at higher bacteria and pH level may be attributed to the activity of Lysinibacillus *fusiformis* and pH), it can be observed from the color gradient that ammonia levels decrease with increase Lysinibacillus *fusiformis* and pH concentration but the changes appear to be gradual which suggest that Lysinibacillus *fusiformis* activity breakdown the ammonia and the higher pH condition facilitate the conversion of ammonium ion NH_4^+ to ammonia gas NH_3. An overly acid or alkaline environment will reduce ammonia removal, and the optimum pH varies with zeolites. In many studies, the optimal pH is about 8, below which H^+ ions increase and compete with NH_4^+ for exchange sites. When pH>8, zeolite may dissolve and NH_4^+converts to NH_3, reducing the removal efficiency. (Huang *et al.*, 2010; Su *et al.*, 2022).

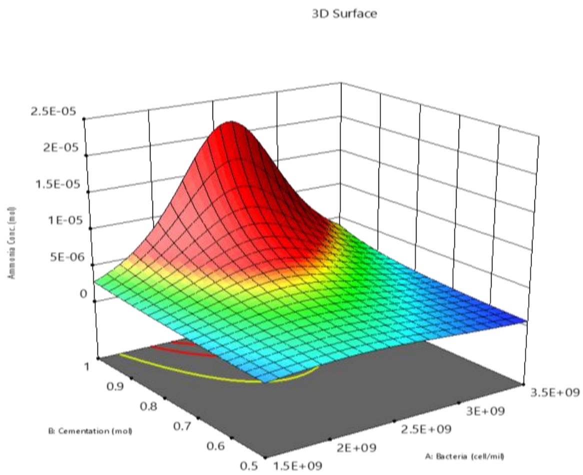

A

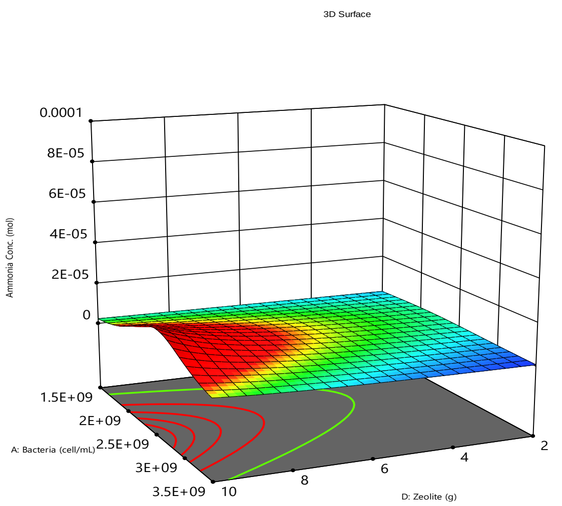

B

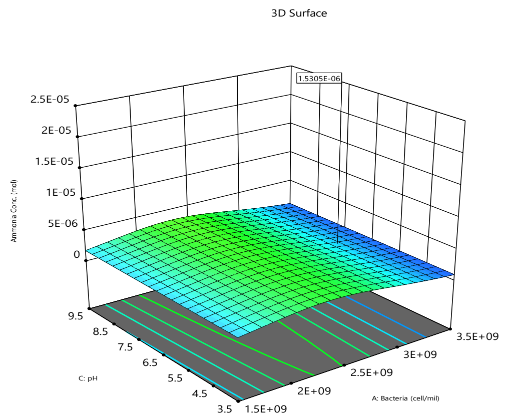

C

Figure 4 Response Surface plot of interaction between (A) Bacteria and Cementation reagent, (B) Bacteria and soil pH, (C) Bacteria and Zeolite for ammonia content

3.6 OPTIMIZATION OF INDEPENDENT VARIABLES

Design expert software was used to create, 3D surface response graphs which show how the concentration of bacteria, cementation reagent concentration, soil pH level, zeolite dose, and compactive effort affected the response variables. These graphs were generated by varying two independent variables within experimental ranges while keeping the other variable at central point. (Fig. A) was generated by varying the concentration of Lysinibacillus fusiformis and cementation reagent at 6.39 pH, 3.92g zeolite and WAS compactive effort, (Fig. B) was generated by varying the concentration of Lysinibacillus fusiformis and soil pH level at o.66mol cementation reagent concentration, 3.92g zeolite and WAS compactive effort, while (Fig. C) was generated by varying the concentration of Lysinibacillus fusiformis and zeolite at 0.66mol concentration of cementation reagent concentration, 6.39 soil pH level and WAS compactive effort respectively. These graphs illustrate the complex interaction among independent variables. Furthermore, numerical optimization was executed by desirability function using Design Expert Software. The goals that were selected for the optimization of MICP stabilized silt-sand soil are concentration of Lysinibacillus fusiformis targeted at 3.0E+09cell/mil. Cementation reagent concentration targeted at 0.66mol, soil pH level targeted at 7.5 pH level, zeolite and compactive effort were in range of experimental data considered, the goal was set to obtain improved silt-sand soil that has lower soil permeability, lower soil erodibility and lower ammonia content generation of MICP process. Sixty-two different solution were found which contain different level of independent variable and the solution with maximum desirability was selected as the optimized MICP silt- sand improvement condition. Combined optimized condition for MICP stabilization of silt-sand were 3.2E+09cell/mil concentration of Lysinibacillus fusiformis, 0.65mol cementation reagent, 6.4 pH level, 3.9g zeolite and WAS compactive effort and the response at these optimized conditions were 6.3E-06cm/sec permeability, 15.93g soil loss (erodibility and 1.53E-06mol ammonia content respectively.

3. 7 VERIFICATION OF THE MODEL

Optimized MICP silt-sand stabilization conditions were used to check the suitability of the model for prediction of response values by performing experiments under the optimized condition. The predicted responses values at the optimized conditions were 6.3E-06cm/sec permeability, 15.93g soil loss (erodibility) and 1.53E-06mol ammonia content while the experimental response values at the optimized condition were 7.2E-06cm/sec permeability, 17.83g soil loss (erodibility and 1.68E-06mol ammonia content respectively.

4.0 CONCLUSION

In this study we have evaluated the influence MICP treatment factors on bio-stabilization of silt-sand and incorporated zeolite in the MICP treatment of silt-sand in order to improve geotechnical properties of silt-sand and reduce ammonia generated during MICP technique. MICP treatment of silt-sand were successfully prepared using experimental design. This study illustrates that response surface methodology is a useful tool to optimize the MICP treatment factors and explore the relationship between independent and response variables. The results of this study disclosed that MICP treatment with zeolite have significant effect on the bio improvement of silt-sand and can reduced the access ammonia generated during MICP treatment process. The current study demonstrates that the quadratic model was sufficient to describe and predict the responses of permeability, erodibility and ammonia content, with the change of independent variables (Lysinibacillus fusiformis, cementation regent, soil pH, zeolite and compactive effort). The optimum condition was obtained through numerical optimization using desirability function. Optimized MICP treatment factors were 3.2E+09cell/mL concentration of Lysinibacillus fusiformis, 0.65mol cementation reagent, 6.4 pH level, 3.9g zeolite under WAS compactive effort respectively. It can be concluded that optimized MICP-zeolite techniques have the potential of improving geotechnical properties of silt-sand and reducing access ammonia generation during MICP process there by making MICP process to be effective and sustainable.

RERERENCES

Al-Thawadi, S.M. (2008) 'High strength in-situ biocementation of soil by calcite precipitating locally isolated ureolytic bacteria', *School of Biological Sciences and Biotechnology*, p. 272.

Dejong, J.T. *et al.* (2013) 'Biogeochemical processes and geotechnical applications: Progress, opportunities and challenges', *Bio- and Chemo- Mechanical Processes in Geotechnical Engineering - Geotechnique Symposium in Print 2013*, (4), pp. 143–157. Available at: https://doi.org/10.1680/bcmpge.60531.014.

DeJong, J.T., Fritzges, M.B. and Nüsslein, K. (2006) 'Microbially Induced Cementation to Control Sand Response to Undrained Shear', *Journal of Geotechnical and Geoenvironmental Engineering*, 132(11), pp. 1381–1392. Available at: https://doi.org/10.1061/(asce)1090-0241(2006)132:11(1381).

Do, J., Montoya, B.M. and Gabr, M.A. (2020) 'Scour mitigation and erodibility improvement using microbially induced carbonate precipitation', *Geotechnical Testing Journal*, 44(5). Available at: https://doi.org/10.1520/GTJ20190478.

Hammes, F. *et al.* (2003) 'Strain-specific ureolytic microbial calcium carbonate precipitation', *Applied and Environmental Microbiology*, 69(8), pp. 4901–4909. Available at: https://doi.org/10.1128/AEM.69.8.4901-4909.2003.

Huang, H. *et al.* (2010) 'Ammonium removal from aqueous solutions by using natural Chinese (Chende) zeolite as adsorbent', *Journal of Hazardous Materials*, 175(1–3). Available at: https://doi.org/10.1016/j.jhazmat.2009.09.156.

Karadag, D. *et al.* (2006) 'Removal of ammonium ion from aqueous solution using natural Turkish clinoptilolite', *Journal of Hazardous Materials*, 136(3), pp. 604–609. Available at: https://doi.org/10.1016/j.jhazmat.2005.12.042.

Liu, J., Li, G. and Li, X. (2021) 'Geotechnical Engineering Properties of Soils Solidified by Microbially Induced CaCO3Precipitation (MICP)', *Advances in Civil Engineering*, 2021. Available at: https://doi.org/10.1155/2021/6683930.

Montoya, B.M., Do, J. and Gabr, M.M. (2018) 'Erodibility of Microbial Induced Carbonate Precipitation-Stabilized Sand under Submerged Impinging Jet', (April 2019), pp. 19–28. Available at: https://doi.org/10.1061/9780784481592.003.

Moravej, S. *et al.* (2018) 'Stabilization of dispersive soils by means of biological calcite precipitation', *Geoderma*, 315(July 2017), pp. 130–137. Available at: https://doi.org/10.1016/j.geoderma.2017.11.037.

Mujah, D., Shahin, M.A. and Cheng, L. (2017) 'State-of-the-Art Review of Biocementation by Microbially Induced Calcite Precipitation (MICP) for Soil Stabilization', *Geomicrobiology Journal*, 34(6), pp. 524–537. Available at: https://doi.org/10.1080/01490451.2016.1225866.

De Muynck, W. *et al.* (2010) 'Influence of urea and calcium dosage on the effectiveness of bacterially induced carbonate precipitation on limestone', *Ecological Engineering*, 36(2), pp. 99–111. Available at: https://doi.org/10.1016/j.ecoleng.2009.03.025.

Soon, N.W. *et al.* (2014) 'Factors Affecting Improvement in Engineering Properties of Residual Soil through Microbial-Induced Calcite Precipitation', *Journal of Geotechnical and Geoenvironmental Engineering*, 140(5), pp. 1–11. Available at: https://doi.org/10.1061/(asce)gt.1943-5606.0001089.

Su, F. *et al.* (2022) 'Combining microbially induced calcite precipitation (MICP) with zeolite: A new technique to reduce ammonia emission and enhance soil treatment ability of MICP technology', *Journal of Environmental Chemical Engineering*, 10(3). Available at: https://doi.org/10.1016/j.jece.2022.107770.

Su, F. and Yang, Y.Y. (2021) 'Microbially induced carbonate precipitation via methanogenesis pathway by a microbial consortium enriched from activated anaerobic sludge', *Journal of Applied Microbiology*, 131(1). Available at: https://doi.org/10.1111/jam.14930.

Warren, L.A. *et al.* (2001) 'Microbially mediated calcium carbonate precipitation: Implications for Interpreting calcite precipitation and for solid-phase capture of inorganic contaminants', *Geomicrobiology Journal*, 18(1), pp. 93–115. Available at: https://doi.org/10.1080/01490450151079833.

Xue, Z.F. *et al.* (2022) 'Catalyzing urea hydrolysis using two-step microbial-induced carbonate precipitation for copper immobilization: Perspective of pH regulation', *Frontiers in Microbiology*, 13(September). Available at: https://doi.org/10.3389/fmicb.2022.1001464.